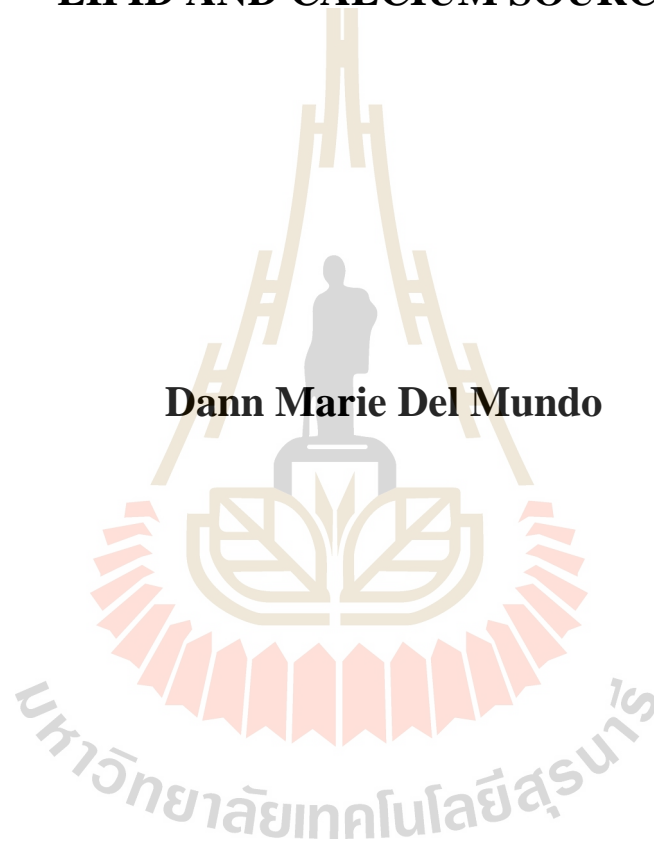


**RHEOLOGY AND MICROSTRUCTURE OF LABORATORY
SCALE MODELS OF FAT, OIL, AND GREASE (FOG)
DEPOSITS PREPARED FROM DIFFERENT
LIPID AND CALCIUM SOURCES**

Dann Marie Del Mundo



A Thesis Submitted in Partial Fulfillment of the Requirements for the

Degree of Doctor of Philosophy in Food Technology

Suranaree University of Technology

Academic Year 2017

กระแสวิทยาและโครงสร้างภายในของตัวอย่างไขมันและน้ำมันสะสมที่เตรียม
ในระดับห้องปฏิบัติการจากไขมันและแคลเซียมต่างชนิดกัน

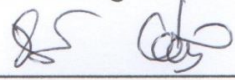


วิทยานิพนธ์นี้เป็นส่วนหนึ่งของการศึกษาตามหลักสูตรปริญญาปรัชญาดุษฎีบัณฑิต
สาขาวิชาเทคโนโลยีอาหาร
มหาวิทยาลัยเทคโนโลยีสุรนารี
ปีการศึกษา 2560

**RHEOLOGY AND MICROSTRUCTURE OF LABORATORY
SCALE MODELS OF FAT, OIL, AND GREASE (FOG)
DEPOSITS PREPARED FROM DIFFERENT LIPID
AND CALCIUM SOURCES**

Suranaree University of Technology has approved this thesis submitted in partial fulfillment of the requirements for the Degree of Doctor of Philosophy.

Thesis Examining Committee



(Assoc. Prof. Dr. Jirawat Yongsawatdigul)

Chairperson



(Assoc. Prof. Dr. Manote Sutheerawattananonda)

Member (Thesis Advisor)



(Asst. Prof. Dr. Jareeya Yimrattanabovorn)

Member



(Dr. Thanawit Kulrattanak)

Member

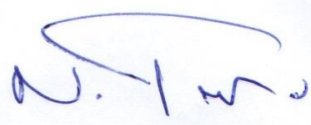


(Asst. Prof. Dr. Siranee Sreesai)

Member



(Prof. Dr. Santi Maensiri)
Vice Rector for Academic Affairs
and Internationalization



(Prof. Dr. Neung Teaumroong)
Dean of Institute of Agricultural Technology

นางสาวแคน มาเรีย เดล มุน ได้ : กระแสวิทยาและโครงสร้างภายในตัวอย่างไขมันและน้ำมัน
สะสมที่เตรียมในระดับห้องปฏิบัติการจากไขมันและแคลเซียมต่างชนิดกัน (RHEOLOGY
AND MICROSTRUCTURE OF LABORATORY SCALE MODELS OF FAT, OIL, AND
GREASE (FOG) DEPOSITS PREPARED FROM DIFFERENT LIPID AND CALCIUM
SOURCES) อาจารย์ที่ปรึกษา : รองศาสตราจารย์ ดร. มาโนชญ์ สุธีรวุฒินานนท์, 138 หน้า.

สารสะสมของไขมัน น้ำมัน และไขมันชั้นคล้ายจาระบีในรูปของสบู่ของแคลเซียมพบว่าเป็น
สาเหตุของน้ำเสียล้นท่อระบายน้ำ โดยเกิดจากการสะสมของสารเหล่านี้ที่ผนังด้านในของท่อระบาย
น้ำ อย่างไรก็ตามแหล่งของแคลเซียมและไขมันที่มีการศึกษามาก่อนหน้านี้มีค่อนข้างจำกัด และยัง
ขาดข้อมูลด้านลักษณะเฉพาะของสบู่บางชนิดไป ดังนั้นงานวิจัยนี้จึงพยายามที่จะศึกษาลึกลงไปผ่าน
การเกิด และความคงตัวของสารสะสมของไขมันเหล่านี้ โดยการเตรียมสบู่ของแคลเซียมที่ได้จาก
เกลือแคลเซียมที่มีความสามารถละลายต่างกัน ร่วมกับไขมันจากหลายแหล่งที่มีสัดส่วน
องค์ประกอบของกรดไขมันแตกต่างกันในระดับห้องปฏิบัติการ แหล่งของแคลเซียมที่ใช้มาจาก
แคลเซียมคลอไรด์และแคลเซียมซัลเฟต ส่วนแหล่งของไขมันและน้ำมันมาจากไก่ หมู ปาล์ม โอลีอิน
ถั่วเหลือง มะกอก และมะพร้าว

จากผลการศึกษาแสดงให้เห็นว่า ปริมาณแคลเซียมเป็นปัจจัยเชิงบวกต่อการเกิดและความคง
ตัวของสบู่ที่ได้ ถึงแม้ว่าสบู่ที่เกิดจากแคลเซียมซัลเฟตจะเกิดการซาปอนนิไฟด์น้อยกว่าสบู่ที่เกิดจาก
แคลเซียมคลอไรด์ แต่ก็ก่อให้เกิดปัญหาการอุดตันในท่อระบายน้ำได้อย่างรวดเร็ว เนื่องจากลักษณะ
ภายนอกที่รวมตัวกันอย่างหลวมๆ ส่วนสบู่ที่ได้จากแคลเซียมคลอไรด์เกิดการซาปอนนิไฟด์สูงกว่า
และเมื่อเกิดการสะสมอยู่ภายในด้านของท่อระบายน้ำทั้งจะเป็นสารสะสมไขมันที่มีจุดหลอมเหลวที่
อุณหภูมิสูง ปัจจัยด้านสัดส่วนของกรดไขมันมีบทบาทสำคัญต่อความคงตัวของสารสะสมไขมัน
เหล่านี้เป็นอย่างมาก ผลรวมของกรดไขมันปาร์เมติก โอเลอิก และลิโนเลอิก ที่มีสัดส่วนเหมาะสม
จะทำให้เกิดสารสะสมไขมันที่เกิดซาปอนนิไฟด์สูง คงตัวต่อความร้อน และต้านทานการไหลได้ดี
สำหรับไขมันจากแหล่งที่แตกต่างกันพบว่า น้ำมันมะพร้าวก่อให้เกิดการอุดตันภายในท่อระบายน้ำ
เร็วกว่าไขมันจากแหล่งอื่น เพราะเกิดเป็นสบู่ได้มากกว่า ส่วนน้ำมันหมูพบว่าเกิดเป็นสารสะสม
ไขมันที่มีจุดหลอมเหลวสูง ความหนืดปรากฏสูง และมีลักษณะคล้ายของแข็งมากกว่าไขมันจาก
แหล่งอื่นๆ จากการตรวจสอบด้วยเทคนิคการหักเหของรังสีเอ็กซ์พบว่า ความคงตัวอุณหภูมิและการ
ต้านทานการไหลของสบู่จากแคลเซียมเหล่านี้มีความเกี่ยวข้องกับโครงสร้างภายในขนาดเล็กที่อัดกัน
แน่น มีลักษณะเป็นแบบผลึก และมีความเป็นรูพรุนน้อย ความคงตัวนี้ยังสัมพันธ์กับการจัดเรียงตัว
กันของโครงสร้างแบบลามลล่าผสม และการเกิดผลึกในระดับสูงภายในโครงสร้าง

DANN MARIE DEL MUNDO : RHEOLOGY AND MICROSTRUCTURE
OF LABORATORY SCALE MODELS OF FAT, OIL, AND GREASE
(FOG) DEPOSITS PREPARED FROM DIFFERENT LIPID AND
CALCIUM SOURCES. THESIS ADVISOR :
ASSOC. PROF. MANOTE SUTHEERAWATTANANONDA, Ph.D.,
138 PP.

FOG DEPOSIT/CALCIUM SOAPS/RHEOLOGY/MELTING/MICROSTRUCTURE/
CRYSTALLINITY

Fat, oil, and grease (FOG) deposit, in the form of calcium soap, was found to cause sanitary sewer overflows due to its adhesion on pipe walls. However, the lipid and calcium sources previously utilized were limited and some soap characteristics were not examined. Hence, this research attempted to probe through the formation and stability of FOG deposits using laboratory-prepared calcium soaps from calcium sources with different solubilities and fats/oils with different fatty acid profiles. Calcium chloride and calcium sulfate were used as the calcium source while the fats and oils of chicken, pork, palm olein, soybean, olive, and coconut were utilized as the lipid source.

Results revealed that the calcium content is a positive indicator of the formation and stability of the soaps. Although less saponified, the calcium sulfate-based soaps are predicted to cause faster sewer blockages due to their bulky appearance, while the highly saponified calcium chloride-based soaps are expected to accumulate on sewer walls due to their higher melting endset. The fatty acid profile also plays a major role

on the stability of FOG deposits. Certain combinations of palmitic, oleic, and linoleic acids generated highly saponified, heat-stable, and flow-resistant FOG deposits. In terms of lipid type, coconut oil is predicted to cause faster sewer blockages as it forms more soaps, whereas pork fat is foreseen to accumulate on pipe walls because it generates soaps with higher melting endset, apparent viscosity, and solid-like characteristics. The higher heat and flow stability of calcium soaps were linked to their tightly-packed, crystal-like, and less porous microstructure. Their stability was also associated with their mixed lamellar structure and higher degree of crystallinity observed through X-ray diffraction technique.

On the whole, the solubility of the calcium source and the fatty acid profile of the lipid source mainly dictate the appearance, melting, rheology, microstructure, and X-ray diffraction of the calcium soaps. The distinct properties of the different calcium soaps would serve as a helpful guide to authorities and institutions in controlling FOG deposit formation and accumulation.

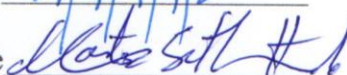
School of Food Technology

Academic Year 2017

Student's Signature



Advisor's Signature



ACKNOWLEDGEMENTS

This endeavor came to fruition through the SUT-PhD Scholarship for ASEAN and University of the Philippines Doctoral Studies Fund.

I am deeply grateful and honored to work with my adviser, Assoc. Prof. Dr. Manote Sutteerawattananonda, who unselfishly imparted his knowledge and expertise in the field of research. His motivation and guidance molded me to become a better version of myself.

I would like to sincerely thank my committee members, Assoc. Prof. Dr. Jirawat Yongsawatdigul, Assist. Prof. Dr. Chareeya Yimrattanabovorn, Dr. Thanawit Kulrattanak, and Assist. Prof. Dr. Siranee Sreesai for their valuable insights and comments in order to improve my manuscript. I would also like to extend my gratitude to my committee members during my thesis proposal, Assist. Prof. Dr. Chantima Deeprasertkul and Assist. Prof. Dr. Panarat Rattanaphanee for their willingness to share their expertise.

I would like express my gratitude to the Synchrotron Light Institute (SLRI), Thailand for allowing me to conduct my ESEM and X-ray diffraction analyses in their facility. I highly appreciate the assistance of Dr. Worawikunya Kiatponglarp and Mr. Anuchit Ruangvittayanon. Special thanks to Dr. Nuntaporn Kamonsutthipaijit for her great contribution in my SAXS and WAXS interpretation and modelling.

I would also like to recognize the staff of the Center for Scientific and Technological Equipment for training me to use their equipment. I sincerely thank my professors for imparting their knowledge, which equipped me to successfully finish

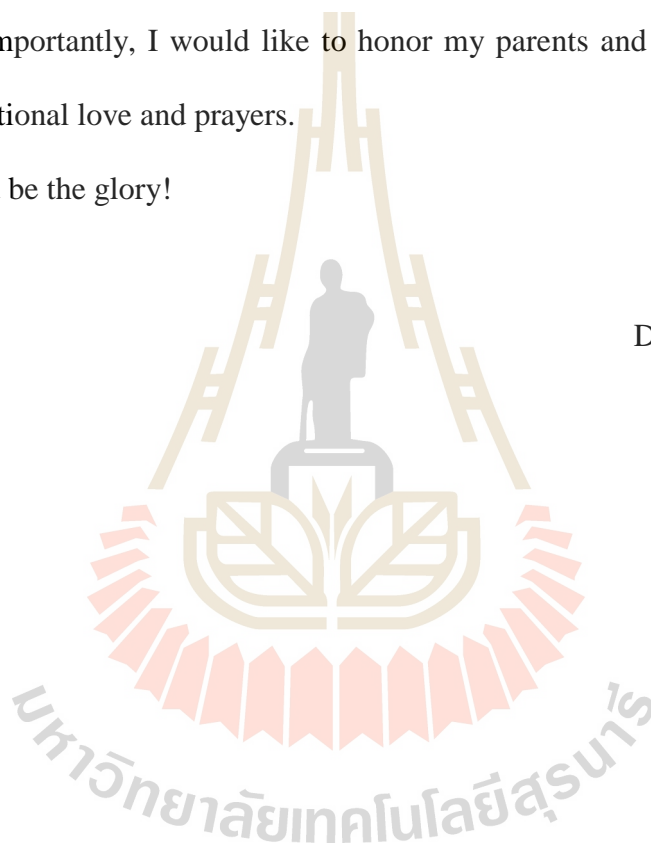
my degree. I am also grateful to my labmates and schoolmates for their kindness and willingness to help.

I would like to acknowledge the assistance of the Center for International Affairs and Center for Library Resources and Educational Media. I am also grateful for the care extended to me by my CFC-SFC family and the Filipino community in Korat. Special mention to Aj. Lilibeth Kantola for treating me like a sister.

Most importantly, I would like to honor my parents and thank my siblings for their unconditional love and prayers.

To God be the glory!

Dann Marie Del Mundo



CONTENTS

| | Page |
|--|-------------|
| ABSTRACT IN THAI..... | I |
| ABSTRACT IN ENGLISH | III |
| ACKNOWLEDGEMENT | V |
| CONTENTS..... | VII |
| LIST OF TABLES | XI |
| LIST OF FIGURES | XIII |
| LIST OF ABBREVIATIONS..... | XXII |
| CHAPTER | |
| I INTRODUCTION | 1 |
| 1.1 Background of the study..... | 1 |
| 1.2 Research objectives of the study | 3 |
| 1.3 Hypotheses of the study | 3 |
| 1.4 Significance of the study | 4 |
| 1.5 Limitation of the study | 5 |
| 1.6 Design route of the study..... | 6 |
| 1.7 Expected results of the study | 9 |
| II LITERATURE REVIEWS | 11 |
| 2.1 Fats and oils production and consumption | 11 |
| 2.2 FOG deposits | 13 |

CONTENTS (Continued)

| | Page |
|---|-----------|
| 2.3 FOG deposit composition..... | 15 |
| 2.3.1 FOG | 16 |
| 2.3.1.1 Description of FOG | 16 |
| 2.3.1.2 Chemical composition of FOG..... | 17 |
| 2.3.1.3 Physical properties of triacylglycerol..... | 18 |
| 2.3.1.4 Sources of FOG | 22 |
| 2.3.2 Fatty acids..... | 23 |
| 2.3.2.1 Chemical composition of fatty acids | 23 |
| 2.3.2.2 Sources of free fatty acids | 25 |
| 2.3.3 Calcium..... | 28 |
| 2.3.3.1 Sources of calcium | 29 |
| 2.4 Formation mechanisms of FOG deposits | 30 |
| 2.5 Confirmatory studies on FOG deposits | 33 |
| 2.5.1 Verification of saponification hypothesis by FTIR analysis | 33 |
| 2.5.1.1 FTIR spectra of FOG deposits and lab- prepared soaps | 34 |
| 2.5.1.2 Properties of FOG deposits and lab- prepared soaps | 42 |
| III MATERIALS AND METHODS | 46 |
| 3.1 Raw materials and chemicals | 46 |

CONTENTS (Continued)

| | Page |
|--|-----------|
| 3.2 Fat rendering..... | 47 |
| 3.3 Production of calcium soaps..... | 47 |
| 3.4 FTIR analysis | 48 |
| 3.5 Fatty acid profiling | 49 |
| 3.6 Calcium content analysis..... | 50 |
| 3.7 Melting endset determination..... | 50 |
| 3.8 Rheological tests..... | 50 |
| 3.8.1 Steady shear characterization | 51 |
| 3.8.2 Oscillatory temperature sweep test..... | 51 |
| 3.9 Microstructure analysis | 52 |
| 3.9.1 ESEM | 52 |
| 3.9.2 CLSM | 52 |
| 3.10 Synchrotron X-ray measurements..... | 53 |
| 3.11 Statistical analysis | 53 |
| IV RESULTS AND DISCUSSION | 54 |
| 4.1 Physical appearance of calcium soaps..... | 54 |
| 4.2 Saponification and yield of calcium soaps..... | 58 |
| 4.2.1 FTIR spectra of raw fats/oils and their calcium soaps..... | 58 |
| 4.2.2 Saponification of calcium soaps..... | 61 |
| 4.2.3 Fatty acid profile of raw fats/oils and their calcium soaps | 64 |

CONTENTS (Continued)

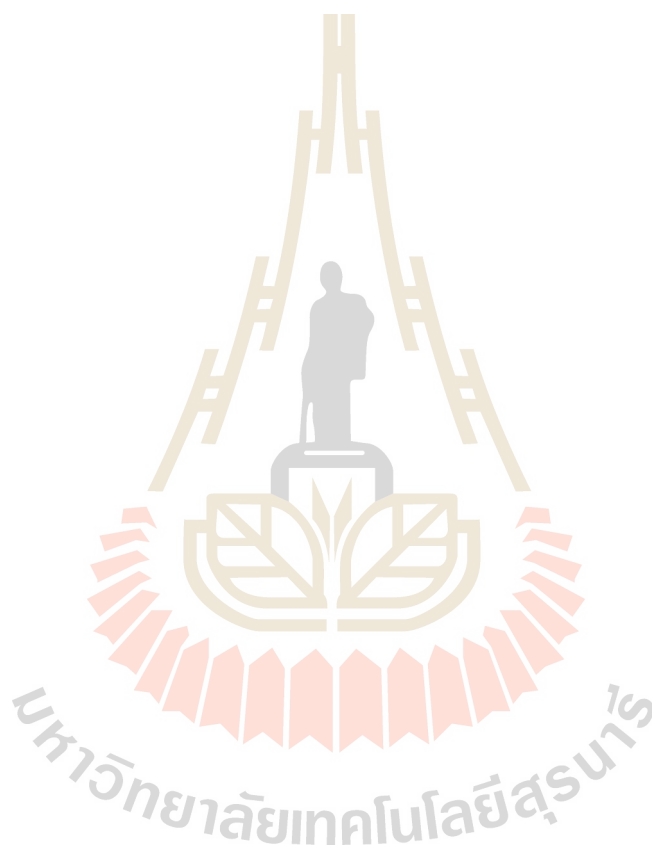
| | Page |
|--|-------------|
| 4.2.4 Yield of calcium soaps | 66 |
| 4.3 Melting endset of raw fats/oils and calcium soaps..... | 69 |
| 4.4 Rheology of calcium soaps..... | 71 |
| 4.4.1 Apparent viscosity | 71 |
| 4.4.2 Viscoelasticity | 75 |
| 4.5 Microstructure of calcium soaps | 83 |
| 4.5.1 ESEM images | 83 |
| 4.5.2 CLSM images | 87 |
| 4.6 X-ray diffraction of calcium soaps | 91 |
| 4.6.1 SAXS diffraction pattern | 91 |
| 4.6.2 WAXS diffraction pattern | 98 |
| 4.7 Correlation of calcium soap composition and physico- chemical properties..... | 101 |
| V CONCLUSION | 104 |
| REFERENCES.. | 106 |
| APPENDIX..... | 131 |
| BIOGRAPHY.. | 138 |

LIST OF TABLES

| Table | Page |
|-------|--|
| 2.1 | 2004/2005 World vegetable oil consumption 12 |
| 2.2 | U.S. fats and oils per capita consumption 12 |
| 2.3 | Annual production of oils and fats (million tonnes) in the years 1998-2002 ... 13 |
| 2.4 | Major compositions of FOG deposits from various sewer lines..... 16 |
| 2.5 | Melting points of triglycerides 19 |
| 2.6 | Melting point of oils and animal fats 20 |
| 2.7 | Systematic, common, and numerical names for fatty acids found in foods 24 |
| 2.8 | Major fatty acid composition of oils and animal fats..... 26 |
| 2.9 | Comparisons of observed wave frequencies among calcium soaps 39 |
| 4.1 | Major fatty acid composition of raw fats/oils and their calcium soaps 64 |
| 4.2 | Summary of the viscoelastic properties of calcium soaps under oscillatory temperature sweep test 81 |
| 4.3 | SAXS data of soaps prepared from calcium chloride and various fat/oil sources..... 94 |
| 4.4 | SAXS data of soaps prepared from calcium sulfate and various fat/oil sources..... 95 |
| 4.5 | Significant correlations between the physico-chemical properties and composition of calcium soaps 102 |

LIST OF TABLES (Continued)

| Table | | Page |
|--------------|--|-------------|
| 4.6 | Significant correlations among the physico-chemical properties of calcium soaps..... | 103 |



LIST OF FIGURES

| Figure | Page |
|--------|---|
| 1.1 | Flow diagram of the research procedure..... 10 |
| 2.1 | FOG deposit turning into a “fatberg” in the sewer system 14 |
| 2.2 | Flow diagram of cassava starch manufacturing process 15 |
| 2.3 | A triglyceride molecule from the reaction of glycerol and fatty acids 17 |
| 2.4 | Proposed mechanism for nucleation of triacylglycerols (TAGs).....21 |
| 2.5 | Structural hierarchy in colloidal fat crystal networks21 |
| 2.6 | Formation of diacylglycerols and fatty acids during triacylglycerol hydrolysis27 |
| 2.7 | Simplified scheme of thermal oxidation of triacylglycerol28 |
| 2.8 | Concrete corrosion induced by the sulfur cycle.....29 |
| 2.9 | Mechanisms of FOG deposit formation in the sewer system31 |
| 2.10 | Saponification reaction in the sewer system.....32 |
| 2.11 | FTIR spectra of sewer and lab samples: (a) FOG deposits from the sewer; (b) lab-prepared FOG deposits; and (c) calcium chloride-based canola oil soap.....35 |
| 2.12 | FTIR spectra of the solids recovered from the saponification set-up: (a) suspended brown particles; (b) white solid at the bottom of the beaker; (c) white solid on concrete surface.....36 |
| 2.13 | FTIR spectra of the solids on concrete with the addition of fatty acids.....36 |

LIST OF FIGURES (Continued)

| Figure | Page |
|--------|--|
| 2.14 | FTIR spectra of soybean oil and solid samples from the reaction of calcium chloride and soybean oil under different pH conditions: (a) pH=9; (b) pH=8; (c) no pH adjustment; (d) pure oil27 |
| 2.15 | Kinetics of calcium-based saponified solids at pH 10 with varying types of fat/oil, calcium forms, and temperatures41 |
| 2.16 | Kinetics of calcium-based saponified solids at pH 14 with varying types of fat/oil, calcium forms, and temperatures41 |
| 2.17 | Shear stress dependence of FOG deposit sub-samples from a manhole beside a pizza restaurant, under oscillation stress sweep of 0.1-100 Pa, $\omega=10$ Hz, and gap of 2 mm: (a) sub-sample 1; (b) sub-sample 243 |
| 2.18 | Shear stress dependence of calcium chloride-based canola oil soaps at pH 10, 22°C, $\omega=10$ Hz, and gap of 1 mm: (a) analysis 1; (b) analysis 244 |
| 2.19 | Shear stress dependence of calcium sulfate-based canola oil soaps at pH 10, 22°C, $\omega=10$ Hz, and gap of 1 mm: (a) analysis 1; (b) analysis 245 |
| 4.1 | A typical calcium soap fraction after centrifugation: (a) excess oil; (b) calcium soap from the second layer; (c) calcium soap from the third layer Secreted metabolites from <i>Lactobacillus</i> sp. 21C2-10 (SML) inhibited55 |

LIST OF FIGURES (Continued)

| Figure | Page |
|---|-------------|
| <p>4.2 Physical appearance of the soaps prepared from calcium chloride and various fat/oil sources (PO = palm olein oil; SO = soybean oil; OO = olive oil; CO = coconut oil; CF = chicken fat; PF = pork fat; the numbers indicate the layer the soaps were taken from the centrifuged mixture: 2= 2nd layer; 3= 3rd layer)</p> | 56 |
| <p>4.3 Physical appearance of the soaps prepared from calcium sulfate and various fat/oil sources (PO = palm olein oil; SO = soybean oil; OO = olive oil; CO = coconut oil; CF = chicken fat; PF = pork fat; the numbers indicate the layer the soaps were taken from the centrifuged mixture: 2= 2nd layer; 3= 3rd layer)</p> | 57 |
| <p>4.4 FTIR spectra of the raw fats/oils and excess fats/oils from saponification reaction: (a) raw fats/oils; (b) excess fats/oils from calcium chloride mixture; (c) excess fats from calcium sulfate mixture (PO = palm olein oil; SO = soybean oil; OO = olive oil; CO = coconut oil; CF = chicken fat; PF = pork fat).....</p> | 58 |
| <p>4.5 FTIR spectra of the calcium soaps taken from the second layer of the centrifuged mixture: (a) calcium chloride source; (b) calcium sulfate source (PO = palm olein oil; SO = soybean oil; OO = olive oil; CO = coconut oil; CF = chicken fat; PF = pork fat)</p> | 60 |

LIST OF FIGURES (Continued)

| Figure | Page |
|---|-------------|
| 4.6 FTIR spectra of the calcium soaps taken from the third layer of the centrifuged mixture: (a) calcium chloride source; (b) calcium sulfate source (PO = palm olein oil; SO = soybean oil; OO = olive oil; CO = coconut oil; CF = chicken fat; PF = pork fat) | 61 |
| 4.7 Percent saponification of the soaps prepared from different fat/oil and calcium sources (PO = palm olein oil, SO = soybean oil, OO = olive oil, CO = coconut oil, CF = chicken fat, PF = pork fat; the numbers indicate the layer the soaps were taken from the centrifuged mixture: 2= 2 nd layer; 3= 3 rd layer)..... | 63 |
| 4.8 Calcium content of the soaps prepared from different fat/oil and calcium sources (PO = palm olein oil, SO = soybean oil, OO = olive oil, CO = coconut oil, CF = chicken fat, PF = pork fat; the numbers indicate the layer the soaps were taken from the centrifuged mixture: 2= 2 nd layer; 3= 3 rd layer) | 63 |
| 4.9 Percent yield of the soaps prepared from different fat/oil and calcium sources (PO = palm olein oil, SO = soybean oil, OO = olive oil, CO = coconut oil, CF = chicken fat, PF = pork fat; the numbers indicate the layer the soaps were taken from the centrifuged mixture: 2= 2 nd layer; 3= 3 rd layer)..... | 67 |

LIST OF FIGURES (Continued)

| Figure | Page |
|--|-------------|
| 4.10 FOG deposit layering: (a) proposed mechanism for FOG deposit layering; (b) FOG deposit layering observed in the sewer (Keener et al., 2008) | 69 |
| 4.11 Melting endset of the raw fats/oils and their calcium soaps (PO = palm olein oil, SO = soybean oil, OO = olive oil, CO = coconut oil, CF = chicken fat, PF = pork fat; the numbers indicate the layer the soaps were taken from the centrifuged mixture: 2= 2 nd layer; 3= 3 rd layer) | 70 |
| 4.12 Apparent viscosity (η) curves at 25°C of calcium soaps prepared from various fats/oils: (a) calcium chloride; (b) calcium sulfate (PO = palm olein oil; SO = soybean oil; OO = olive oil; CO = coconut oil; CF = chicken fat; PF = pork fat; the numbers indicate the layer the soaps were taken from the centrifuged mixture: 2= 2 nd layer; 3= 3 rd layer) | 73 |
| 4.13 Apparent viscosity (η_{100} at 25°C) of the soaps prepared from different fat/oil and calcium sources (PO = palm olein oil, SO = soybean oil, OO = olive oil, CO = coconut oil, CF = chicken fat, PF = pork fat; the numbers indicate the layer the soaps were taken from the centrifuged mixture: 2= 2 nd layer; 3= 3 rd layer) | 74 |

LIST OF FIGURES (Continued)

| Figure | Page |
|--|------|
| 4.14 Temperature stress dependence of the soaps prepared from calcium chloride and various fats/oils (PO = palm olein oil; SO = soybean oil; OO = olive oil; CO = coconut oil; CF = chicken fat; PF = pork fat; the numbers indicate the layer the soaps were taken from the centrifuged mixture: 2= 2 nd layer; 3= 3 rd layer) | 79 |
| 4.15 Temperature stress dependence of the soaps prepared from calcium sulfate and various fats/oils (PO = palm olein oil; SO = soybean oil; OO = olive oil; CO = coconut oil; CF = chicken fat; PF = pork fat; the numbers indicate the layer the soaps were taken from the centrifuged mixture: 2= 2 nd layer; 3= 3 rd layer) | 80 |
| 4.16 Tan δ of the soaps at 25°C prepared from different fat/oil and calcium sources (PO = palm olein oil, SO = soybean oil, OO = olive oil, CO = coconut oil, CF = chicken fat, PF = pork fat; the numbers indicate the layer the soaps were taken from the centrifuged mixture: 2= 2 nd layer; 3= 3 rd layer) | 82 |
| 4.17 ESEM image (5000x, 20 μ m) of the soaps prepared from calcium chloride and various fat/oil sources (PO = palm olein oil; SO = soybean oil; OO = olive oil; CO = coconut oil; CF = chicken fat; PF = pork fat; the numbers indicate the layer the soaps were taken from the centrifuged mixture: 2= 2 nd layer; 3= 3 rd layer) | 84 |

LIST OF FIGURES (Continued)

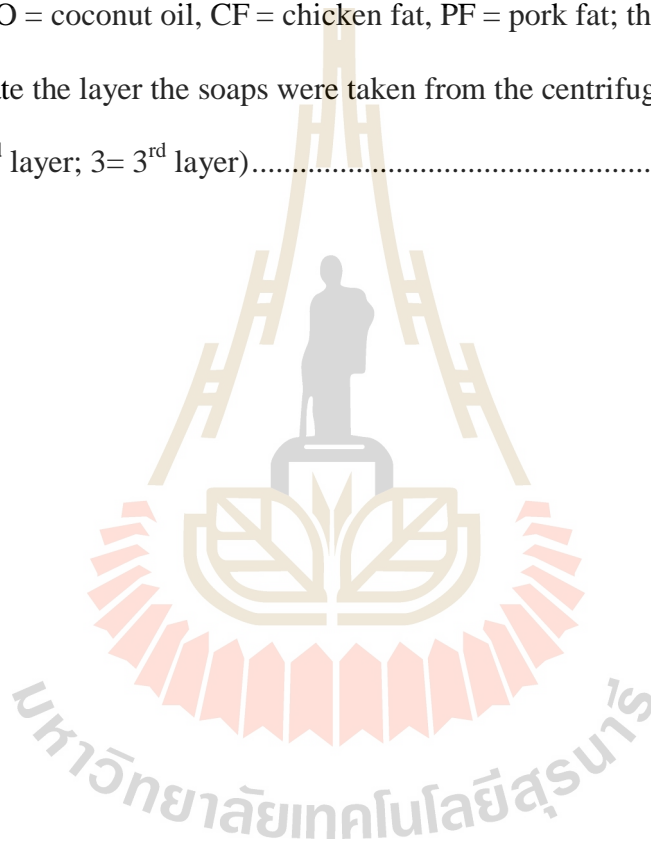
| Figure | Page |
|---|-------------|
| 4.18 ESEM image (5000x, 20 μ m) of the soaps prepared from calcium sulfate and various fat/oil sources (PO = palm olein oil; SO = soybean oil; OO = olive oil; CO = coconut oil; CF = chicken fat; PF = pork fat; the numbers indicate the layer the soaps were taken from the centrifuged mixture: 2= 2 nd layer; 3= 3 rd layer) | 86 |
| 4.19 CLSM 3-D image of the soaps prepared from calcium chloride and various fat/oil sources soaps (PO = palm olein oil; SO = soybean oil; OO = olive oil; CO = coconut oil; CF = chicken fat; PF = pork fat; the numbers indicate the layer the soaps were taken from the centrifuged mixture: 2= 2 nd layer; 3= 3 rd layer) | 88 |
| 4.20 CLSM 3-D image of the soaps prepared from calcium sulfate and various fat/oil sources soaps (PO = palm olein oil; SO = soybean oil; OO = olive oil; CO = coconut oil; CF = chicken fat; PF = pork fat; the numbers indicate the layer the soaps were taken from the centrifuged mixture: 2= 2 nd layer; 3= 3 rd layer) | 89 |
| 4.21 Percent void of the soaps prepared from different fat/oil and calcium sources (PO = palm olein oil, SO = soybean oil, OO = olive oil, CO = coconut oil, CF = chicken fat, PF = pork fat; the numbers indicate the layer the soaps were taken from the centrifuged mixture: 2= 2 nd layer; 3= 3 rd layer)..... | 90 |

LIST OF FIGURES (Continued)

| Figure | Page |
|--|-------------|
| 4.22 Void circularity of the soaps prepared from different fat/oil and calcium sources (PO = palm olein oil, SO = soybean oil, OO = olive oil, CO = coconut oil, CF = chicken fat, PF = pork fat; the numbers indicate the layer the soaps were taken from the centrifuged mixture: 2= 2 nd layer; 3= 3 rd layer)..... | 90 |
| 4.23 SAXS diffraction patterns of the calcium soaps prepared from various fats/oils: (a) calcium chloride; (b) calcium sulfate (PO = palm olein oil; SO = soybean oil; OO = olive oil; CO = coconut oil; CF = chicken fat; PF = pork fat; the numbers indicate the layer the soaps were taken from the centrifuged mixture: 2= 2 nd layer; 3= 3 rd layer)..... | 92 |
| 4.24 Proposed lamellar plane models of the calcium soaps from various fat/oil sources: (a) uniform lamellar plane; (b) mixed lamellar planes; (c) distributed lamellar plane | 97 |
| 4.25 WAXS diffraction patterns of calcium soaps prepared from various fats/oils: (a) calcium chloride; (b) calcium sulfate (PO = palm olein oil; SO = soybean oil; OO = olive oil; CO = coconut oil; CF = chicken fat; PF = pork fat; the numbers indicate the layer the soaps were taken from the centrifuged mixture: 2= 2 nd layer; 3= 3 rd layer) | 99 |

LIST OF FIGURES (Continued)

| Figure | Page |
|--|-------------|
| <p>4.26 Percent crystallinity of soaps prepared from different fat/oil and calcium sources (PO = palm olein oil, SO = soybean oil, OO = olive oil, CO = coconut oil, CF = chicken fat, PF = pork fat; the numbers indicate the layer the soaps were taken from the centrifuged mixture: 2= 2nd layer; 3= 3rd layer).....</p> | 100 |



LIST OF ABBREVIATIONS

| | | |
|---------|---|---|
| ANOVA | = | Analysis of variance |
| ATR | = | Attenuated reflectance |
| BSR | = | Business for Social Responsibility |
| CF | = | Chicken fat |
| CLSM | = | Confocal laser scanning microscope |
| CO | = | Coconut oil |
| DAWR | = | Department of Agriculture and Water Resources (Australia) |
| DI | = | Deionized |
| DLVO | = | Derjaguin, Landau, Verwey, and Overbeek |
| DSC | = | Differential scanning calorimetry |
| EPA | = | Environmental Protection Agency |
| EPD | = | Environmental Protection Department (Hong Kong) |
| FAO | = | Food and Agriculture Organization |
| FAs | = | Fatty acids |
| FFAs | = | Free fatty acids |
| FOG | = | Fat, oil, and grease |
| FSEs | = | Food service establishments |
| FTIR | = | Fourier-transform infrared spectroscopy |
| GC-FID | = | Gas chromatography-flame ionization detector |
| ICP-OES | = | Inductively coupled plasma optical emission spectrometry |
| MICC | = | Microbiologically induced concrete corrosion |

LIST OF ABBREVIATIONS (Continued)

| | | |
|-------|---|---|
| MUFAs | = | Mono-unsaturated fatty acids |
| NEA | = | National Environment Agency (Singapore) |
| OO | = | Olive oil |
| PF | = | Pork fat |
| PO | = | Palm olein oil |
| PUFAs | = | Polyunsaturated fatty acids |
| SAXS | = | Small angle X-ray scattering |
| SEM | = | Scanning electron microscope |
| SFA | = | Saturated fatty acid |
| SFAs | = | Saturated fatty acids |
| SFC | = | Solid fat content |
| SLRI | = | Synchrotron Light Research Institute |
| SO | = | Soybean oil |
| SPSS | = | Statistical Package for the Social Sciences |
| SSOs | = | Sanitary sewer overflows |
| UFA | = | Unsaturated fatty acid |
| WAXS | = | Wide angle X-ray scattering |
| WEPA | = | Water Environment Partnership in Asia |
| WCHD | = | Washtenaw County Health Department (Michigan) |

CHAPTER I

INTRODUCTION

1.1 Background of the study

The global trend in fat and oil consumption has already changed as oil-processed foods are more in demand and oil mills and refineries are expanding (Alade et al., 2011). The predicted world consumption of fats/oils in 2017/2018 is estimated at 226 million tonnes, entailing a year-on-year growth of around 3% (FAO, 2017). This development is linked to elevated fat, oil, and grease (FOG) wastes, which primarily come from domestic, commercial, and industrial sources (Arthur and Blanc, 2013; Husain et al., 2014). FOG has the ability to solidify and adhere to the surface of the pipes and can hold other solid wastes to form into a “fatberg” that hinders the smooth flow of wastewater in the sewer system (Wallace et al., 2016). In fact, FOG deposition had caused around 50% and 75% of sewer blockages in the US and UK, correspondingly (EPA, 2004; Mills, 2010). This can be translated to an annual additional maintenance and rehabilitation cost of \$25 billion and £15 million for the US and UK, respectively (Mills, 2010; WCHD, 2018).

Keener et al. (2008) categorized FOG deposits as metallic salts of fatty acids, accumulated lipid wastes, and misidentified mineral deposits. It was hypothesized that FOG deposits were formed through saponification and aggregation of unreacted calcium and free fatty acids in the sewer environment (He et al., 2013; He et al., 2011; Keener et al., 2008). The free fatty acid is a product of chemical and microbial

hydrolysis of oil (Iasmin et al., 2014; Keener et al., 2008; Williams et al., 2012), while the available calcium is a result of water hardness, concrete corrosion, and microbial reactions (He et al., 2013; He et al., 2011; Williams et al., 2012). Saponification occurs when free fatty acids react with the positively charged calcium ions to form calcium-based fatty acid salts (He et al., 2011). The high pH condition needed for saponification is provided by the alkaline detergents, degreasers, and sanitizers typically used in food service establishments (FSEs) (Keener et al., 2008).

Previous studies produced laboratory-prepared calcium soaps under different conditions to investigate the FOG deposit formation mechanism in the sewer system. He et al. (2013) scrutinized the roles of palmitic, oleic, and linoleic acids on saponification reaction and found out that palmitic acid led to faster soap formation, while oleic acid resulted in higher amounts of solids formed. They also revealed that harder deposits were formed with highest oleic to palmitic acid ratio. On the other hand, Iasmin et al. (2014) and Iasmin et al. (2016) studied the roles of fat/oil type, calcium source, pH, and temperature on FOG formation kinetics. Based on their results, saponification was greater with oil and calcium sulfate and it was facilitated at higher pH and temperature.

The existing researches on laboratory-prepared FOG deposits mainly focused on calcium chloride-based soaps from canola oil and beef tallow, which are not commonly consumed and highly produced worldwide. Although calcium chloride is a known food additive (García et al., 1996; Madani et al., 2016) and agent for wastewater treatment (AlMubaddal et al., 2009; Ren et al., 2016), past investigations hinted that the calcium ions in the sewer system primarily come from microbiologically induced concrete corrosion (MICC), which generates calcium

sulfate (Gu et al., 2015; He et al., 2013; Iasmin et al., 2016; Iasmin et al., 2014). Therefore, it is worthwhile to conduct a comprehensive evaluation on the characteristics of the soaps produced from both calcium chloride and calcium sulfate in order to determine the effect of calcium source solubilities on FOG deposit formation and properties. It is also more realistic to utilize various fats and oils in the soap formation since they represent different types of lipid wastes with varying fatty acid composition.

1.2 Research objectives of the study

The main objective of this study was to investigate the influence of fat/oil type and calcium sources on the formation and stability of FOG deposits.

The specific objectives were as follows:

1. To calculate the degree of saponification and yield of the calcium soaps.
2. To evaluate the physico-chemical properties of the soaps such as calcium content, fatty acid profile, melting endset, viscosity, viscoelasticity, and crystallinity.
3. To determine the microstructure and lamellar phase structure of the calcium soaps.

1.3 Hypothesis of the study

It was predicted that calcium soaps produced from fats/oils with different fatty acid profile and calcium source solubilities would represent a certain type of FOG deposit with different characteristics and stability.

The specific hypotheses were as follows:

1. The more soluble calcium chloride would produce calcium soaps with

higher yield and degree of saponification than the less soluble calcium sulfate.

2. The highly saturated fats and oils would generate calcium soaps that are more heat-stable, flow-resistant, and solid-like.

3. The heat and rheological stability of calcium soaps are associated with their microstructure and X-ray diffraction pattern.

1.4 Significance of the study

Previous works on FOG deposit formation mainly focused on calcium chloride soaps produced from canola oil and beef tallow, which may not sufficiently represent the FOG deposits in the sewer system. Therefore, this research included calcium sulfate, a known product of concrete corrosion, as another type of calcium source. Moreover, the fats and oils of palm olein, soybean, olive, coconut, chicken, and pork were also considered for saponification to cover the lipid sources with different fatty acid profiles.

In the past studies, the assessed properties of the calcium soaps were also limited, which may not comprehensively describe the stability of FOG deposits. Thus, this study advanced the understanding of FOG deposit characteristics with the inclusion of steady shear characterization, oscillatory temperature sweep, microstructure, Small Angle X-ray Scattering (SAXS) and Wide Angle X-ray Scattering (WAXS) analyses. To the extent of our knowledge, this research undertaking pioneered the incorporation of these parameters in evaluating the stability of FOG deposits.

In this work, the properties evaluated were physical appearance, saponification, yield, fatty acid profile, calcium content, melting endset, apparent viscosity, viscoelasticity, microstructure, lamellar phase structure and crystallinity. Determining

the yield of the soaps from different fat/oil and calcium sources could give information which kind of fat/oil-calcium source combination may produce the greatest amount of FOG deposit; while evaluating their other properties could reveal their specific identity and stability. Particularly, the melting endset may depict the peak temperature at which the FOG deposits will eventually destabilize in the sewer system, whereas the rheological behavior may illustrate the resistance to flow and rigidity of the FOG deposits under sewer conditions. The soap composition and quantifiable properties were subjected to correlation analysis to identify their significant influence on FOG deposit formation and stability.

The data gathered in this study may help determine the risk and seriousness of FOG deposits formed from different types of fat/oil and calcium sources. Particularly, the results may disclose the fat/oil-calcium source combination that can produce a large amount and highly stable FOG deposit. Therefore, the outcome of this research can be a helpful guide to establishments and authorities in marking the possible FOG deposit hotspots based on their production or usage of a particular fat/oil and exposure to different calcium sources. This would also allow them to plan more effective control and preventive measures for FOG deposits.

1.5 Limitation of the study

In the actual sewer environment, the composition of FOG deposits is dependent on the cooking/production activities of the household, food service establishments, and industries (Arthur and Blanc, 2013; He et al., 2017; Husain et al., 2014). However, based on previous investigations, the major components of FOG deposits in the sewer system are fats/oils, fatty acids, and calcium (Keener et al., 2008; Montefrio et al.,

2010; He et al., 2011; Williams et al., 2012; Husain et al., 2014). Hence, this study focused on utilizing different fats/oils and calcium sources to produce calcium soaps, which served as models of FOG deposits. Unlike the FOG deposits on site, the laboratory-prepared FOG deposits were made from uncooked or unprocessed fats and oils. They were also free from other wastes and compounds typically found in the sewer. These conditions were considered to initially and clearly establish the profile of FOG deposits from different fats/oils. Moreover, the formulation of Iasmin et al. (2014), which had a fixed quantity of calcium source, was employed to produce the soaps. This was followed in order to know the effects of calcium source solubility limit on the yield and characteristics of the resulting soaps. In addition, compared to commercial soaps that are normally created at higher temperatures (100-115°C) (Iasmin et al., 2014; Poulenat et al., 2003), this study employed a lower temperature-based saponification process (He et al., 2011, He et al., 2013; Iasmin et al., 2014). This was done in order to closely mimic the temperature of a sewer environment, which only ranges from 5-25°C.

1.6 Design route of the study

To produce different FOG deposit models in the form of calcium soaps, this study used six kinds of fats/oils and two types of calcium compounds. The fats/oils were palm olein, soybean, olive, coconut, chicken, and pork, while the calcium sources were calcium chloride and calcium sulfate. The vegetable oils were directly used for saponification reaction, whereas the animal fats were produced by initially rendering the adipose tissues of chicken and pork according to the method of Rohman

and Che Man (2011), with some modifications. As previously mentioned, Calcium soaps were produced using the formulation of Iasmin et al. (2014).

This study employed a number of tests to establish the identity and properties of the different calcium soaps. The analyses are briefly described below while details of each method are elaborated in Chapter III. The flow diagram of the research procedure is presented in Figure 1.1.

1. Saponification

The solids as well as the excess lipid recovered from the centrifuged mixture underwent FTIR analysis to verify their identity and determine the efficiency of the saponification process. The characteristic soap bands were recorded and the percent saponification was calculated following the equation of Iasmin et al. (2014).

2. Yield

The solids or the crude soaps recovered from the centrifuged mixture were weighed to calculate the percent yield of the calcium soaps.

3. Fatty acid profiling

The fatty acid composition of the raw fats/oils and their soaps was evaluated to ascertain the influence of carbon chain length and unsaturation on the properties of the calcium soaps. The fatty acid profile was determined following the method of Panpipat and Yongsawatdigul (2008), with some modifications.

4. Calcium content analysis

The calcium content of the soaps was evaluated to uncover how the calcium source solubilities affected the saponification and stability of the soaps. The calcium content of the soaps was analyzed using the method of Trampitsch (2009).

5. Melting endset analysis

The melting endset of the raw fats/oils and their corresponding soaps was determined in order to clarify the effect of saponification on the melting profile of the soaps. The melting endset serves as an indicator of the heat stability of FOG deposits in the sewer environment. The analysis was undertaken using the procedure of Tiekou Nassu and Guaraldo Gonçalves (1995).

6. Rheological tests

The calcium soaps were subjected to rheological tests such as steady shear characterization and oscillatory temperature sweep to respectively record their apparent viscosity and viscoelasticity. These parameters describe the resistance to flow and rigidity of the FOG deposits in the sewer environment. The steady shear characterization was analyzed applying the method of Ikhu-Omoregbe and Bushi (2008).

7. Microstructure analysis

The microstructure of the calcium soaps was observed under Environmental Scanning Electron Microscope (ESEM) and Confocal Laser Scanning Microscope (CLSM). ESEM has the ability to show the structural networks and aggregation of the soaps, while CLSM has the capacity to reveal the porosity and void circularity of the soaps. The samples viewed through CLSM were particularly prepared following the procedure of Wu et al., (2013), with some modifications.

8. Synchrotron X-ray analyses

The SAXS and WAXS X-ray diffraction patterns of the soaps were recorded in order to identify their structural phase and crystallinity, correspondingly. The data

were analyzed using SAXSIT version 4.34 developed by Rugmai and Soontaranon (2017).

9. Statistical Tests

One-way Analysis of Variance (ANOVA) together with Tukey Post Hoc Test was employed to statistically establish the differences of each quantifiable soap property among the fat/oil-calcium combinations. Pearson Correlation was also used to identify the factors that have significant correlations.

1.7 Expected results of the study

Based on the different analyses involved in this study, the expected results were as follows:

1. To establish the infrared spectra, fatty acid, and melting endset profiles of raw fats/oils and their corresponding calcium soaps.
2. To determine the efficiency of the saponification reaction on each fat/oil-calcium source combination based on percent saponification.
3. To characterize the calcium soaps based on their heat stability, rheology, microstructure, lamellar phase structure, and crystallinity.

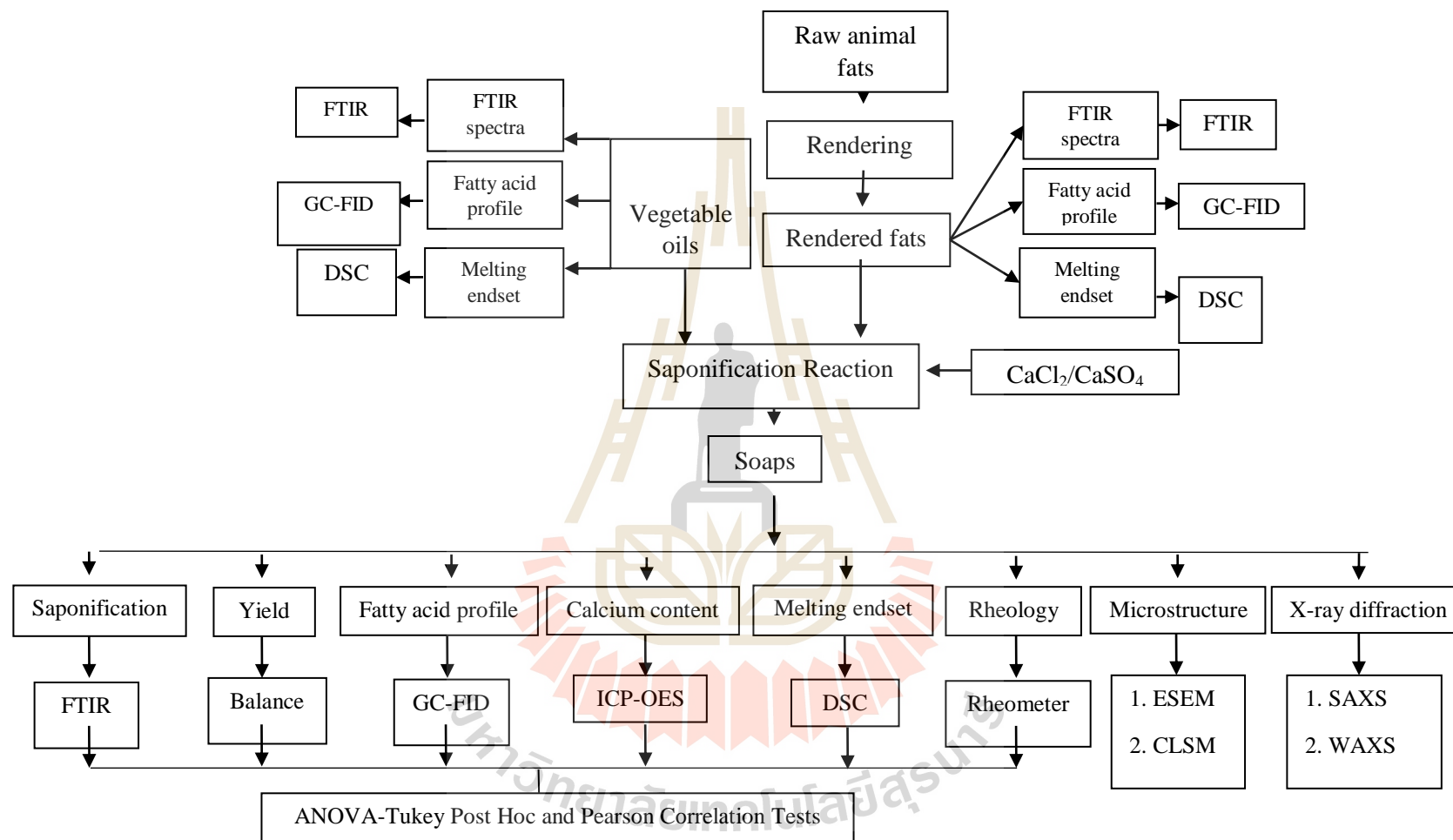


Figure 1.1 Flow diagram of the research procedure.

CHAPTER II

LITERATURE REVIEWS

2.1 Fats and oils production and consumption

Climate and resource availability influence the eating habits of people from different continents. People from central and northern Europe acquire their edible fats from animals; thus, they utilize solid fats, such as butter, lard, and tallow in their pastry and fried products. Whereas, people in southern Europe, Asia, and Africa obtain their edible oils from vegetable sources; hence, their food products, which are usually sauces and dressings, are cooked from liquid oil. On the other hand, fat/oil technology has made the United States a consumer of almost every available fat and oil in the form of cooking or salad oil, butter, margarine, spreads, and shortenings (O' Brein, 2009).

Palm oil and soybean oil are the leading oils consumed worldwide (Table 2.1). In the US alone, there is a consistent increase in vegetable oil consumption from 1950-2005 (Table 2.2), although animal consumption gradually declined in the same years (O' Brein, 2009). According to the recent report of FAO (2017), soybean and palm oil are still projected to be the highly consumed oil commodity with 57% consumption growth. Overall, the predicted world consumption of fats/oils in 2017/2018 is estimated at 226 million tonnes, entailing a year-on-year growth of around 3%. The high demand for soybean and palm oil is reflected in their production pattern. From 1998-2002, soybean oil was highly produced worldwide followed by palm olein oil. In the case of animal fats, tallow was highly produced followed by lard (Table 2.3) (Gunstone, 2004). For

2017/2018, FAO (2017) forecasted that the global fat/oil production will continue to expand reaching 226.5 million tonnes.

Table 2.1 2004/2005 World vegetable oil consumption (O' Brein, 2009).

| Rank order | With U.S. usage | | Without U.S. usage | | Consumption, % | |
|---------------|-------------------|----------------|--------------------|----------------|----------------|--------|
| | Oil | Million lbs | Oil | Million lbs | U.S. | World* |
| 1 | Palm | 72,292 | Palm | 71,039 | 4.7 | 33.1 |
| 2 | Soybean | 69,828 | Soybean | 51,873 | 67.8 | 24.2 |
| 3 | Canola | 34,474 | Canola | 32,569 | 7.2 | 15.2 |
| 4 | Sunflower | 18,678 | Sunflower | 18,319 | 1.4 | 8.5 |
| 5 | Peanut | 11,088 | Peanut | 10,817 | 1 | 5.1 |
| 6 | Cottonseed | 10,098 | Cottonseed | 9,238 | 3.3 | 4.3 |
| 7 | Palm kernel | 8,316 | Palm kernel | 7,787 | 2 | 3.6 |
| 8 | Coconut | 7,260 | Coconut | 6,134 | 4.3 | 2.9 |
| 9 | Olive | 6,270 | Olive | 5,756 | 1.9 | 2.7 |
| 10 | Corn ^a | 2,483 | Corn | 798 | 6.4 | 0.4 |
| | Total | 240,787 | | 214,330 | 100 | 100 |

*without US consumption

Table 2.2 U.S. fats and oils per capita consumption (O' Brein, 2009).

| Consumption | Pounds per person | | | | | | |
|----------------|-------------------|------|------|------|------|------|------|
| | 1950 | 1960 | 1970 | 1980 | 1990 | 2000 | 2005 |
| Vegetable oils | 24 | 26.7 | 39 | 44.7 | 52.5 | 63 | 75.2 |
| Animal fats | 21.9 | 18.5 | 14.1 | 12.3 | 8.5 | 10.2 | 10.4 |
| Total | 45.9 | 45.3 | 53.1 | 57 | 61 | 73.2 | 85.6 |

Table 2.3 Annual production of oils and fats (million tonnes) in the years 1998-2002 (Gunstone, 2004).

| Commodity | Year | | | | |
|---------------------------|-------|-------|-------|-------|-------|
| | 1998 | 1999 | 2000 | 2001 | 2002 |
| Four major oils | | | | | |
| Soybean | 24.01 | 24.78 | 25.53 | 27.79 | 29.75 |
| Palm | 17.15 | 20.62 | 21.87 | 23.92 | 25.03 |
| Rapeseed | 12.29 | 13.21 | 14.47 | 13.69 | 13.33 |
| Sunflower | 8.41 | 9.29 | 9.7 | 8.14 | 7.61 |
| Nine minor vegetable oils | | | | | |
| Cottonseed | 4.06 | 3.9 | 3.87 | 4.05 | 4.18 |
| Groundnut | 4.5 | 4.7 | 4.55 | 5.06 | 5.3 |
| Sesame | 0.71 | 0.69 | 0.71 | 0.74 | 0.83 |
| Corn | 1.87 | 1.93 | 1.97 | 1.96 | 2.02 |
| Olive | 2.59 | 2.47 | 2.54 | 2.76 | 2.66 |
| Palmkernel | 2.19 | 2.56 | 2.69 | 2.93 | 3 |
| Coconut | 3.15 | 2.4 | 3.28 | 3.51 | 3.11 |
| Linseed | 0.69 | 0.73 | 0.7 | 0.65 | 0.63 |
| Castor | 0.44 | 0.43 | 0.5 | 0.51 | 0.44 |
| Four animal oils and fats | | | | | |
| Butter | 5.76 | 5.92 | 6.04 | 6.1 | 6.3 |
| Lard | 6.52 | 6.62 | 6.67 | 6.72 | 6.91 |
| Tallow | 7.81 | 8.17 | 8.19 | 8.15 | 8.4 |
| Fish | 0.89 | 1.41 | 1.42 | 1.13 | 0.97 |
| Total | 103 | 109.9 | 114.7 | 117.8 | 120.5 |

2.2 Probiotics

The consumption of fats and oils is linked to elevated fat, oil, and grease (FOG) waste in the sewer system. FOG, a by-product of food processing, restaurant, and household activities (Arthur and Blanc, 2013; He et al., 2017; Husain et al., 2014), has the tendency to reach into the sewer if not disposed properly (He et al., 2011; Husain et al.,

2014; Keener et al., 2008; Montefrio et al., 2010; Williams et al., 2012). FOG wastes from multiple point sources are prone to accumulate in the sewer and form into FOG deposit, which eventually becomes a “fatberg” when non-flushable wastes are attached to it (Wallace et al., 2016) (Figure 2.1). In September 2017, Thames Water discovered one of the biggest “fatbergs” ever seen in London. It measured more than 800 feet long, which is more than twice the length of two football pitches. It also weighed around 130 metric tonnes, which is similar to the weight of 11 double-decker buses (Figure 2.2) (Osborne, 2017). The detrimental consequences of FOG deposit range from an isolated case of clogged domestic pipe to a temporary closure of a sewer system due to complete blockage and sanitary sewer overflows (SSOs) (Wallace et al., 2016). Aside from the costly and laborious rehabilitation requirements, these occurrences pose a threat to public health and environment (He et al., 2013).



Figure 2.1 FOG deposit turning into a “fatberg” in the sewer system (Thames Water, 2017).

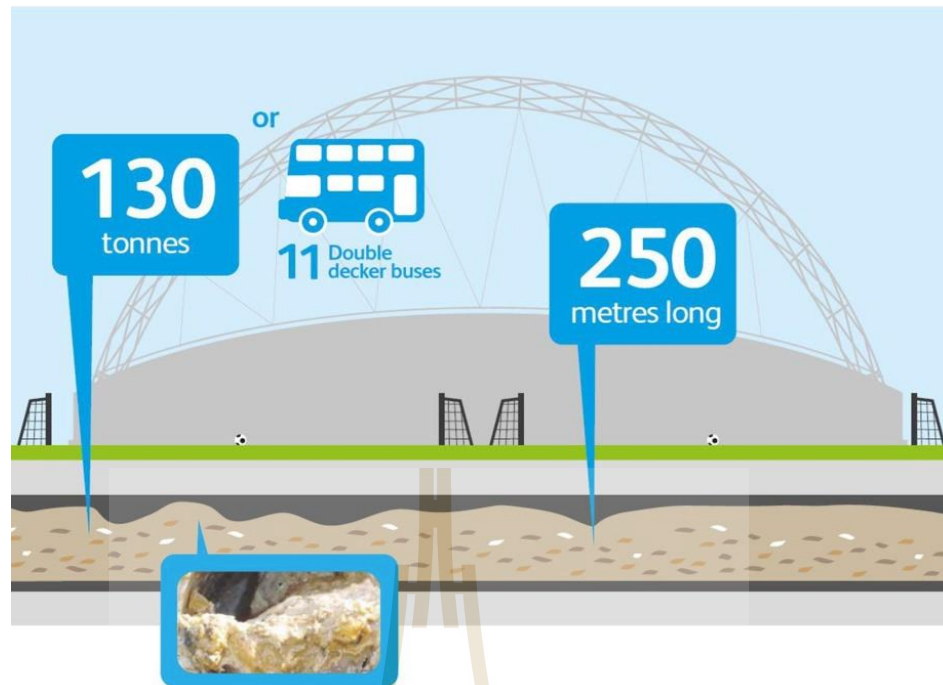


Figure 2.2 Recently discovered “fatberg” in London (Osborne, 2017).

2.3 FOG deposit composition

The perennial problem of sewer blockages has brought the attention of a group of scientists from the US, UK, Singapore, and Malaysia to investigate the cause of these incidences. The results of their investigation are summarized in Table 2.4. As shown, the data revealed that regardless of the country and sample areas, the deposits commonly contain FOG, calcium, and fatty acids (FAs). The fatty acid components identified from the FOG deposits in the sewer system include palmitic, stearic, oleic, and linoleic acids (Williams et al., 2012). Among these, palmitic and oleic acids occur in larger amounts.

Therefore, acid and bile tolerance are important for stability and resistance of viable probiotic bacteria in bile and acid due to large amount of probiotics which pass through the gastro-intestinal tract and provide health benefits.

Table 2.4 Major compositions of FOG deposits from various sewer lines.

| | References | | | | |
|----------|---|---|---|---|---|
| | Keener et al., 2008 (US) | Montefrio et al., 2010 (Singapore) | He et al., 2011 (US) | Williams et al., 2012 (UK) | Husain et al., 2014 (Malaysia) |
| Source | city sewer | school canteen grease interceptor | apartment, food service establishments, shopping center | pumping stations, Sewer manholes, sewer works | food restaurant manhole |
| Fat/oil | 0->100% | not analyzed | 26-49% | 1.2-18.1% | 0.10%* |
| FAs | | | | | |
| palmitic | 10.9-89.5% | 38.30% | 38.7-64.7% | 70% | not analyzed |
| oleic | 6.75-70.4% | 36.90% | 37% | 40% | not analyzed |
| Calcium | 35-18600 mg/L | not analyzed | 900 mg/L - 51400 mg/L* | 10940 mg/L* | 1.96 mg/L |

*converted

2.3.1 FOG

2.3.1.1 Description of FOG

FOG, also known as grease trap waste or brown grease, is the layer of lipid-rich material from wastewater produced during cooking and food processing. It typically contains food scraps, meat fats, lard, tallow, cooking oil, butter, margarine, sauces, gravy, dressings, deep-fried food, baked goods, and cheeses.

Depending on the saturation of the carbon chain, FOG can be a solid or viscous liquid (Husain et al., 2014).

2.3.1.2 Chemical composition of FOG

Fats and oils are the basic constituents of FOG deposit, which belong to the triacylglycerol group of lipid components (Fennema et al., 2008). One type of lipid is called a triglyceride, an ester derived from glycerol combined with three fatty acid molecules (Figure 2.3) (Soult, 2016). Each fatty acid may contain a different number of carbon, degree of unsaturation, and branching (da Silva Lannes and Ignácio, 2013; Fennema et al., 2008; O' Brein, 2009).

Triacylglyceride (TAG) mixtures, such as fats and oils, are the most abundant lipids in food. The chemical and physical properties of fats and oils are basically dictated by their fatty acid profile and the position of the fatty acids within the TAG molecule (O' Brein, 2009). Fat is a solid or pasty triglyceride mixture at room temperature (around 20°C), while oil is a liquid triglyceride mixture at room temperature (Valenzuela and Valenzuela, 2013).

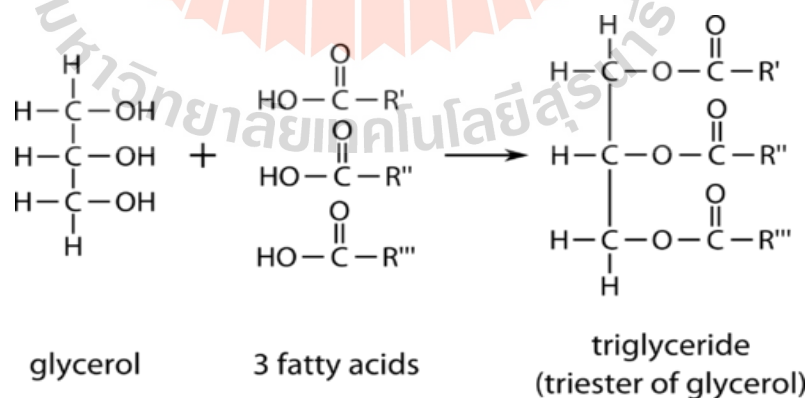


Figure 2.3 A triglyceride molecule from the reaction of glycerol and fatty acids (Soult, 2016).

2.3.1.3 Physical properties of triacylglycerol

Examples of triacylglycerols, which are highly utilized in food industries, are edible fats and oils. Their physical properties are highly dependent on the structure, size, interactions, and organization of the triacylglycerol molecules that they are made of (Fennema et al., 2008; Rosell, 1999).

Melting

The melting point of a pure triacylglycerol is dependent on its chain length, branching, degree of unsaturation of fatty acids, and the position of fatty acids along the glycerol molecule (Fennema et al., 2008). The presence of only straight-chain saturated fatty acid in a triglyceride molecule results in a tight crystal lattice, which requires a lot of energy to be destroyed and melted. Table 2.5 presents the influence of molecular structure on the melting point of triglycerides. It shows that melting point is higher with longer carbon chain length, while melting point is lower with the presence of more double bonds within the carbon chain (Rosell, 1999). A pure triglyceride melts at a distinct temperature while edible fats melt at a wide range of temperature because they contain various types of triglycerides (Fennema et al., 2008).

Natural fats, which primarily contain saturated fatty acids, are solid at room temperature. Similarly, triglycerides with predominantly *trans*-unsaturated fatty acids are also tightly packed and do not melt readily. Triglycerides that are composed mainly of bent chains of *cis*-unsaturated fatty acids have a crystal lattice that is not tightly packed. Thus, they appear liquid at room temperature or can easily be melted (Fennema et al., 2008). The melting point of common oils and animal fats are listed in Table 2.6.

Table 2.5 Melting points of triglycerides (Rosell, 1999).

| Triglyceride | Molecular feature | Approximate melting point (°C) |
|---------------------|--------------------------|---|
| Tristearin | C18:0 | 73 |
| Tripalmitin | C16:0 | 66.5 |
| Trielaidin | C18:1 (<i>trans</i>) | 42 |
| Triolein | C18:1 (<i>cis</i>) | 5.5 |
| Trilinolein | C18:2 (<i>cis</i>) | -12.9 |
| Trilinolenin | C18:3 (<i>cis</i>) | -24 |

Crystallization

Fats are considered as the main structural constituents of various food products. Specifically, fat crystallization mainly affects the consistency, stability, and other mechanical properties of products. Crystallization follows the process of nucleation and crystal growth. Figure 2.4 illustrates the proposed mechanism for nucleation of triacylglycerols (TAGs). The straight chains indicate crystallized TAGs, whereas the bent chains indicate fluid TAGs (da Silva Lannes and Ignacio, 2013).

In nucleation, the natural ordering of the liquid phase of lipids leads to crystal formation. Rapid cooling of liquid lipids produces a diffuse crystalline phase, which usually results in a glassy state with randomly organized molecules. However, slower cooling allows the lipid molecules to organize into lamellae and finally form coherent, three-dimensional crystals (Metin and Hartel, 2005).

Figure 2.5 presents the structural hierarchy within fat crystal networks. The solid lipids in semi-solid products, which typically occur as a three-dimensional colloidal fat crystal network, determine the physical properties of the product. During

crystallization, fat crystals tend to aggregate, in a similar manner as colloidal gels, to form clusters. The clusters further aggregate into flocs and finally form into a network (da Silva Lannes and Ignacio, 2013; Tang and Marangoni, 2006).

Table 2.6 Melting point of common oils and animal fats.

| Lipid type | Melting point (°C) | References |
|-------------------|-------------------------------|--|
| Oils | | |
| Canola | -10 | dos Santos et al., 2016 |
| | -10 | Engineering ToolBox, 2008 |
| Coconut | 26 | Ghotra et al., 2002 |
| | 25 | Engineering ToolBox, 2008 |
| Olive | 7 | Naghshineh, et al., 2010 |
| | -6 | Engineering ToolBox, 2008 |
| Palm | 41 | Tieko Nassu and Guaraldo Gonçalves, 1995 |
| | 39 | Ghotra et al., 2002 |
| | 35 | Engineering ToolBox, 2008 |
| Palm olein | 29 | Tieko Nassu and Guaraldo Gonçalves, 1995 |
| | 22 | Koushki et al., 2015 |
| Soybean | -6 | Tieko Nassu and Guaraldo Gonçalves, 1995 |
| | -16 | Engineering ToolBox, 2008 |
| Animal fats | | |
| Chicken fat | 40 | Arnaud et al., 2004 |
| | 23-40 | Alm, 2013 |
| Pork fat (lard) | 43 | Ghotra et al., 2002 |
| | 41 | Engineering ToolBox, 2008 |
| | 34-44 | Alm, 2013 |
| Beef fat (tallow) | 48 | Ghotra et al., 2002 |
| | 42 | Engineering ToolBox, 2008 |
| | 40-50 | Alm, 2013 |

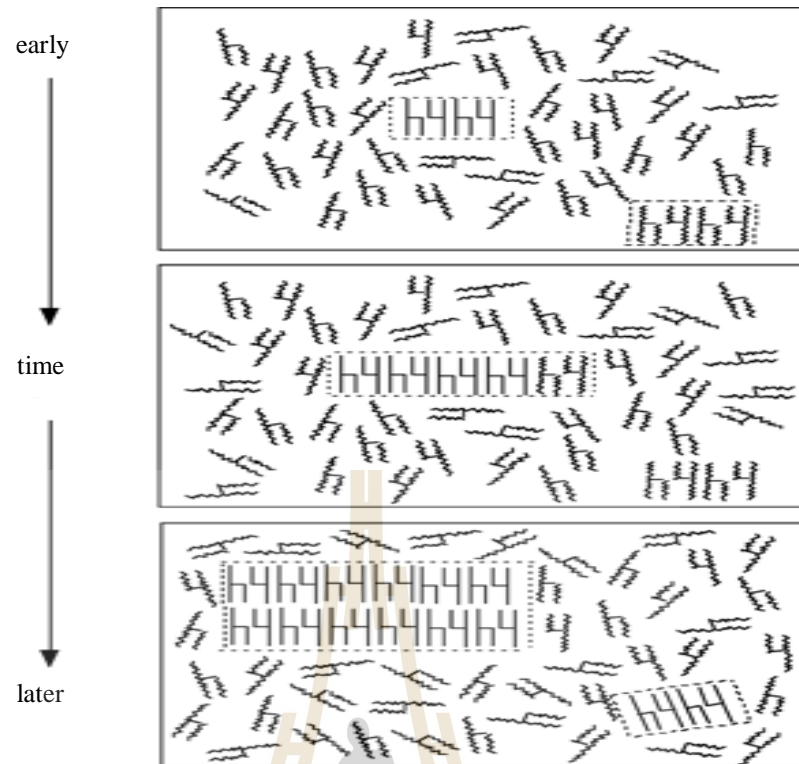


Figure 2.4 Proposed mechanism for nucleation of triacylglycerols (TAGs) (da Silva Lannes and Ignacio, 2013).

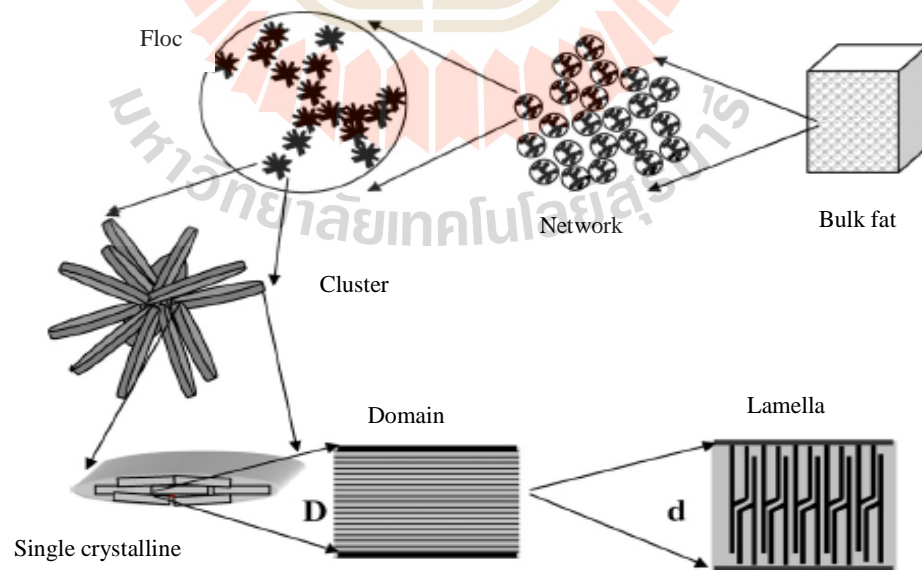


Figure 2.5 Structural hierarchy in colloidal fat crystal networks (Tang and Marangoni, 2006).

Rheology

Most “solid fats” are made up of a mixture of fat crystals dispersed in a liquid oil matrix. The concentration, morphology, interactions, and organizations of the fat crystals present in the system affect the rheological properties of these solid fats. Usually, solid fats display a behavior called as “plasticity” by which they behave like a solid below the yield stress or a critical applied stress, but behaves like a liquid above the yield stress (Fennema et al., 2008; da Silva Lannes and Ignacio, 2013). Typically, yield stress increases with higher solid fat content (SFC) and the extension of three-dimensional networks throughout the volume of the system. In reality, solid fats show a non-ideal plastic behavior as they can exhibit shear thinning above the yield stress or show viscoelasticity below the yield stress. On the other hand, most liquid oils behave like Newtonian liquids at room temperature (Fennema et al., 2008).

2.3.1.4 Sources of FOG

According to Arthur and Blanc (2013), the three main sources of FOG in the sewer system are domestic, commercial, and industrial. The contribution of sewer blockages due to domestic source is 55% (Scottish Water, 2012). However, the change of the eating habits of people, particularly their preference of eating outside their homes, has resulted in flourishing food service establishments (FSEs) (Husain et al., 2014). In Thailand, high concentration of FOG was analyzed from the effluent of restaurants that serve fried chicken, seafood, French fries, and salad dressings (Stoll and Gupta, 1997). In the commercial category, the FSEs emerge to be the major source of FOG waste. In fact, Arthur and Blanc (2013) reported that 80% of FOG-related blockages in the sewer system are found to occur in areas with high concentrations of FSEs. This supports the findings of He et al. (2011) that as the density of commercial food preparation facilities increases, the amount of FOG being discharged also increases.

On the other hand, the industrial sector, which includes abattoirs, rendering plants, and food processors, also contributes to FOG waste (Arthur and Blanc, 2013). The oil milling industries are also identified as industrial source of FOG waste (Husain et al., 2014). Nevertheless, the effluent from oil milling plants is controlled by licensing and legislation (Arthur and Blanc, 2013).

2.3.2 Fatty acids

2.3.2.1 Chemical composition of fatty acids

Fatty acids comprise the main component of lipid, which is composed of aliphatic chain and carboxylic acid group. Majority of the fatty acids contain even number of carbons positioned in a straight chain. This is due to the biological process of fatty acid elongation in which two carbons are added at a time. However, fatty acids with odd carbon numbers can be found in microorganisms and dairy fats (Fennema et al., 2008). Fatty acids are classified based on their saturation and chain length. Saturated fatty acids (SFAs) have no double bonds in the hydrocarbon chain. On the other hand, unsaturated fatty acids (UFAs) have hydrocarbon chain that has at least one double bond and can be further classified into mono-unsaturated fatty acids (MUFAs) and polyunsaturated fatty acids (PUFAs). MUFAs have hydrocarbon chain consisting of single double bond while PUFAs have hydrocarbon chain with more than one double bond (Rosell, 1999). Table 2.7 presents the list of fatty acids commonly found in foods.

In terms of chain length, fatty acids are termed as short-chain fatty acids if they contain four to ten carbons (C4 to C10); medium-chain fatty acids if they have twelve to fourteen carbons (C12 to C14); long-chain fatty acids if they consist of sixteen to eighteen carbons (C16 to C18); and very long-chain fatty acids if they carry twenty or more carbons (\geq C20). The chemical and physical properties of various types of fatty acids, such as their melting point and solubility, highly depend on the number of

carbon atoms and the presence of double bonds in their molecule. Fatty acids with a higher number of carbon atoms in their chain length exhibit higher melting points. However, fatty acids containing double bonds have lower melting points. Therefore, even if fatty acids contain the same number of carbon atoms, a saturated structure behaves like a solid or semi-solid at room temperature, while the unsaturated structure exhibits a liquid or semi-solid property at room temperature (Valenzuela and Valenzuela, 2013).

Table 2.7 Systematic, common, and numerical names for fatty acids found in foods (Fennema et al., 2008).

| Systematic Name | Common Name | Numerical Abbreviation |
|--|-------------|------------------------|
| Saturated fatty acids | | |
| Hexanoic | Caproic | 6:00 |
| Octanoic | Caprylic | 8:00 |
| Decanoic | Capric | 10:00 |
| Dodecanoic | Lauric | 12:00 |
| Tetradecanoic | Myristic | 14:00 |
| Hexadecanoic | Palmitic | 16:00 |
| Octadecanoic | Stearic | 18:00 |
| Unsaturated fatty acids | | |
| <i>cis</i> -9-Octadecenoic | Oleic | 18:1 Δ 9 |
| <i>cis</i> -9- <i>cis</i> -12,Octadecadienoic | Linoleic | 18:2 Δ 9 |
| <i>cis</i> -9- <i>cis</i> -12, <i>cis</i> -15- Octadecatrienoic | Linolenic | 18:3 Δ 9 |
| <i>cis</i> -5- <i>cis</i> -8, <i>cis</i> -11- <i>cis</i> -14- Eicosatetraenoic | Arachidonic | 20:4 Δ 9 |
| <i>cis</i> -5- <i>cis</i> -8, <i>cis</i> -11- <i>cis</i> -14- <i>cis</i> - 17-Eicosapentaenoic | EPA | 20:5 Δ 5 |
| <i>cis</i> -4- <i>cis</i> -7, <i>cis</i> -10- <i>cis</i> -13- <i>cis</i> - 16- <i>cis</i> -19-Docosahexaenoic | DHA | 22:6 Δ 4 |

2.3.2.2 Sources of free fatty acids

The evaluated FOG deposits were found to be predominantly made up of palmitic acid followed by oleic acid. The FOG deposits were assumed to come from cooking oils, but Williams et al. (2012) observed that most fresh oils mainly contain oleic acid than palmitic acid (Table 2.8). Hence, the free fatty acids analyzed from the deposits were considered to be products of microbial, chemical, and enzymatic hydrolysis of oil (Iasmin et al., 2014; Keener et al., 2008; Williams et al., 2012).

Hydrolysis is known to affect fats and oils due to the action of moisture (Daborganes, 2011). It mainly occurs in lipids with short chain and unsaturated fatty acids because they are more soluble in water (Choi and Chang, 2012; Fennema et al., 2008; Shahidi and Zhong, 2005). During frying, water, oxygen, and steam initiate the chemical changes in the oil and food. The ester linkage of triacylglycerols is attacked by water to release free fatty acids, glycerol, and di- and mono-acylglycerols (Choi and Chang, 2012; Scrimgeour, 2005). Figure 2.6 shows the breakdown of triacylglycerol molecule during hydrolysis. In the drainage system, FFAs can also be generated through alkali-driven hydrolysis due to the prolonged exposure and mixing of FOG, moisture, and calcium hydroxide from concrete corrosion (He et al., 2013; Iasmin et al., 2014).

Microbial activity also contributes to the generation of FFA in the sewer. It was found out that numerous microorganisms were identified to degrade FOG with the aid of extracellular lipases. Moreover, lipases from food wastes, commercial detergents, and soaps were also presumed to catalyze FOG hydrolysis (He et al., 2017; Montefrio et al., 2010).

Table 2.8 Major fatty acid composition of common oils and animal fats.

| Lipid type | Major fatty acids (%) | | | | | References |
|---------------|-----------------------|-------|-------|-------|-------|------------------------|
| | C12:0 | C14:0 | C16:0 | C18:1 | C18:2 | |
| Oils | | | | | | |
| Canola | | | 4 | 75 | 12 | Gupta, 2005 |
| | | | 4 | 64 | 19 | Fennema et al., 2008 |
| | | | 5 | 54 | 26 | Marikkar et al., 2002 |
| Coconut | 49 | 22 | 8 | 6 | | Bhatnagar et al., 2009 |
| | 51 | 19 | 8 | 5 | | Jayadas and Nair, 2006 |
| Olive | | | 10 | 78 | 7 | Scrimgeour, 2005 |
| | | | 13 | 71 | 10 | Williams et al., 2012 |
| | | | 14 | 71 | 10 | Fennema et al., 2008 |
| Palm | | | 44 | 40 | 10 | Scrimgeour, 2005 |
| | | | 41 | 44 | 9 | Montoya et al., 2014 |
| | | | 44 | 39 | 10 | Mancini et al., 2015 |
| Palm olein | | | 39-43 | 40-44 | 12-14 | Gupta, 2005 |
| | | | 38-42 | 41-44 | 10-13 | Koushki et al., 2015 |
| Soybean | | | 11 | 22 | 53 | Scrimgeour, 2005 |
| | | | 10 | 55 | 28 | Gupta, 2005 |
| | | | 11 | 23 | 53 | Fennema et al., 2008 |
| Fats | | | | | | |
| Chicken | | | 22 | 39 | 16 | Goodrum et al., 2002 |
| | | | 25 | 40 | 18 | Lee and Foglia, 2000 |
| | | | 28 | 44 | 14 | Fennema et al., 2008 |
| Pork (lard) | | | 24 | 44 | 11 | Williams et al., 2012 |
| | | | 27 | 44 | 11 | Scrimgeour, 2005 |
| | | | 25 | 45 | 10 | Fennema et al., 2008 |
| Beef (tallow) | | | 25 | 42 | 18 | Marikkar et al., 2002 |
| | | | 26 | 39 | 2 | Fennema et al., 2008 |
| | | | 26 | 31 | 2 | Scrimgeour, 2005 |
| | | | 29 | 31 | 2 | Marikkar et al., 2002 |

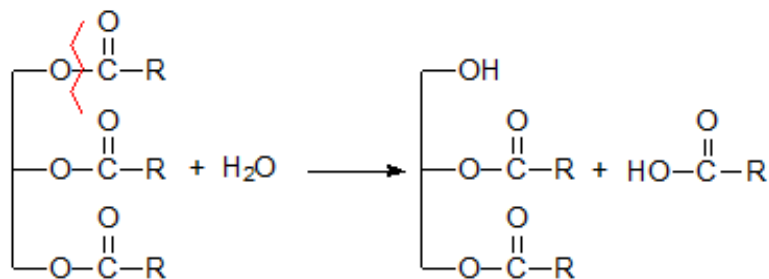


Figure 2.6 Formation of diacylglycerols and fatty acids during triacylglycerol hydrolysis (Daborganes, 2009).

FOG is also vulnerable to deterioration through lipid oxidation. The reaction process can be accelerated by the application of heat, as in the case of deep-fat frying. This cooking method can induce thermal oxidation that changes the color of the oil. It also increases foaming, viscosity, free fatty acid and polar matter contents (Shahidi and Zhong, 2005). Thermally induced lipid oxidation, which occurs during baking or frying, are very complex since oxidative and thermal reactions are simultaneously involved. Particularly, as the temperature is increased, the solubility of oxygen is reduced significantly but all the oxidation reactions are accelerated (Daborganes, 2009). The oxidation process occurs through a series of chain reactions such as initiation, propagation, and termination depicted in Figure 2.7.

As shown in Figure 2.7, RH represents the triacylglycerol molecule that undergoes oxidation in one of its unsaturated fatty acyl groups. During the initiation stage, an alkyl radical is produced by the abstraction of a hydrogen radical from an unsaturated fatty acid. In the propagation stage, the alkyl radical further reacts with oxygen to form peroxy radicals. Consequently, peroxy radicals react with new triacylglycerol molecules to yield hydroperoxides and new alkyl radicals. Lastly, in the

termination stage, radicals combine to form non-radical species, which are relatively stable (Dobarganes, 2009).

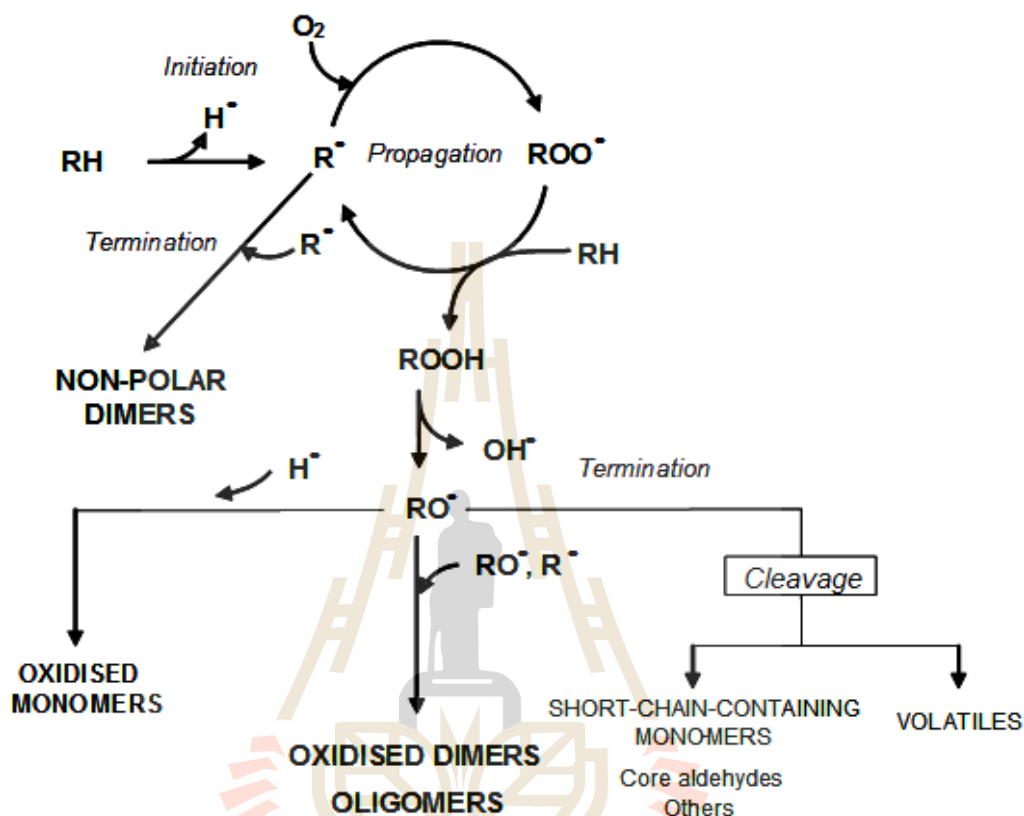


Figure 2.7 Simplified scheme of thermal oxidation of triacylglycerol (Dobarganes, 2009).

2.3.3 Calcium

Among the ninety chemical elements that exist naturally in the earth's crust, twenty-five elements are present in living cells of plants and animals. Calcium is one of the major elements in biological systems (Fennema et al., 2008). Hence, it is inevitable that calcium present in food and environment may also reach the sewer.

2.3.3.1 Sources of calcium

Calcium cation (Ca^{2+}) is naturally present in water and is one of the principal cations that cause water hardness (Sawyer, 2003; Williams et al., 2012). However, Keener et al. (2008) found no correlation between water hardness and calcium content in FOG deposits, but in the preceding investigation conducted by Williams et al. (2012), there was increased calcium content in FOG deposits with increased water hardness.

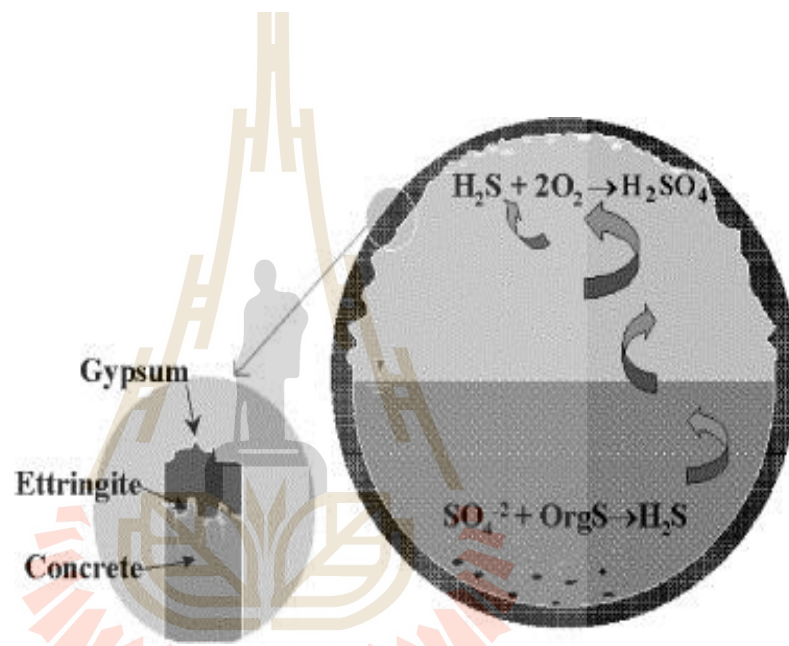


Figure 2.8 Concrete corrosion induced by the sulfur cycle (Roberts et al., 2002).

Furthermore, calcium can also be produced from microbiologically induced concrete corrosion (MICC) (He et al., 2013; He et al., 2011; Romanova et al., 2014; Williams et al., 2012). Concrete is still a major constituent of the sewer system throughout the world (Roberts et al., 2002). The sulfur cycle in the sewage collection system facilitates concrete corrosion (Figure 2.8). In the sewer, the sulfate-reducing bacteria in biofilms produce hydrogen sulfide, which is converted to partially reduced sulfur compounds. Eventually, sulfur-oxidizing bacteria convert the sulfur

compounds to sulfuric acid in the presence of oxygen and moisture. The sulfuric acid reacts with the binder of the concrete producing ettringite and gypsum (calcium sulfate) (Davis et al., 1998; George, 2012; Roberts et al., 2002).

2.4 Formation mechanisms of FOG deposits

Based on the physical properties and visual characteristics of the FOG deposits evaluated by Keener et al. (2008), their group theorized that FOG deposits can be formed through saponification. Particularly, oil constituents interact with calcium in the wastewater and form into metallic salts of fatty acids. On the other hand, FOG deposits can also be merely solid substances that are formed through the physical accumulation of oils, or just simply mineral deposits that are misidentified as FOG deposits. Succeeding investigations clarified how FOG deposits develop. He et al. (2013) first proposed the formation mechanisms of FOG deposits in the sewer system (Figure 2.9). The four major components that essentially contribute to FOG deposit formation in the sewer system include FOG or oil, free fatty acids, calcium, and water.

Oil serves as a carrier and minor source of free fatty acids (FFAs). FFAs, which are also generated during cooking or microbial activities in the grease interceptor, float on the wastewater surface and come in contact with calcium from wastewater or concrete corrosion. In the sewer environment, FFAs and calcium chemically react to form calcium salts of fatty acids. Saponification takes place at a faster rate when FFAs and calcium are present in the oil/water or oil/concrete interface. The accumulation of FOG deposits occurs when the saponified solid attached on the sewer walls draws unreacted FFAs. The adhered FFAs attract calcium or other metal cations through van der Waals attraction and electrostatic repulsion (DLVO theory). Eventually, saponification reoccurs and results in additional soap layer in the deposit. As long as the reactants are present and the sewer

environment is suitable for the reaction to take place, the same process continues leading to FOG deposit build up (He et al., 2013).

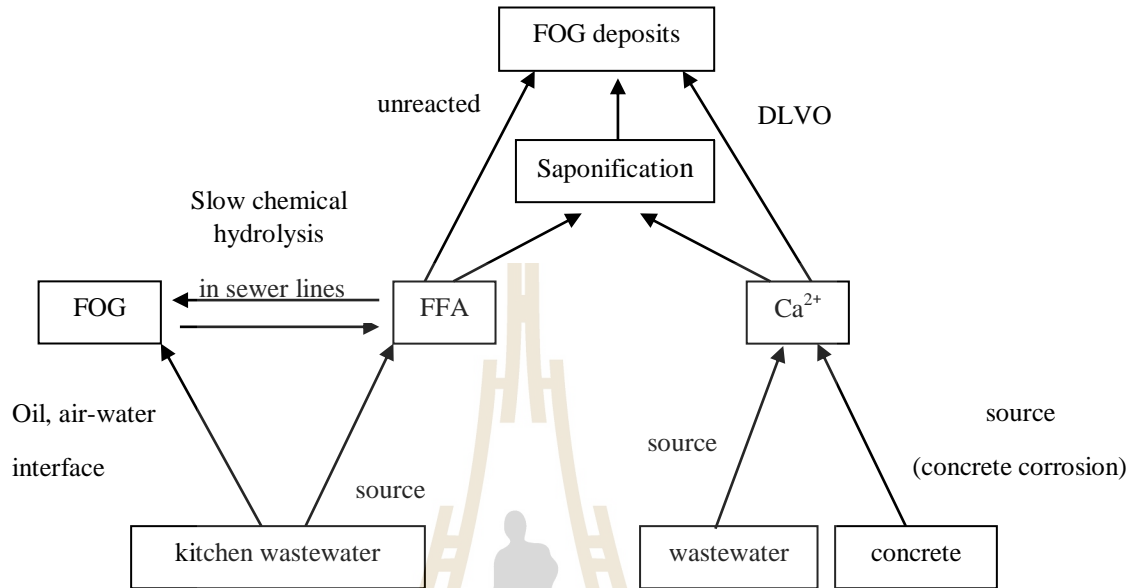
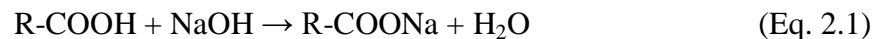


Figure 2.9 Mechanisms of FOG deposit formation in the sewer system (He et al., 2013).

Saponification already arises during cooking and can still continue to occur in the sewer system. Initially, frying may release the fatty acid in fats and oils and these free fatty acids easily undergo saponification in the presence of a catalyst, such as sodium hydroxide or potassium hydroxide, which is naturally found in raw foods or ingredients (Eq. 2.1) (Keener et al., 2008; Husain et al., 2014).



As the fat and oil wastes reach the sewer system, the triacylglycerols can also be saponified to produce metallic soap (Eq. 2.2) (He et al., 2011; Husain et al., 2014). The alkaline detergents, degreasers, and sanitizers commonly used in FSEs provide the available oxidizer to catalyze saponification in the sewer system (Keener et al., 2008).



Furthermore, the calcium ions present in the sewer system may react with the free fatty acid component of the soap to produce lime soaps (Eq. 2.3) (Nora et al., 2005). The general saponification reaction in the production of insoluble calcium-based fatty acid salts is illustrated in Figure 2.10.

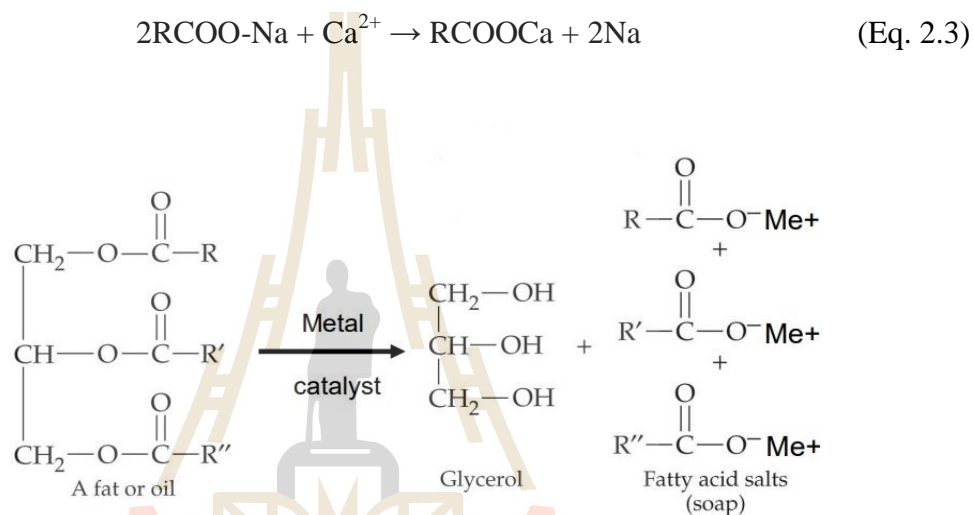


Figure 2.10 Saponification reaction in the sewer system (Ducoste, 2013).

In another study, Poulenat et al. (2004) synthesized sodium, lithium, and calcium soaps from high oleic sunflower oil by double decomposition reactions. The production was done in a 250-ml reactor, in the presence of nitrogen, with agitation at 200-250 rpm. Their study confirmed that solubilities of organic and inorganic compounds can be categorized based on the anion. In the case of hydroxides, sulfates, carbonates, and oleates in water, the solubilities decline along the cation series: $\text{Na} > \text{Li} > \text{Ca}$. Specifically, the soap conversion yields (measured in calcium content) of the calcium soaps are presented in Eqs. 2.4, 2.5, and 2.6.



2.5 Confirmatory studies on FOG deposits

The environmental conditions in the sewer system are not similar to the conditions used in commercial soap manufacture. Commercial soaps are conventionally prepared under boiling conditions (100°C), while the typical temperature of the sewer system only ranges from 5-25°C (Iasmin et al., 2014). Thus, in order to mimic the soaps produced from a sewer environment, He et al. (2011), He et al. (2013), and Iasmin et al. (2014) employed a lower temperature-based saponification process. Laboratory-prepared calcium soaps were purposely created to provide experimental evidence that FOG deposits are indeed calcium-based fatty acid salts.

2.5.1 Verification of saponification hypothesis by FTIR analysis

FTIR has been widely used to identify the FOG in water, oily substances in various chemical processes, *trans* fat in food, fatty acids, and fatty acid salts. To verify the saponification hypothesis, characteristic soap bands should be detected in FOG deposits. According to Poulenat et al. (2003), characteristic soap bands are divided into four regions. Region 1 is from 3000-4000 cm⁻¹ that is linked to O-H stretching vibration of hydrated water. Soaps have broad and distinct absorption at 3400 cm⁻¹ that is related to hydrogen bonding and the polar head groups of the soap molecule. Region 2 is from 1350-1800 cm⁻¹, which is the carboxylic group of fatty acid metallic soap. The frequency

of ester bond in triglycerides at 1745 cm^{-1} should disappear in calcium soap formation. Region 3 consists of band near 720 cm^{-1} that is associated to the rocking vibration of successive methylene groups in calcium and metallic soaps. Region 4 involves the absorption band of the calcium-oxygen bond at 665 cm^{-1} .

2.5.1.1 FTIR spectra of FOG deposits and lab-prepared soaps

He et al. (2011) initiated the investigation on saponified FOG deposits. Their group analyzed the solids recovered from three different sewer lines, used the effluent to produce FOG deposits under laboratory conditions, and created calcium chloride-based soaps using canola oil. The FTIR spectra of FOG deposits in the sewer, lab-based FOG deposits, and calcium soap are presented in Figure 2.11.

The FTIR analyses revealed that each kind of sample has distinct FTIR spectra. This may be attributed to the environmental conditions and the reactants used for saponification. Particularly, the differences in the FTIR spectra observed in the FOG deposits from different sampling sites (Figure 2.11a) may be caused by the kind of waste being released into the sewer line. Overall, although the sewer FOG deposits, lab-based FOG deposits, and calcium soap had distinct FTIR profile, they all displayed the characteristic four regions of soap. The results verified the initial assumption of Keener et al. (2008) that FOG deposits may be metallic salts of fatty acids formed by saponification.

He et al. (2013) further advanced their investigation on the mechanism of FOG deposit formation in the sewer line by studying the laboratory models of soap from concrete, specific fatty acids, and calcium chloride-soybean oil reaction. The solids obtained from the bottom of the beaker (Figure 2.12b) and concrete surface (Figure 2.12c) were identified as soaps based on their FTIR spectra. This confirms the role of concrete in soap formation. On the other hand, the solids made from oleic,

linoleic, and palmitic acids were also verified as soaps according to their FTIR profile. However, band shifting and the differences in absorbance intensities indicate that the process of saponification is different between unsaturated and saturated fatty acids (Figure 2.13). Furthermore, it was recognized that the formation of calcium chloride-based soap is facilitated at pH 8 and 9 (Figure 2.14).

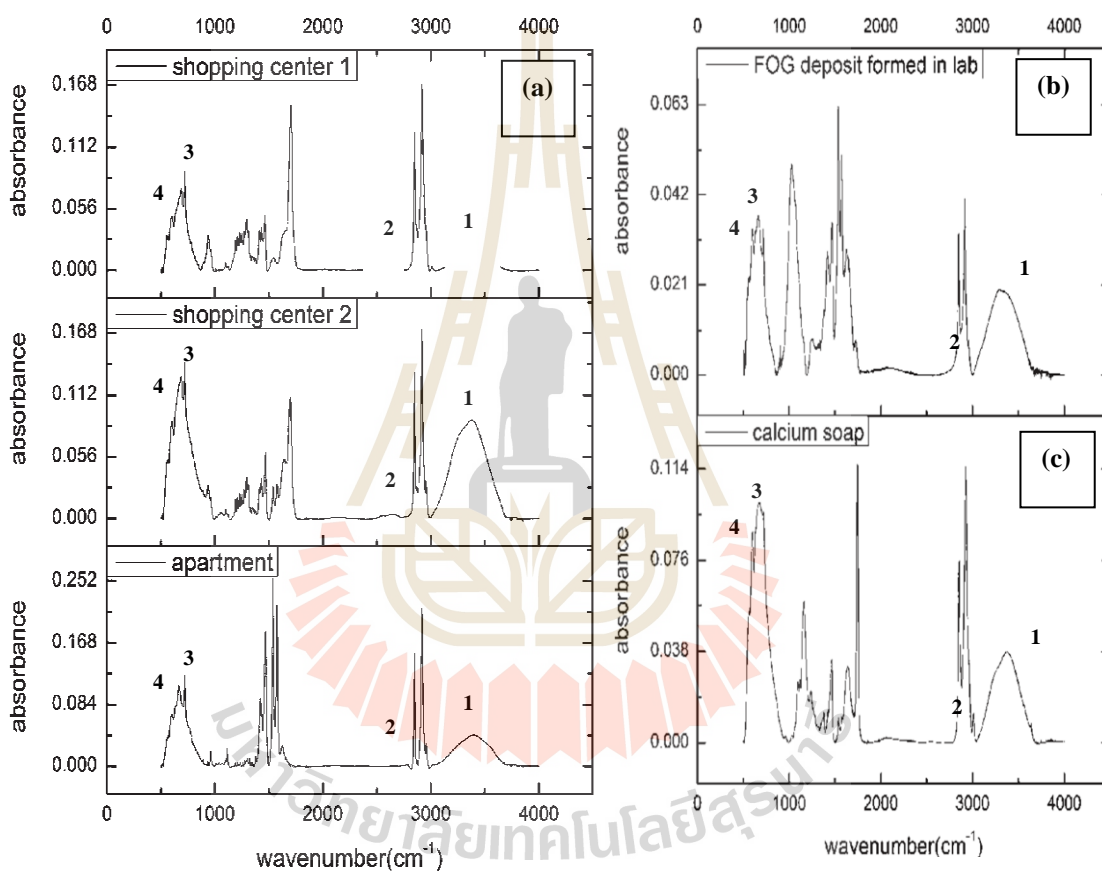


Figure 2.11 FTIR spectra of sewer and lab samples: (a) FOG deposits from the sewer; (b) lab-prepared FOG deposits; and (c) calcium chloride-based canola oil soap (He et al., 2011).

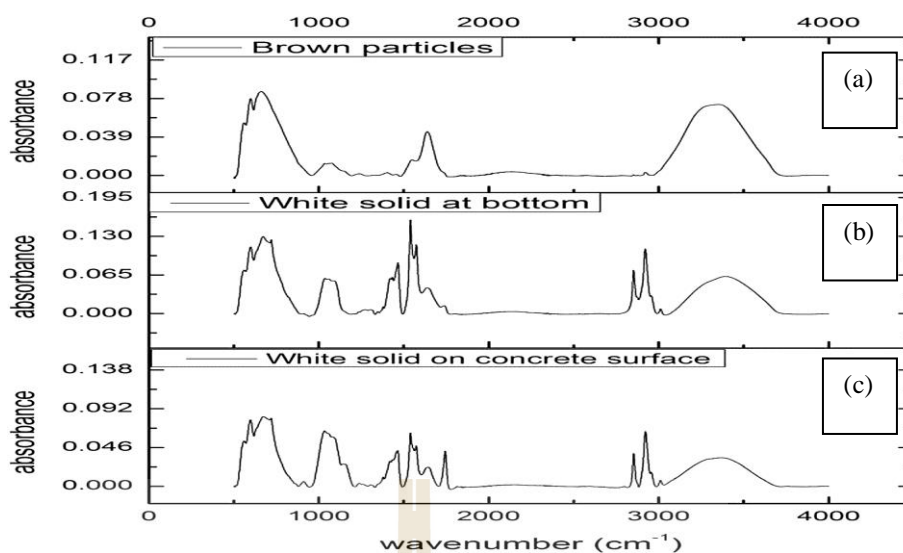


Figure 2.12 FTIR spectra of the solids recovered from the saponification set-up: (a) suspended brown particles; (b) white solid at the bottom of the beaker; (c) white solid on concrete surface (He et al., 2013).

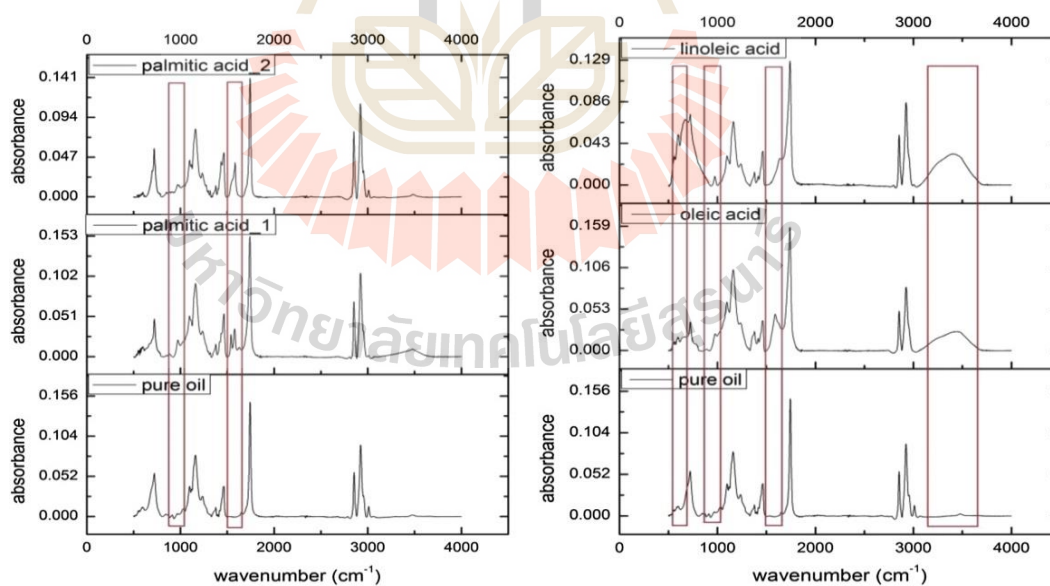


Figure 2.13 FTIR spectra of the solids on concrete with the addition of fatty acids (He et al., 2013).

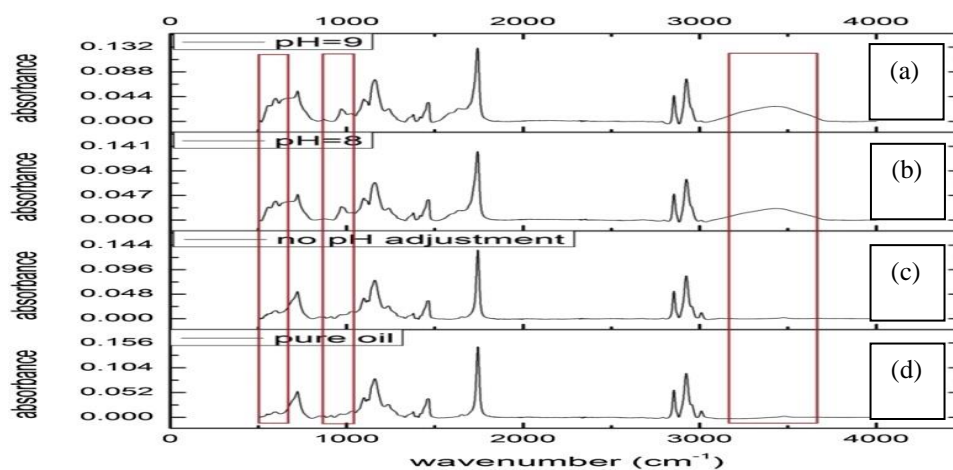


Figure 2.14 FTIR spectra of soybean oil and solid samples from the reaction of calcium chloride and soybean oil under different pH conditions: (a) pH=9; (b) pH=8; (c) no pH adjustment; (d) pure oil (He et al., 2013).

Iasmin et al. (2014) investigated the effect of the type of fat/oil and calcium source on the formation of FOG deposits. Specifically, canola oil and beef tallow were utilized as the lipid source, while calcium chloride, calcium sulfate, and calcium hydroxide were used as the calcium source. With the emphasis on calcium chloride-based soaps, the canola soap showed strong absorption in the metal-oxygen region, while beef tallow soap prepared at 45°C displayed weak absorption in the same region. This implies that beef tallow, being highly saturated, has slower alkali hydrolysis kinetics than the canola oil. The FTIR analysis revealed that all soaps showed signature bands of calcium-based fatty acid salts. They exhibited strong metal-oxygen bonds (around 670 cm^{-1}) and hydroxyl bonds (around 3400 cm^{-1}) (Table 2.9). The locations of the characteristic soap bands were slightly shifted due to the variation of reactants and progression of saponification reaction.

Iasmin et al. (2016) further studied the FOG deposit formation kinetics at varying pH and temperatures. The calcium chloride and calcium sulfate soap

mixtures were allowed to react for eight hours and their rate of reaction was recorded. At pH 10, calcium sulfate-based canola oil soap, which was prepared at 45°C, registered the highest saponification of almost 90%, while calcium chloride-based beef tallow (BT) soap at 45°C had the least saponification at around 20% (Figure 2.15). On the other hand, at pH 14, calcium sulfate-based canola oil soap, which was prepared at 22°C, reflected the highest saponification at about 70%, while calcium chloride-based beef tallow soap at 45°C had the lowest saponification at about 20% (Figure 2.16).

Consistently, calcium sulfate-based canola oil soaps exhibited the highest saponification regardless of pH condition. It was speculated that the metal oxygen band of the unreacted calcium sulfate may have also contributed to the values of saponification. Additionally, beef tallow produced the lowest amount of saponified solids. It was theorized that beef tallow requires more thermal energy to produce a considerable amount of soap since it is solid at room temperature. Based on the saponification kinetics, four types of alkali driven hydrolysis that may influence FOG deposit formation were proposed: (1) fast hydrolysis during the cooking process when fat comes in contact with moisture; (2) hydrolysis near the grease interceptor due to the release of high alkaline detergents; (3) hydrolysis along the sewer line caused by the prolonged contact and/or mixing of unreacted fat and moisture; and (4) hydrolysis of the entrapped or adsorbed oil at the sewer crown induced by the release of gypsum (CaSO_4).

Table 2.9 Comparisons of observed wave frequencies among calcium soaps (Iasmin et al., 2014).

| Frequencies (cm ⁻¹)* | | | | | Assignments |
|----------------------------------|----------------------------------|------------------------------------|---|---|--|
| Canola with CaCl ₂ | Canola with CaSO ₄ | Canola with Ca(OH) ₂ | Beef Tallow with CaCl ₂ @22°C | Beef Tallow with CaCl ₂ @45°C | |
| | | 3639 (n, w) | | | Non bonded hydroxyl group, OH ⁻ stretch |
| | | | | 3558 (n, vw) | Tertiary alcohol, OH ⁻ stretch |
| 3367 (b, ms) | 3331 (b, ms) | 3381 (b, ms) | 3464 (b, vw) | 3390 (b, vw) | Hydroxyl group. H-bonded OH ⁻ stretch |
| 3010(vw) | | 3011 (vw) | 3001 (vw) | | Stretching =CH-H |
| 2924 (s) | 2923 (vs) | | | | Asymmetric stretching CH ₂ , C-H |
| 2857 (w) | 2853 (s) | | | | Symmetric stretching CH ₂ , C-H |
| 1744 (s) | 1744 (vs) | 1744 (w) | 1739 (vs) | 1741 (vs) | Stretching C=O (ester) |
| | | | 1702 (vw) | 1696 (vw) | C=C stretching |
| 1637 (s) | 1650 (w) | 1641 (w) | | 1640 (vw) | |
| | | 1570 (ms) | | | Asymmetric stretching COO ⁻ , C-O (ω ₂) |
| | | 1541 (ms) | | | |
| 1456 (w) | 1463 (w) | 1462 (s) | 1463 (w) | 1461 (w) | |
| | | 1419 (s) | 1420 (vw) | | |
| | | | 1404 (vw) | | |
| | | | 1385 (vw) | 1380 (vw) | Symmetric stretching COO ⁻ , C-O (ω ₁) |
| | 1377 (vw) | 1313 (w) | 1353 (vw) | | |

Table 2.9 Comparisons of observed wave frequencies among calcium soaps (Iasmin et al., 2014) (Continued).

| Frequencies (cm ⁻¹)* | | | | | Assignments |
|----------------------------------|----------------------------------|------------------------------------|---|---|--|
| Canola with CaCl ₂ | Canola with CaSO ₄ | Canola with Ca(OH) ₂ | Beef Tallow with CaCl ₂ @22°C | Beef Tallow with CaCl ₂ @45°C | |
| | | 1279 (w) | | | Twist and wag CH ₂ |
| 1234 (w) | 1236 (w) | 1240 (w) | 1243 (w) | 1232 (w) | Skeletal C-C vibrations |
| | | | 1231 (w) | | Rocking CH ₃ |
| 1159 (s) | 1154 (vs) | 1164 (w) | 1171 (vs) | 1169 (ms) | Deformation COOR |
| 1103 (w) | 1117 (vs) | 1107 (w) | 1101 (w) | 1103 (w) | Glycerin |
| | 1096 (vs) | 1046 (w) | 1066 (vw) | | Glycerin |
| | 967 (vw) | | 965 (vw) | 964 (vw) | Glycerin |
| | | 914 (w) | | | Bending deformation COO ⁻ (ω ₃) or glycerin |
| | | | 837 (vw) | | |
| | 721 (vs) | 713 (vs) | 722 (w) | 720 (s) | Rocking (CH ₂) _n , n > 4 |
| | | | 697 (vw) | | |
| 675 (vs) | 673 (vs) | 674 (vs) | | 685 (w) | Ca-O bond |
| | | | 645 (vw) | | OH ⁻ out-of-plane bend |
| 599 (vs) | 593 (vs) | 601 (vs) | | 591 (w) | |

*vs- very strong (>80% range/guideline); s- strong (>60 and ≤80); ms- medium strong (>40 and ≤60); vw (>20 and ≤40); w- weak (≤20); b- broad (from visual appearance); n-narrow (from visual appearance).

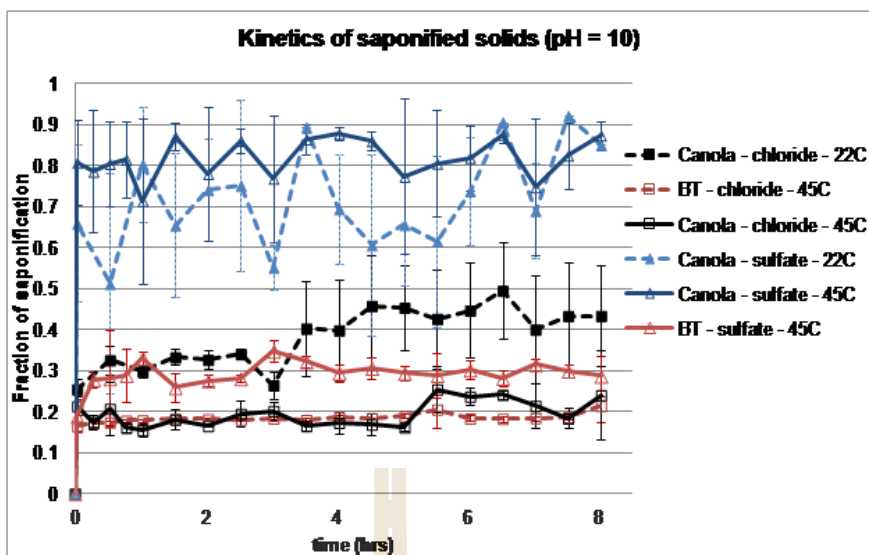


Figure 2.15 Kinetics of calcium-based saponified solids at pH 10 with varying types of fat/oil, calcium forms, and temperatures (Iasmin et al., 2014).

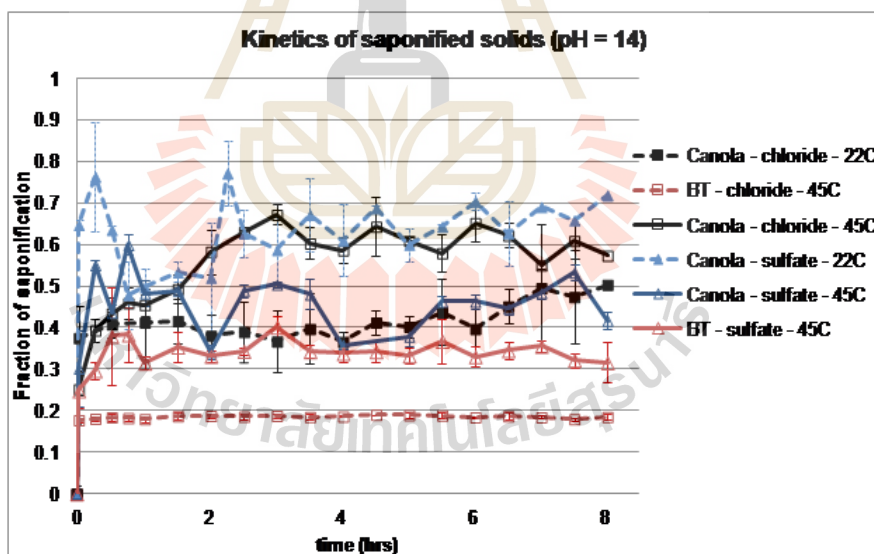


Figure 2.16 Kinetics of calcium-based saponified solids at pH 14 with varying types of fat/oil, calcium forms, and temperatures (Iasmin et al., 2014).

2.5.1.2 Properties of FOG deposits and lab-prepared soaps

Private and public wastewater utilities are expected to maintain free-flowing sanitary collection systems. However, once FOG leaks from the grease interceptor or is deliberately thrown into the drainage system, it tends to stick to the wall of the sewer pipes, which causes clogging over time. In effect, the restriction of flow of sewage due to clogged pipes eventually leads to sanitary sewer overflows (SSOs) (Husain et al., 2014; Keener et al., 2008). The adhesive property of FOG deposit is therefore an important parameter to be considered in finding solutions for SSOs. Keener et al. (2008) evaluated the FOG deposits sampled from 23 locations around the United States. It was found out that the yield strength of FOG deposits ranged from 4.50-34.25 kPa. The sample with the lowest yield strength was suspected to be formed from simple FOG accumulation, while samples with higher yield strength were assumed to be formed by chemical reaction. In another investigation, Williams et al. (2012) evaluated the FOG deposits from nine locations across England. It was identified that the hardness index of the samples ranged from 9.56-14.8 mm, which were generally softer than solid fats such as lard and butter. Moreover, the melting point of the samples registered a mean range of 30.7-33.6°C.

Iasmin et al. (2014) probed into the viscoelasticity of FOG deposits and laboratory-prepared soap by subjecting them to oscillatory stress sweep analysis. The type of test was done to determine the storage modulus (G') and loss modulus (G'') of the samples, by which a higher G' than G'' entails a more elastic behavior. Figure 2.17 presents the shear stress dependence of two FOG deposit sub-samples from a manhole of a pizza restaurant. The first sub-sample registered a G' and G'' range of 10^{-1} and 10^3 Pa (Figure 2.17a), while the second sub-sample recorded a G'

and G'' range of 10^2 and 10^8 Pa (Figure 2.17b). The variation of G' and G'' values in the samples supported the assumption that FOG deposits in the sewer system are calcium-based fatty acid salts with layered combinations of debris. Moreover, both samples showed stability as they transformed from viscous to elastic under shear stress.

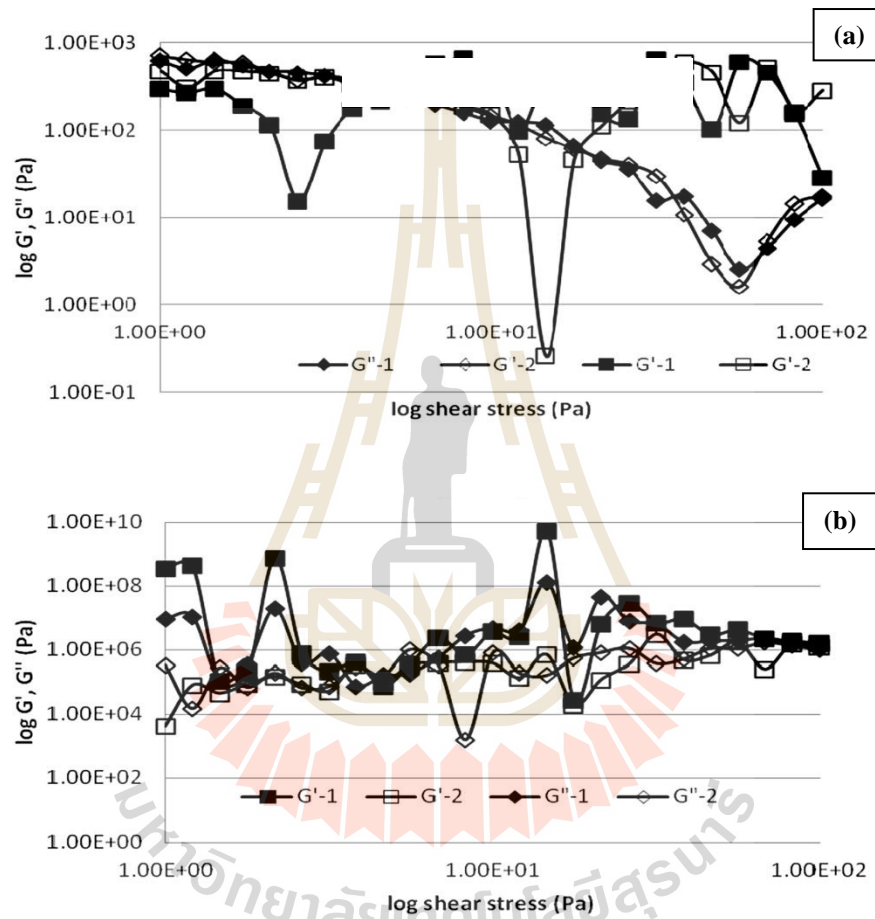


Figure 2.17 Shear stress dependence of FOG deposit sub-samples from a manhole beside a pizza restaurant, under oscillation stress sweep of 0.1- 100 Pa, $\omega=10$ Hz, and gap of 2 mm: (a) sub-sample 1; (b) sub-sample 2 (Iasmin et al., 2014).

Similarly, the behavior of laboratory-prepared soap from canola and calcium chloride was also noted to be like a viscoelastic gel or solid as shown in Figure 2.18. The G' and G'' values of the samples, which ranged from 10^{-1} to 10^3 Pa, were not significantly different. Furthermore, a gel point was particularly observed in the samples where G' crossed G'' signaling a transition from viscous to elastic behavior as shear is increased. The minor differences in their profile may be due to soap crystal sizes.

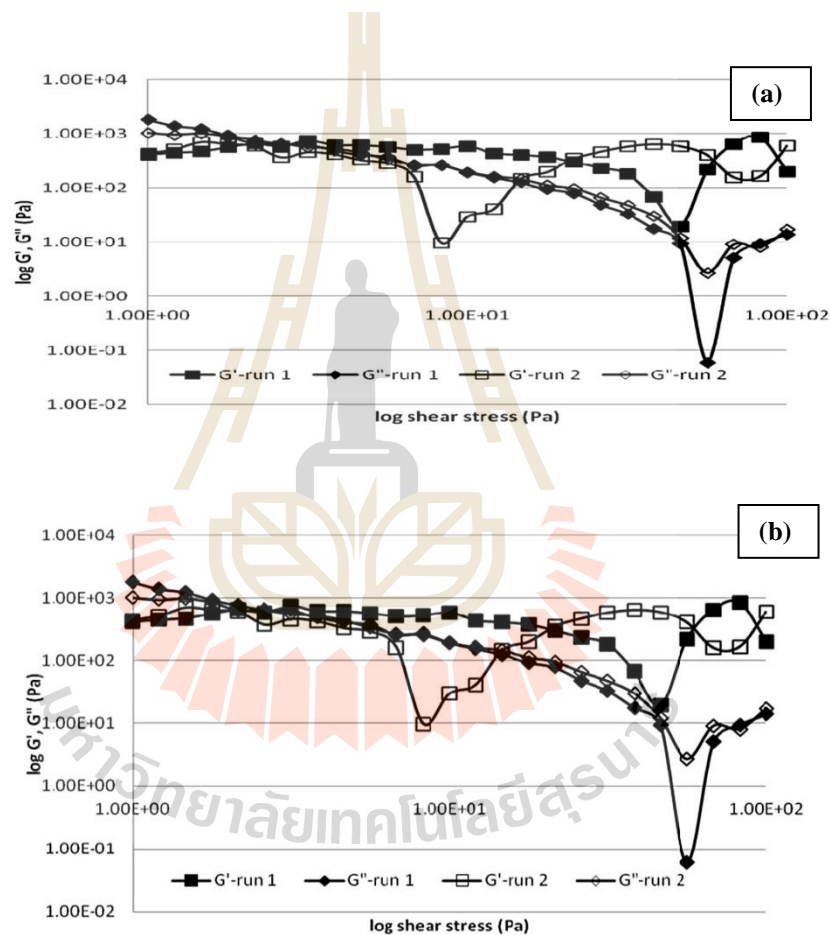


Figure 2.18 Shear stress dependence of calcium chloride-based canola oil soaps at pH 10, 22°C, $\omega=10$ Hz, gap=1 mm: (a) analysis 1; (b) analysis 2 (Iasmin et al., 2014).

On the other hand, laboratory-prepared soap from canola and calcium sulfate exhibited a steady decreasing trend in G' and G'' as more shear was applied (Figure 2.19). Nevertheless, its G' was still slightly higher than G'' . Overall, the G' and G'' values recorded from calcium sulfate-based canola oil soap were still higher (10^2 to 10^5 Pa) than calcium chloride-based soaps.

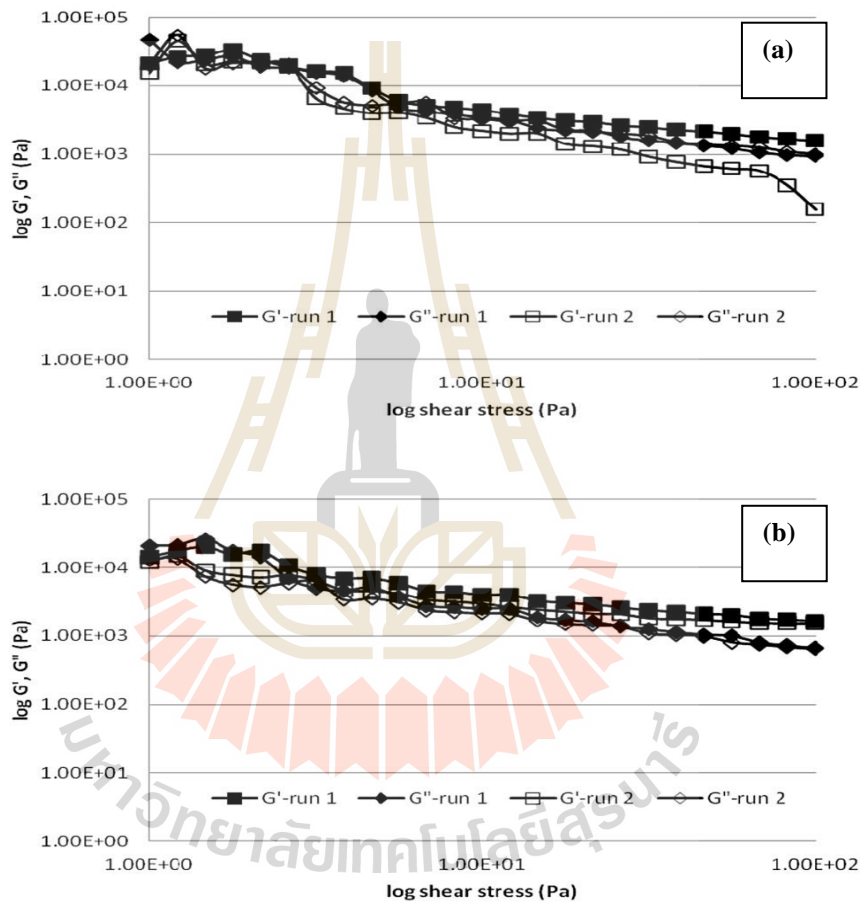


Figure 2.19 Shear stress dependence calcium sulfate-based canola oil soaps at pH 10, 22°C, $\omega=10$ Hz, gap=1 mm: (a) analysis 1; (b) analysis 2 (Iasmin et al., 2014).

CHAPTER III

MATERIALS AND METHODS

3.1 Raw materials and chemicals

The vegetable oils utilized in this study include: a) Home Fresh Mart Soybean Oil (total fat 15 g, 23%; saturated fat 2.5 g, 12%); b) Home Fresh Mart Refined Palm Olein oil from Pericarp (total fat 14 g, 22%; saturated fat 6 g, 30%); c) Naturel Coconut Cooking Oil (total fat 14 g, 22%; saturated fat 13 g, 65%); and d) Sabroso Olive Oil Full Bodied and Mild (total fat 14 g, 22%; saturated fat 2 g, 10%). The soybean oil is manufactured by Thanakorn Vegetable Oil Products Company Limited, the palm olein oil and coconut oil are manufactured by Lam Soon Thailand Public Company Limited, and the olive oil is distributed by Sino-Pacific Trading Thailand Company Limited. The animal fats used for rendering include: a) pork loin fat produced by PS Food Product Company Limited; and b) chicken fat purchased from Nakhon Ratchasima local wet market. The chemicals used for saponification were anhydrous calcium chloride (CaCl_2 , $\geq 90\%$, 110.99 g/mol), anhydrous calcium sulfate (CaSO_4 , 97%, 136.14 g/mol), and sodium hydroxide (NaOH , $\geq 97\%$, anhydrous, 39.997 g/mol), purchased from Carlo Erba Reagents, Italmar, Thailand Company Limited. Deionized (DI) water was used to prepare the solutions.

3.2 Fat rendering

The vegetable oils were directly utilized for the reaction but the animal fats underwent rendering following the procedure of Rohman and Che Man (2011), with some modifications. The ground adipose tissues of pork and chicken were heated in an oven (Memmert, Schwabach, Germany) at 100°C for 2 hours. After the specified time, the melted fat was strained through a triple-folded Muslin cloth. The filtered fats then underwent centrifugation (Hitachi CR22GIII, Tokyo, Japan) at 3000 rpm for 20 minutes at 30°C. After centrifugation, the decanted fat was again filtered through triple-folded Muslin cloth, ready for saponification reaction.

3.3 Production of calcium soap

Alkali hydrolysis, similar to the method used by Iasmin et al. (2014) was adopted to produce calcium soaps. Sodium hydroxide (0.6 wt%) was dissolved in deionized water (14.9 wt%) and anhydrous calcium compound (9.8 wt%) was added, stirred until dissolved, and allowed to cool at room temperature. After cooling, the vegetable oil or melted fat (74.7 wt%) was gradually added to the mixture and stirred at 450 rpm for four hours using an overhead stirrer (IKA® RW 20 Digital, Staufen, Germany). The mixtures with vegetable oil underwent room temperature saponification, while those with animal fat were exposed at 45°C using a water bath (Memmert, Schwabach, Germany) to avoid fat solidification. Modifications were made in terms of sampling because the soap mixtures were allowed to cure at room temperature for 7 days. After the curing period, the calcium soap mixtures were centrifuged at 3000 rpm for 20 minutes at 30°C to separate the solids formed from the rest of the unreacted components. The excess fat/oil was decanted and the soaps were

scraped off from the container. A smooth soap was taken from the second layer of the mixture, while a coarse and moist soap was taken from the third bottom layer of the mixture. The coarse soap was drained for 2 minutes to separate the liquid portion. Each component of the mixture was quantified to calculate the amount of soap produced (yield). The obtained calcium soaps were considered as crude as they did not undergo further purification.

3.4 FTIR analysis

FTIR-ATR data of the fat/oil sources and crude soap components were recorded using FTIR microscope (Bruker Tensor 27, Ettlingen, Germany). Each sample was placed on an attenuated reflectance (ATR) cell equipped with platinum single crystal and scanned 64 times at a range of 4000-400 cm^{-1} . The readings were computed using OPUS 7.2 software. For the soaps, percent saponification was calculated according to the formula used by Iasmin et al. (2014) (Eq. 3.1). Characteristic soap bands represent the metal-oxygen bond vibration around 670 cm^{-1} , carboxylate ion symmetric stretching vibration between 1300-1420 cm^{-1} , and carboxylate ion asymmetric stretching vibration between 1550-1610 cm^{-1} . The carbonyl band around 1745 cm^{-1} signifies the presence of unreacted fat/oil.

% saponification =

$$\frac{\text{absorbance (670 cm}^{-1}\text{+ between 1300 and 1420 cm}^{-1}\text{+ between 1550 and 1610 cm}^{-1}\text{)}}{\text{absorbance (670 cm}^{-1}\text{+between 1300 and 1420 cm}^{-1}\text{+between 1550 and 1610 cm}^{-1}\text{+1745 cm}^{-1}\text{)}} \times 100 \quad (3.1)$$

3.5 Fatty acid profiling

The fatty acid profile of the fats and oils and their calcium soaps was determined following the method of Panpipat and Yongsawatdigul (2008), with some modifications. Each tube containing 25 mg of sample was added with 1.5 mL freshly prepared methanolic NaOH (0.5M) and was immediately purged with nitrogen. Samples were incubated for 2 minutes in a water bath at 80-100°C. After cooling, each tube was added with 2 mL BF₃ and spiked with 1 mL C17:0 as an internal standard. Each tube was again purged with nitrogen gas, capped, and returned to the water bath for 30 minutes. After cooling, each tube was added with 1 mL isooctane and vortexed for 1 minute. It was further added with 5 mL saturated NaCl solution, vortexed for 30 seconds, and allowed to form layers. The top layer comprising the fatty acid methyl esters (FAMES) was collected and placed in a new test tube. The sample was re-extracted by adding 2 mL isooctane. The tubes containing the FAMES were dried at 30°C under nitrogen gas using TurboVap® LV (Caliper Life Sciences, Massachusetts, USA). After drying, each sample was solubilized with 1mL isooctane and vortexed for 30 seconds before it was transferred to a vial. FAMES were analyzed using 7890A GC Systems (Agilent Technologies, Delaware, USA) fitted with fused silica capillary column (SPTM-2560 Supelco, Pennsylvania, USA) with gas chromatography-flame ionization detector (GC-FID) and helium as the carrier gas. The peak areas of the samples, relative to the added internal standard, were compared to the FAME standard mixture (Supelco™ 37 Component FAME Mix, Pennsylvania, USA) in order to determine the percent concentration of each fatty acid.

3.6 Calcium content analysis

The calcium content of the crude soaps was analyzed following the method specified by Trampitsch (2009). In brief, 100 mg of each dried sample was acidified with 8 mL concentrated nitric acid and 2 mL hydrogen peroxide and left overnight in the fume hood. Thereafter, they were digested in the Multiwave 3000 Reaction System chamber (Anton Paar, Graz, Austria). After digestion, the diluted samples, together with blanks and standards, were introduced to Optima 8000 ICP-OES Spectrometer (PerkinElmer, Massachusetts, USA) for calcium content determination.

3.7 Melting endset determination

The melting profile of the fat and oil sources and calcium soaps was determined through Differential Scanning Calorimetry (DSC 204 F1, NETZSCH, Germany) using the method of Tiekko Nassu and Guaraldo Gonçalves (1995). About 6-9 mg of soap was placed in a hermetically sealed aluminum pan and run against an empty pan as the reference. Samples were heated to 80°C for 5 minutes at a rate of 10°C/min to destroy any prior crystalline structure. After this period, they were cooled to -50°C for 5 minutes at a rate of 10°C/min. After reaching the cooling condition, they were reheated to 80°C for 5 minutes at a rate of 10°C/min to record their melting endset.

3.8 Rheological tests

The rheological properties of the calcium soaps were determined using AR2 Rheometer (TA Instruments, Delaware, USA). TA® plate/plate geometry with 60 mm diameter and 1 mm gap was used to evaluate the rheology of the paste-like soaps from the second layer; while TA® concentric cylinder (Model# 545611.901), cup (Model#

545630.001), and vaned rotor (Model# 546026.901) with 4 mm gap was utilized to analyze the coarse soaps from the third layer.

3.8.1 Steady shear characterization

The steady shear data (shear stress and shear rate) of the soaps were obtained by exposing the samples to increasing shear rate of 0.1-800 s⁻¹ at 25°C (Ikhu-Omoregbe and Bushi, 2008). The apparent viscosity, which describes the resistance to flow of the soaps, was derived from the shear stress and shear rate data using Eq. 2:

$$\eta = f(\dot{\gamma}) = \frac{\sigma}{\dot{\gamma}} \quad (3.2)$$

where η is the apparent viscosity, σ is the shear stress, and $\dot{\gamma}$ is the shear rate (Steffe, 1996).

3.8.2 Oscillatory temperature sweep test

In order to determine the viscoelasticity of the calcium soaps, their storage modulus (G') and loss modulus (G'') were recorded through oscillatory temperature sweep test from 5-60°C with a specific stress within their linear viscoelastic region (LVR). The LVR was initially identified through oscillatory stress sweep test from 0.1-100 Pa at 1.0 Hz and at 60°C.

From the temperature sweep plot, the $\tan \delta$ (G''/G') at 25°C was calculated. G' represents a solid-like response, while G'' represents a liquid-like response (da Silva Lannes and Ignacio, 2013). A predominantly elastic or solid-like behavior is indicated by $\tan \delta$ lesser than 1, while a predominantly viscous or liquid-like behavior is signified by $\tan \delta$ greater than 1 (Choi and Chang, 2012).

3.9 Microstructure analysis

3.9.1 ESEM

The microstructure of the calcium soaps was observed under environmental scanning electron microscope (SEM Quanta 450, FEI, Oregon, USA). A small portion of each calcium soap sample was placed on a disposable vinyl specimen mold (Tissue-Tek®) and fixed with O.C.T. compound (Tissue-Tek®). Each sample was frozen by soaking it into liquid nitrogen and then freeze fractured. The fractured component was immediately transferred to a sample holder and placed in the SEM chamber for scanning. The microstructure of the soaps was observed at 5000x magnification.

3.9.2 CLSM

To determine the void area/porosity and void circularity of the calcium soaps, the samples were viewed through confocal laser scanning microscope (Nikon Ti-E A1RSi, New York, USA). Samples for CLSM were separately prepared following the procedure of Wu et al. (2013), with modification. Initially, the raw fats and oils were dyed before they were used for saponification reaction. Nile red (Acros Organics™) was added to the fat/oil at 0.01 mg per gram of fat/oil. The mixture was stirred in the dark for two hours at 450 rpm and then used for the production of calcium soaps as described in Section 3.3. A small portion of each soap sample was placed on a glass slide and secured with a cover slip that was sealed with a nail polish. Each specimen was scanned using an oil immersion objective lens (60x, 1.50 NA). Solid state laser was used to excite the dye at 488 nm and the detection of emission spectra was recorded at 532 nm. For each sample, the field of observation was randomly selected and its interior was scanned to at least 20 layers. From the scanned

layers, five layers were randomly chosen for the calculation of void area and circularity using NIS-Elements AR software (New York, USA). A void with a perfect circle is signified by a circularity value of 1.0, while a more elongated polygon or irregular void is indicated by a circularity value approaching zero (Rasband, 2000).

3.10 Synchrotron X-ray measurements

SAXS and WAXS measurements were performed at BL1.3W Siam Photon Laboratory of Synchrotron Light Research Institute (SLRI), Nakhon Ratchasima, Thailand. Synchrotron X-ray energy at 9.0 KeV, monochromatized by a double multilayer monochromator (W/B4C), was used to determine the diffraction patterns of the calcium soap samples. SAXS and WAXS sample to detector distances were at 1711.2 mm and 122.819 mm, respectively. Samples were fixed in a copper frame with a square aperture of 40x10 mm² and tests were conducted at 25°C. SAXS and WAXS profiles were recorded through MAR-CCD (Rayonix SX165) detector at 30 s exposure time. The data were analyzed using SAXSIT version 4.34 (Rugmai and Soontaranon, 2017). SAXS and WAXS diffraction patterns were plotted at a q range of 0.14-3.74 nm⁻¹ and 3.63-36.35 nm⁻¹, respectively.

3.11 Statistical analysis

SPSS Statistics 17.0 (SPSS Inc., Illinois, USA) was used for One-way Analysis of Variance (ANOVA) and Tukey Post Hoc Test to compare the significant differences among the group of samples. Pearson Correlation was also employed to determine the significant association of the quantifiable soap parameters. Statistical significance is indicated by p-value <0.05. All quantitative tests were conducted in triplicate.

CHAPTER IV

RESULTS AND DISCUSSION

4.1 Physical appearance of calcium soaps

In the soap-making process, the rapid mixing of the reactants produced a water-in-oil type of emulsion. During agitation, the calcium chloride soap mixtures showed more uniform and finer emulsion, while the calcium sulfate soap mixtures appeared marshmallow-like similar to the observation of Iasmin et al. (2014). Both types of emulsion became phase separated when mixing was ceased. Thus, centrifugation was employed in order to obtain a more homogeneous sample and practically isolate the crude soaps from the rest of the components. After centrifugation, three distinct soap fractions were observed (Figure 4.1). The first layer was the excess fat/oil, while the second and third layers were crude soaps with characteristic appearance and texture. The verification of their identities was done using FTIR and discussed in Section 4.2.1.

The separated crude calcium soaps from the second and third layer are presented in Figures 4.2 and 4.3. All soaps from the second layer were paste-like, which may be due to their direct exposure to the excess fat/oil. On the other hand, the soaps from the third layer were coarse, which may be attributed to the unreacted calcium particles that settled at the bottom of the container after centrifugation. As shown, palm olein oil, olive oil, and chicken fat produced yellow-colored soaps of decreasing intensities, while coconut oil, soybean oil, and pork fat produced whitish soaps of decreasing intensities. The color and solubility of the calcium source affected the appearance and texture of the

soaps. The soaps from calcium chloride were darker in color compared to the soaps from calcium sulfate. Their distinct appearance was similar to the observation of Iasmin et al. (2014). Moreover, the calcium chloride-based soaps taken from the second layer of the mixture were in the form of a thin paste, while the calcium sulfate-based soaps from the same layer were in the form of a thick paste. The calcium chloride-based soaps isolated from the third layer of the mixture were sandy and watery, while the calcium sulfate-based soaps from the same layer were lumpy and bulky. Overall, the calcium chloride-based soybean oil soaps exhibited the thinnest and most watery emulsion, whereas the calcium sulfate-based pork fat soaps exhibited the thickest and hardest emulsion. The viscosity and hardness of these soaps were verified quantitatively and discussed in Section 4.4.

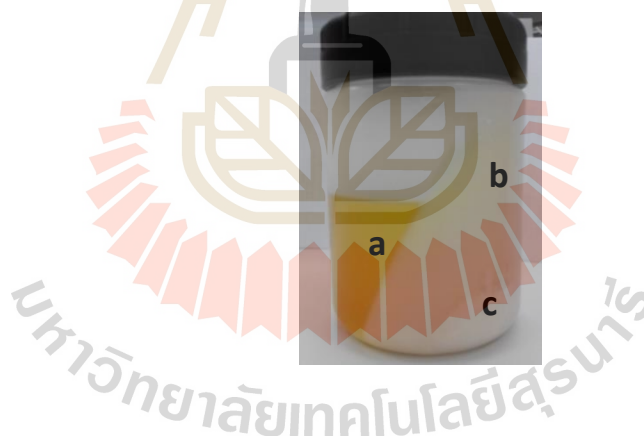


Figure 4.1 An example of a calcium soap fraction after centrifugation (palm oil-calcium chloride mixture): (a) excess oil; (b) calcium soap from the second layer; (c) calcium soap from the third layer.



Figure 4.2 Physical appearance of the soaps prepared from calcium chloride and various fat/oil sources (PO = palm olein oil; SO = soybean oil; OO = olive oil; CO = coconut oil; CF = chicken fat; PF = pork fat; the numbers indicate the layer the soaps were taken from the centrifuged mixture: 2= 2nd layer; 3= 3rd layer).

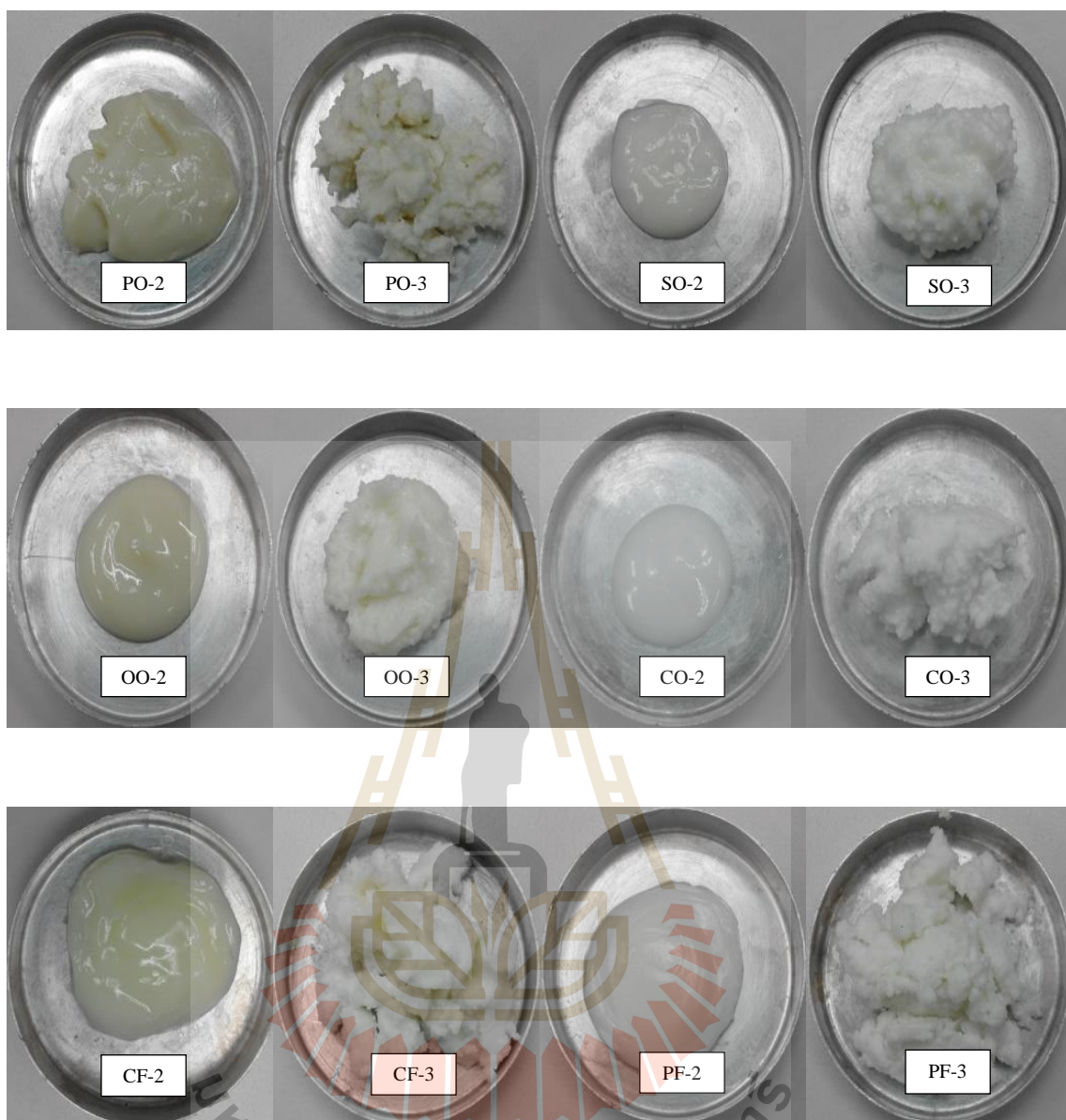


Figure 4.3 Physical appearance of the soaps prepared from calcium sulfate and various fat/oil sources (PO = palm olein oil; SO = soybean oil; OO = olive oil; CO = coconut oil; CF = chicken fat; PF = pork fat; the numbers indicate the layer the soaps were taken from the centrifuged mixture: 2= 2nd layer; 3= 3rd layer).

4.2 Saponification and yield of calcium soaps

4.2.1 FTIR spectra of raw fats/oils and their calcium soaps

The three distinct layers formed after the centrifugation of the soap mixtures underwent FTIR analysis to verify their identity. The liquid samples taken from the first layer of the centrifuged mixture were confirmed as excess fat/oil as their FTIR spectra resembled their raw fat/oil source (Figure 4.4). The bands of the excess fat/oil corresponded to the bands of the raw fat/oil used for the reaction that showed dominant spectra of triglyceride.

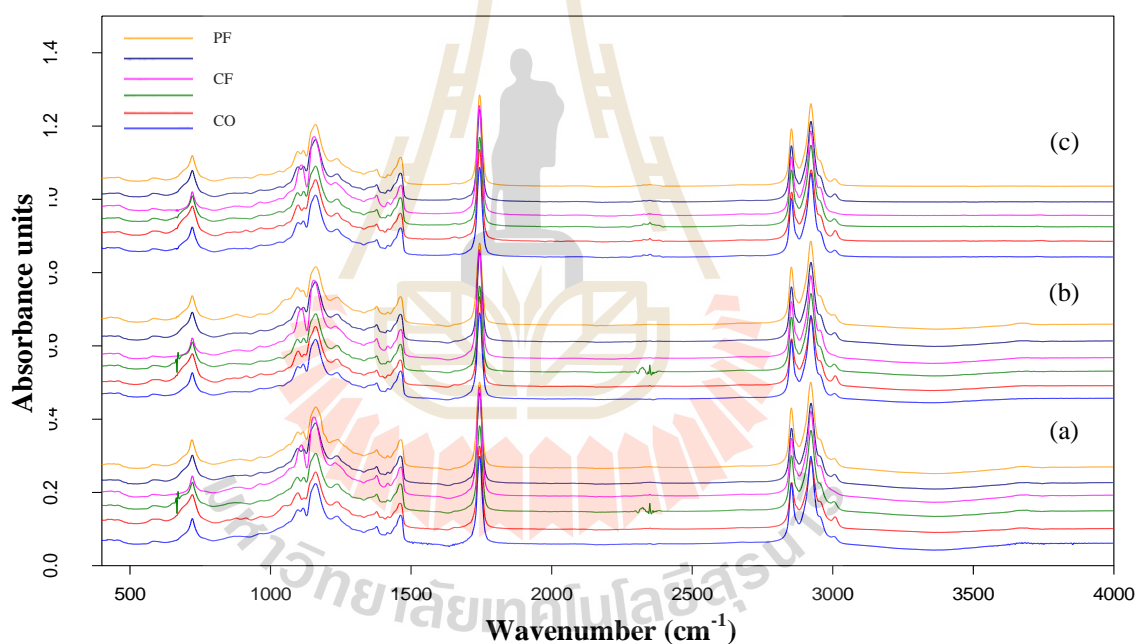


Figure 4.4 FTIR spectra of the raw fats/oils and excess fats/oils from saponification reaction: (a) raw fats/oils; (b) excess fats/oils from calcium chloride mixture; (c) excess fats from calcium sulfate mixture (PO = palm olein oil; SO = soybean oil; OO = olive oil; CO = coconut oil; CF = chicken fat; PF = pork fat).

As shown in Figure 4.4, the main peaks of the triglyceride functional groups displayed by the fats and oils were the =C-H (cis) stretching vibration around 3006 cm^{-1} , -C-H (CH_3) asymmetric stretching vibration at 2953 cm^{-1} , -C-H (CH_2) asymmetric stretching vibration at 2924 cm^{-1} , -C-H (CH_2) symmetric stretching vibration at 2853 cm^{-1} , -C=O (ester) stretching vibration at 1745 cm^{-1} , -C-H (CH_2) scissoring bending vibration at 1465 cm^{-1} , =C-H (cis) rocking bending vibration at 1417 cm^{-1} , -C-H (CH_3) symmetric bending vibration at 1377 cm^{-1} , -C-O stretching vibrations at 1238 cm^{-1} , 1163 cm^{-1} , 1118 cm^{-1} , and 1097 cm^{-1} , and $-(\text{CH}_2)_n-$ rocking vibration at 723 cm^{-1} (Guillen and Cabo, 1997; Lerma-García et al., 2010; Rohman and Che Man, 2011; Yang et al., 2005). Each type of fat/oil has a specific band intensity and frequency of maximum absorbance, which can be explained by its nature and components (Guillen and Cabo, 1997). In this study, the absorbance around 1745 cm^{-1} was considered to calculate the percent saponification of the crude calcium soaps as it gauges how much fat/oil was consumed in the reaction (He et al., 2011; Iasmin et al., 2014).

After the saponification process, the solids recovered from the second layer and third layer of the mixture were verified as calcium soaps based on their FTIR profile (Figures 4.5 and 4.6). The characteristic soap bands observed from the samples were the carboxylate ion symmetric stretching vibration between 1300 and 1420 cm^{-1} , carboxylate ion asymmetric stretching vibration between 1550 and 1610 cm^{-1} , and the metal-oxygen bond vibration around 670 cm^{-1} (He et al., 2011; Iasmin et al., 2014; Poulenat et al., 2003). It is visually noticeable that saponification caused the distinct appearance of bands between 1550 and 1610 cm^{-1} . Saponification also led to intense absorption at 670 cm^{-1} and 3400 cm^{-1} . The absorbance at 3400 cm^{-1} , which signifies the bound water associated with calcium soap, was also very evident in the studies of Iasmin et al. (2016), Iasmin et al. (2014), He et al. (2013), and He et al. (2011).

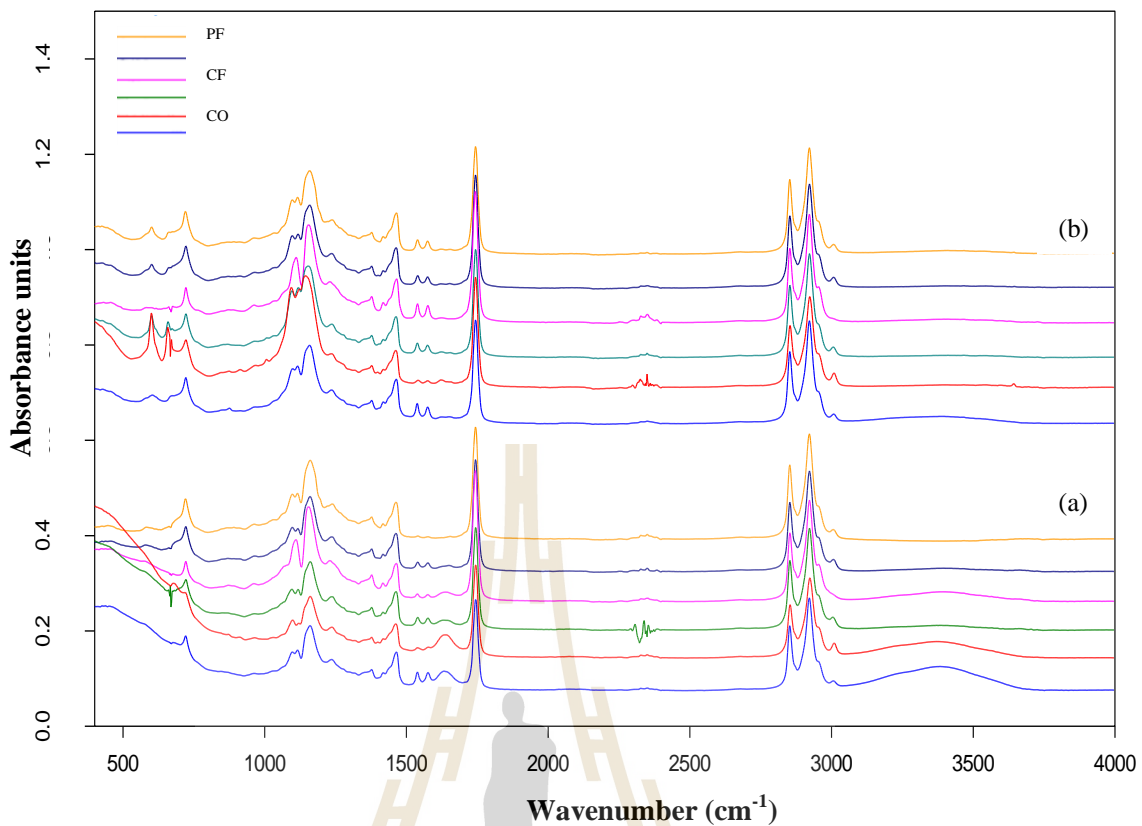


Figure 4.5 FTIR spectra of the calcium soaps taken from the second layer of the centrifuged mixture: (a) calcium chloride source; (b) calcium sulfate source (PO = palm olein oil; SO = soybean oil; OO = olive oil; CO = coconut oil; CF = chicken fat; PF = pork fat).

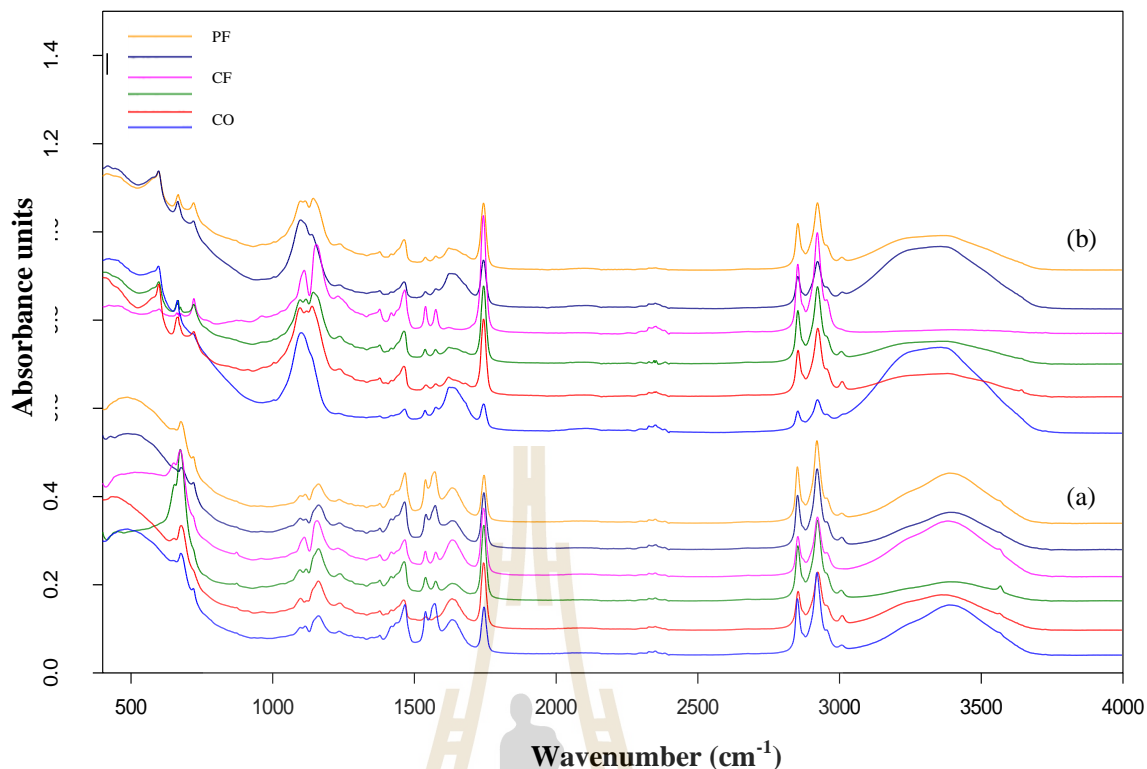


Figure 4.6 FTIR spectra of the calcium soaps taken from the third layer of the centrifuged mixture: (a) calcium chloride source; (b) calcium sulfate source (PO = palm olein oil; SO = soybean oil; OO = olive oil; CO = coconut oil; CF = chicken fat; PF = pork fat).

4.2.2 Saponification of calcium soaps

The degree of saponification of the calcium soaps was calculated based on their FTIR spectra. As shown in Figure 4.7, regardless of the calcium source, the soaps obtained from the third layer of the mixture generally had higher percent saponification compared to their counterpart from the second layer. This was due to their higher absorbance of characteristic soap bands. It is evident that the soaps from the third layer displayed more intense metal-oxygen bond vibration at 670 cm^{-1} , which is assumed to be caused by saponified solids and unreacted calcium (Iasmin et al., 2016). As previously

mentioned, the calcium particles preferentially settled in the third layer due to centrifugation. According to Iasmin et al. (2016), unreacted calcium can be considered as a false positive indicator of saponification because it has a similar peak with calcium-based saponified solids at about 670 cm^{-1} . The soaps from the third layer also had higher absorbance around 3400 cm^{-1} that represents the O-H stretching vibration of hydrated water in soap (He et al., 2011; Iasmin et al., 2016; Iasmin et al., 2014; Poulenat et al., 2003). As stated by Gross et al. (2017), metal ions can produce porous FOG deposits that can hold water. Since the soaps from the third layer had more calcium content (Figure 4.8), they absorbed more water into their matrix. Moreover, the soaps from the third layer generally exhibited lower absorbance at 1745 cm^{-1} , which implies that more fat/oil was consumed in the saponification reaction. In contrast, the high absorbance at 1745 cm^{-1} recorded from the soaps from the second layer reveals the presence of more unreacted fat/oil. This is expected since the soaps from the second layer were directly exposed to the excess fat/oil after centrifugation. Actually, the soap from the second layer functioned as an interface between the excess fat/oil and the soap from the third layer. As reported by He et al. (2013), oil can serve as a source of free fatty acid after alkaline hydrolysis or it can act as a carrier of pre-hydrolyzed free fatty acid and aid the saponification interface reaction. Therefore, the unreacted fats/oils can still be further transformed into FOG deposits given their prolonged exposure and interaction with water, oxygen, alkali, and available calcium cation (Choi and Chang, 2012; He et al., 2013; Iasmin et al., 2014).

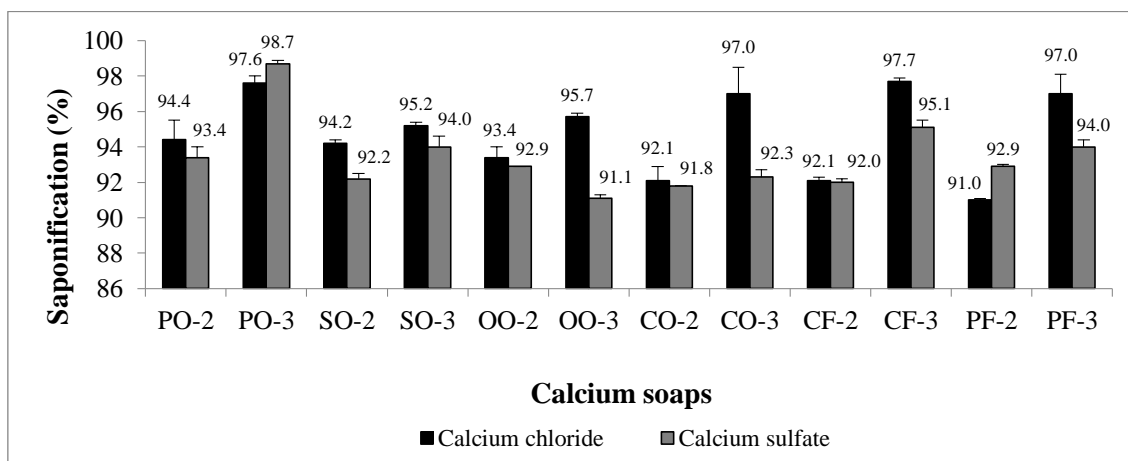


Figure 4.7 Percent saponification of the soaps prepared from different fat/oil and calcium sources (PO = palm olein oil, SO = soybean oil, OO = olive oil, CO = coconut oil, CF = chicken fat, PF = pork fat; the numbers indicate the layer the soaps were taken from the centrifuged mixture: 2= 2nd layer; 3= 3rd layer).

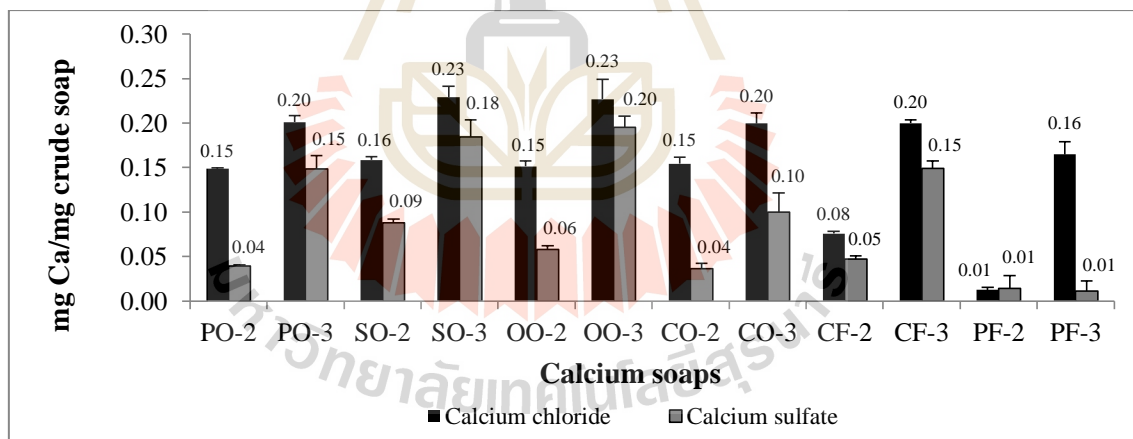


Figure 4.8 Calcium content of the soaps prepared from different fat/oil and calcium sources (PO = palm olein oil, SO = soybean oil, OO = olive oil, CO = coconut oil, CF = chicken fat, PF = pork fat; the numbers indicate the layer the soaps were taken from the centrifuged mixture: 2= 2nd layer; 3= 3rd layer).

4.2.3 Fatty acid profile of raw fats/oils and their calcium soaps

The fatty acid composition of the raw fats/oils and their corresponding soaps was analyzed in order to determine the effect of the saponification reaction on the fatty acid profile of the fats/oils. It was identified that the fatty acid profile of the raw fats and oils was not significantly altered by the saponification process (Table 4.1). This coincided with the reports of Iasmin et al. (2014) and Poulenat et al. (2004). Therefore, this parameter can trace the identity of the fat/oil waste in newly-formed FOG deposits (Keener et al., 2008; Montefrio et al., 2010; Williams et al., 2012).

Regardless of the calcium source, the results revealed that calcium soaps that contained a combination of palmitic acid, C16:0 (\approx 21-39%) and oleic acid, C18:1 (\approx 40-42%) were highly saponified. Specifically, palm olein oil, chicken fat, and pork fat soaps from the third layer consistently exhibited higher percent saponification (Figure 4.7).

Table 4.1 Major fatty acid composition of raw fats/oils and their calcium soaps.

| Samples* | Fatty acid composition (%) | | | | | |
|----------|-----------------------------|-----------------------------|--------------------------------|------------------------------|--------------------------------|------------------------------|
| | C12:0 | C14:0 | C16:0 | C18:0 | C18:1 | C18:2 |
| Raw | | | | | | |
| PO | | 1.0 \pm 0.0 ^{ab} | 38.4 \pm 0.1 ^k | 4.2 \pm 0.0 ^{abc} | 43.2 \pm 0.1 ⁱ | 11.6 \pm 0.0 ^c |
| SO | | | 11.4 \pm 0.0 ^{abc} | 3.8 \pm 0.1 ^{abc} | 22.4 \pm 0.1 ^b | 55.0 \pm 0.2 ^{jk} |
| OO | | | 11.8 \pm 0.2 ^{abc} | 3.2 \pm 0.0 ^{ab} | 75.2 \pm 0.4 ^l | 7.2 \pm 0.2 ^b |
| CO | 44.0 \pm 0.4 ^a | 22.4 \pm 0.5 ^d | 12.5 \pm 0.4 ^{abc} | 3.8 \pm 0.1 ^{abc} | 9.2 \pm 0.3 ^a | 2.7 \pm 0.1 ^a |
| CF | | 0.6 \pm 0.0 ^{ab} | 27.0 \pm 0.6 ^h | 5.7 \pm 0.1 ^{bcd} | 39.1 \pm 0.3 ^{defg} | 20.7 \pm 0.5 ^g |
| PF | | 1.4 \pm 0.0 ^{ab} | 23.7 \pm 0.2 ^{efgh} | 12.2 \pm 0.3 ^f | 40.7 \pm 0.3 ^{fghi} | 16.6 \pm 0.2 ^e |

*PO = palm olein oil; SO = soybean oil; OO = olive oil; CO = coconut oil; CF = chicken fat; PF = pork fat; the numbers indicate the layer the soaps were taken from the centrifuged mixture: 2= 2nd layer; 3= 3rd layer.

**Values followed by the same letter within the column are not significantly different ($p < 0.05$).

Table 4.1 Major fatty acid composition of raw fats/oils and their calcium soaps
(Continued).

| Samples* | Fatty acid composition (%) | | | | | |
|-------------------|----------------------------|-----------------------|-------------------------|-------------------------|----------------------------|------------------------|
| | C12:0 | C14:0 | C16:0 | C18:0 | C18:1 | C18:2 |
| CaCl ₂ | | | | | | |
| PO-2 | | 1.1±0.0 ^{ab} | 37.2±0.5 ^{jk} | 4.8±1.0 ^{abcd} | 38.6±0.3 ^{defgh} | 16.5±1.2 ^e |
| PO-3 | | 1.0±0.1 ^{ab} | 38.7±0.8 ^k | 4.2±0.1 ^{abc} | 40.2±0.6 ^{efghi} | 14.4±0.7 ^d |
| SO-2 | | | 12.9±0.5 ^{abc} | 3.7±0.2 ^{abc} | 23.2±0.7 ^{bc} | 54.2±0.6 ^{jk} |
| SO-3 | | | 13.6±0.6 ^{bc} | 4.2±0.5 ^{abc} | 23.0±0.8 ^{bc} | 52.9±1.2 ^j |
| OO-2 | | | 20.6±4.0 ^{de} | 4.3±0.9 ^{abc} | 62.4±3.7 ^j | 11.4±1.1 ^c |
| OO-3 | | | 18.8±0.5 ^d | 7.1±3.7 ^d | 62.3±2.7 ^j | 11.3±0.6 ^c |
| CO-2 | 44.4±0.2 ^a | 24.1±1.2 ^e | 14.0±0.7 ^c | 4.5±0.3 ^{abcd} | 7.9±0.9 ^a | 1.7±0.1 ^a |
| CO-3 | 45.6±1.7 ^a | 22.7±0.1 ^d | 12.6±1.1 ^{abc} | 3.8±0.3 ^{abc} | 8.2±1.0 ^a | 1.9±0.2 ^a |
| CF-2 | | 0.9±0.5 ^{ab} | 25.6±1.4 ^{gh} | 6.1±1.0 ^{cd} | 36.4±1.5 ^{de} | 22.8±1.3 ^h |
| CF-3 | | 0.7±0.0 ^{ab} | 24.2±0.5 ^{fgh} | 5.7±0.1 ^{bcd} | 35.9±0.9 ^d | 24.0±0.4 ^{hi} |
| PF-2 | | 1.6±0.1 ^b | 23.1±0.6 ^{efg} | 13.0±0.7 ^{ef} | 36.5±0.0 ^{def} | 20.1±1.1 ^{fg} |
| PF-3 | | 1.4±0.1 ^{ab} | 21.1±1.3 ^{def} | 12.3±0.5 ^{ef} | 41.8±0.7 ^{ghi} | 18.2±0.8 ^{ef} |
| CaSO ₄ | | | | | | |
| PO-2 | | 1.1±0.0 ^{ab} | 34.0±0.5 ^{ij} | 4.3±0.1 ^{abc} | 39.2±0.1 ^{defghi} | 17.7±0.6 ^e |
| PO-3 | | 1.0±0.1 ^{ab} | 30.8±0.9 ⁱ | 3.8±0.1 ^{abc} | 42.4±0.4 ^{hi} | 20.4±0.2 ^g |
| SO-2 | | | 10.5±0.4 ^{ab} | 3.3±0.1 ^{ab} | 23.6±0.3 ^{bc} | 53.1±0.4 ^{jk} |
| SO-3 | | | 9.9±0.2 ^a | 3.3±0.1 ^{ab} | 26.8±0.2 ^c | 56.3±0.2 ^l |
| OO-2 | | | 13.8±0.2 ^{bc} | 2.8±0.1 ^a | 67.2±0.3 ^k | 13.2±0.3 ^{cd} |
| OO-3 | | | 14.4±0.2 ^c | 2.9±0.4 ^a | 68.7±1.0 ^k | 12.5±0.1 ^{cd} |
| CO-2 | 46.4±0.9 ^a | 21.1±0.6 ^c | 11.3±0.6 ^{abc} | 3.3±0.2 ^{ab} | 8.4±0.4 ^a | 2.1±0.2 ^a |
| CO-3 | 44.6±0.6 ^a | 21.1±0.1 ^c | 11.7±0.5 ^{abc} | 3.5±0.2 ^{abc} | 8.8±0.1 ^a | 2.1±0.0 ^a |
| CF-2 | | 0.5±0.0 ^a | 22.8±0.1 ^{efg} | 5.0±0.0 ^{abcd} | 38.6±0.1 ^{defgh} | 25.0±0.1 ⁱ |
| CF-3 | | 0.5±0.0 ^a | 23.3±0.2 ^{efg} | 4.8±0.2 ^{abcd} | 39.6±0.2 ^{defghi} | 24.7±0.1 ⁱ |
| PF-2 | | 1.4±0.1 ^{ab} | 24.6±2.5 ^{gh} | 14.2±1.6 ^f | 43.2±4.6 ⁱ | 17.0±0.4 ^e |
| PF-3 | | 1.3±0.0 ^{ab} | 22.8±0.1 ^{efg} | 10.9±0.1 ^e | 43.3±0.1 ⁱ | 17.4±0.1 ^e |

*PO = palm olein oil; SO = soybean oil; OO = olive oil; CO = coconut oil; CF = chicken fat; PF = pork fat; the numbers indicate the layer the soaps were taken from the centrifuged mixture: 2= 2nd layer; 3= 3rd layer.

**Values followed by the same letter within the column are not significantly different (p<0.05).

4.2.4 Yield of calcium soaps

In this study, the process of saponification was done at a lower temperature to simulate the sewer condition, unlike the normal commercial/metal soap production that employs boiling condition. The modified saponification process resulted to the presence of excess fats/oils and calcium compounds. When centrifugation was employed after the reaction time, the excess calcium particles preferentially accumulated at the bottom of the bottle and contributed to the amount of solids in the third layer. As shown in Figure 4.9, the soaps from the third layer had significantly higher yield or total solids formed compared to the soaps from the second layer. In general, calcium sulfate-based soaps from the third layer had the higher yield.

Among the soaps, calcium sulfate-based coconut oil soap from the third layer had the highest soap yield (32.1%) that was followed by calcium sulfate-based soybean oil soap from the same layer (28.4%). Interestingly, calcium chloride-based coconut oil soap and calcium chloride-based soybean oil soap from the third layer only produced small amount of solids (12.7% and 7.2%, respectively). Hence, the trend in the yield may be linked to the availability of the calcium compounds and their solubility. Calcium chloride and calcium sulfate solubilities (expressed as mass percent of solute) at 25°C are 44.83 and 0.21, correspondingly (Haynes, 2010). It is hypothesized that the greater amount of solids formed from calcium sulfate soap mixtures were due to the presence of more excess calcium sulfate. Calcium sulfate has a low solubility product constant, K_{sp} of 2×10^{-5} at 25°C (Sawyer et al., 2003). Thus, based on the soap formulation of Iasmin et al. (2014) (9.8 wt% calcium compound per 14.9 wt% water), calcium sulfate reached its saturation point (Sawyer et al., 2003). This proves the initial assumption of Keener et al. (2008) and He et al. (2011) that mineral deposits also contribute to the formation of solids in the sewer.

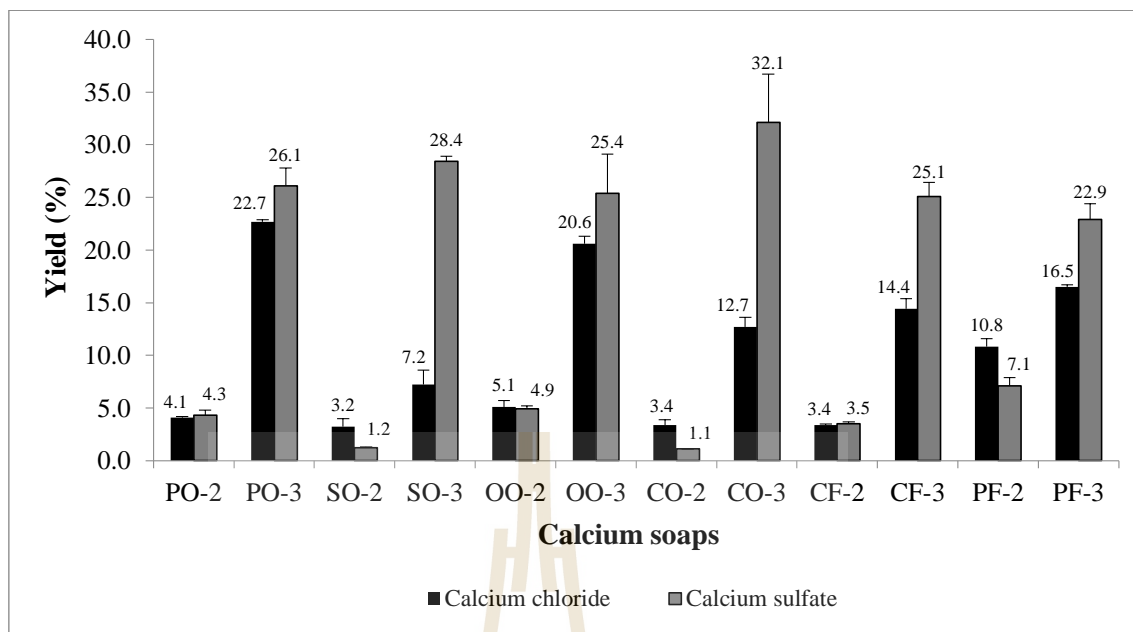


Figure 4.9 Percent yield of the soaps prepared from different fat/oil and calcium sources (PO = palm olein oil, SO = soybean oil, OO = olive oil, CO = coconut oil, CF = chicken fat, PF = pork fat; the numbers indicate the layer the soaps were taken from the centrifuged mixture: 2= 2nd layer; 3= 3rd layer).

Although calcium sulfate-based soaps generally had higher yield or solids formed compared to calcium chloride-based soaps, their degree of saponification was lower than calcium chloride-based soaps. This is the case since calcium sulfate is less soluble; thus, lesser calcium ions in the solution reacted with the fats/oils. As a consequence, the reaction produced soaps with lower calcium content. This supported the observation of Iasmin et al. (2014), which revealed that the calcium content of calcium sulfate-based soaps from canola oil and beef tallow were lower compared to their counterpart using calcium chloride.

Based on the yield and saponification readings, it can be deduced that the high solids formed after the reaction time do not directly translate to high percent saponification. For instance, calcium sulfate-based coconut oil soap from the third layer, which registered the highest yield among the samples (Figure 4.9), had relatively low percent saponification (Figure 4.7). This verified the assumption that FOG deposits are not exclusively products of chemical reaction but also physical accumulation of unreacted calcium and fatty acids (Gu et al., 2015; He et al., 2013; He et al., 2011).

The trend in the yield and saponification values provides additional evidence that FOG deposits may also consist of crystallized fatty acids (Gross et al., 2017) or oil accumulations without saponification (Keener et al., 2008). Overall, the results substantiated the proposed mechanism of FOG deposit formation by He et al. (2013), which states that FOG deposit is a combination of saponified solids and aggregates of excess calcium, unreacted free fatty acids, and debris in the drainage system. As illustrated in Figure 4.10a, the metallic salt (RCOOCa) serves as a core adhered to the sewer wall. The fat/oil waste (RCOOR), which is drawn onto the core, functions as a carrier of free fatty acids (RCOOH). The calcium cations (Ca^{2+}) that are present in concrete corrosion or wastewater are attracted to the free fatty acids (DLVO theory). Eventually, the physical aggregation results in more saponified solids causing greater FOG deposit build up and layering. FOG deposit becomes bigger and harder to manage if solid wastes and other compounds from the wastewater are attached to it forming a “fatberg” (Wallace et al., 2016). The proposed mechanism may be used to describe the observed layering in FOG deposit from the sewer, which specifically showed layers of debris intermixed with hardened FOG (Figure 4.10b) (Keener et al., 2008).

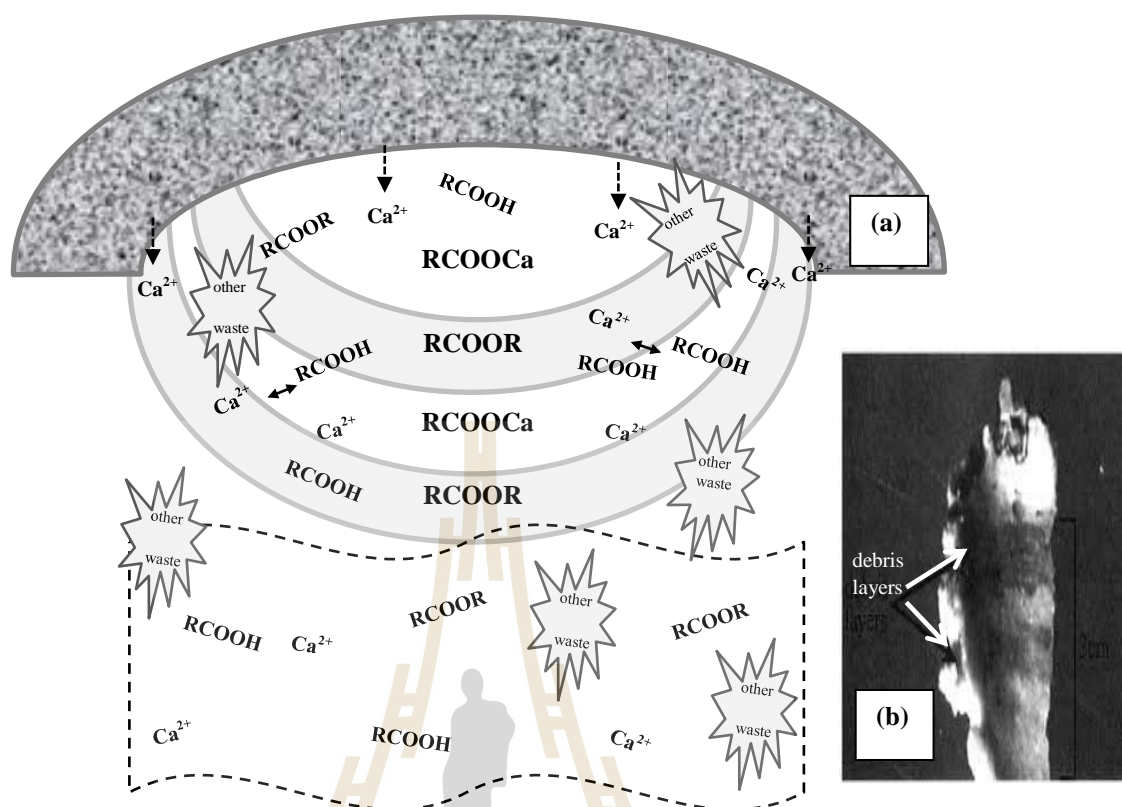


Figure 4.10 FOG deposit layering: (a) proposed mechanism for FOG deposit layering; (b) FOG deposit layering observed in the sewer (Keener et al., 2008).

4.3 Melting endset of raw fats/oils and calcium soaps

This study emphasized on the melting endset of the calcium soaps to detect the possible temperature at which the FOG deposits will be destabilized. As shown in Figure 4.11, the average melting endset of fats/oils and their corresponding soaps was very diverse. Saponification had caused these fats and oils to behave differently. Among the raw fats/oils, soybean oil exhibited the lowest melting endset since it contains a high percentage of long chain polyunsaturated fatty acid (C18:2). On the other hand, chicken fat manifested the highest melting endset, which was not significantly different from pork fat and coconut oil. These lipids melted at higher temperature because of their fatty

acid composition. Specifically, chicken and pork fat is mainly made up of long chain saturated fatty acids (C16:0 and C18:0) and long chain mono-unsaturated fatty acid (C18:1), while coconut oil is largely comprised of medium chain saturated fatty acid (C12:0 and C14:0) (Table 4.1).

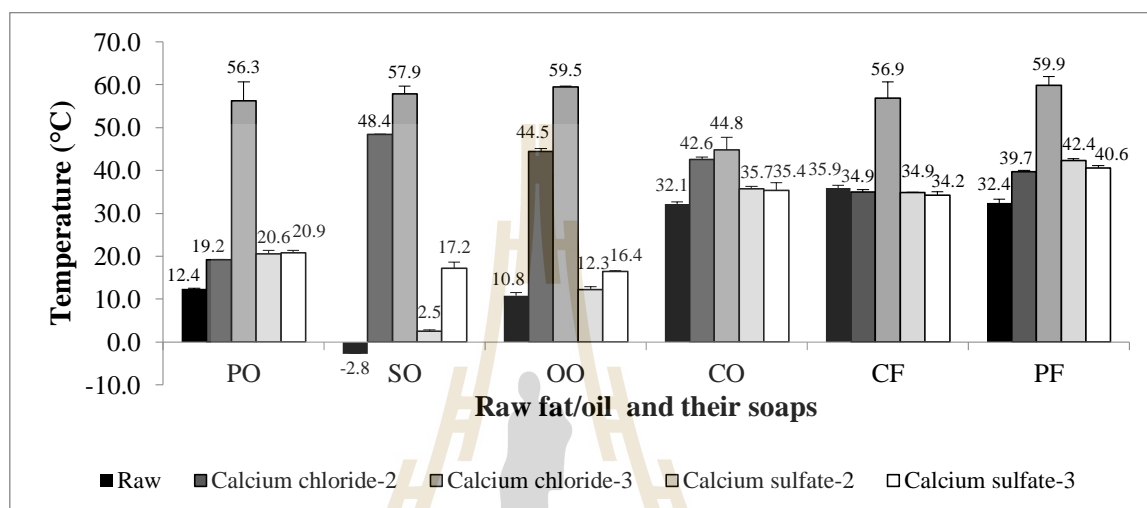


Figure 4.11 Melting endset of the raw fats/oils and their calcium soaps (PO = palm olein oil, SO = soybean oil, OO = olive oil, CO = coconut oil, CF = chicken fat, PF = pork fat; the numbers indicate the layer the soaps were taken from the centrifuged mixture: 2= 2nd layer; 3= 3rd layer).

The melting endset of the soaps produced was greatly influenced by the type of calcium source and calcium content. Particularly, the melting endset readings recorded from calcium sulfate-based soaps were considerably lower (2.5-42.4°C) compared to the readings from calcium chloride-based soaps (19.2-59.9°C). This is because calcium sulfate-based soaps had lower percent saponification, more unreacted fat, and lesser calcium content. Statistically, calcium content and melting endset has a positive linear relationship ($r = 0.345$), which justified the report of Williams et al. (2012).

Considering a maximum sewer temperature of 25°C (Iasmin et al., 2014), only calcium chloride-based palm olein oil soap from the second layer as well as calcium sulfate-based palm olein oil, soybean oil, and olive oil soaps can be potentially destabilized. However, industrial wastewater may reach up to 50°C (Ashan et al., 2005; Fabiyi and Larrea, 2015); thus, more types of calcium soaps may be destabilized in such temperature. Further, the more heat-stable soaps such as calcium chloride-based soaps from the third layer are not expected to largely accumulate in areas where automatic dishwashers are used since the water temperature setting of dishwashers is as high as 71°C (Emmel et al., 2003; Heger, 2017). It is anticipated that during the cleaning period, the warmer wastewater will weaken all types of calcium soaps.

In terms of the effect of fat/oil source on the melting endset of the soaps, results revealed that regardless of the calcium source, pork fat soaps from the third layer consistently had the highest melting endset. This signifies that the abundance of calcium and the presence of palmitic acid ($\approx 21\text{-}23\%$), oleic acid ($\approx 42\text{-}43\%$), and linoleic acid ($\approx 17\text{-}18\%$) can generate more heat-stable FOG deposits. As a consequence, the deposits tend to adhere and accumulate on the sewer walls. Additionally, the results imply that FOG deposits formed from a corroded sewer environment (high levels of calcium sulfate) and highly unsaturated oils such as soybean and olive oils are unstable even at sewer temperature below 20°C.

4.4 Rheology of calcium soaps

4.4.1 Apparent viscosity

In order to visualize the flow behavior of the calcium soaps, their apparent viscosity (η) was examined at increasing shear rate and a constant temperature of 25°C. As shown in Figure 4.12, the η values of the soaps decreased as shear rate increased. At

the initial shear rate of 1.0 s^{-1} , calcium chloride-based soaps generally had higher apparent viscosity (between $10^2 \text{ Pa}\cdot\text{s}$ and $10^3 \text{ Pa}\cdot\text{s}$) than calcium sulfate-based soaps (between $10^1 \text{ Pa}\cdot\text{s}$ and $10^3 \text{ Pa}\cdot\text{s}$). However, at 100 s^{-1} onwards, calcium chloride-based soaps indicated a weaker structure as their apparent viscosity reduced more drastically (up to $10^{-2} \text{ Pa}\cdot\text{s}$) than calcium sulfate-based soaps ($10^{-1} \text{ Pa}\cdot\text{s}$). The apparent viscosity-shear rate plot is useful in choosing the shear rate setting of fluid movers or pumps to destabilize a certain type of FOG deposit.

Considering a shear rate of 100 s^{-1} at 25°C , a clear distinction between calcium chloride and calcium sulfate-based soaps was observed (Figure 4.13). Per soap layer, calcium chloride-based soaps commonly exhibited lower apparent viscosity readings (η_{100}) compared to calcium sulfate-based soaps. Moreover, calcium chloride-based soaps from the third layer had generally lower apparent viscosity than calcium chloride-based soaps from the second layer. This may be caused by their grainy and moister texture. In contrast, calcium sulfate-based soaps from the third layer had higher apparent viscosity than calcium sulfate-based soaps from the second layer. This can be attributed to their lumpy appearance.

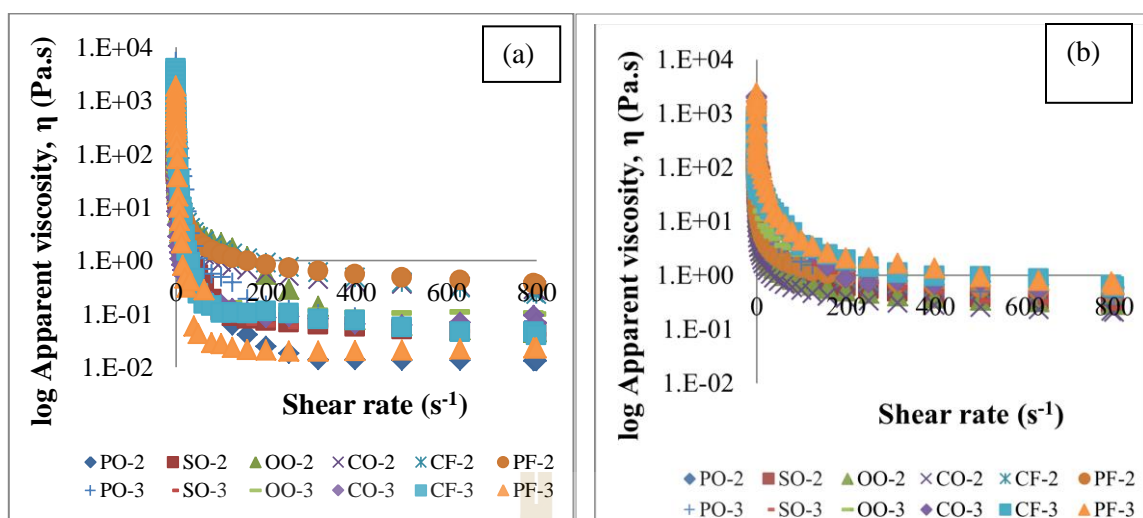


Figure 4.12 Apparent viscosity (η) curves at 25°C of calcium soaps prepared from various fats/oils: (a) calcium chloride; (b) calcium sulfate (PO = palm olein oil; SO = soybean oil; OO = olive oil; CO = coconut oil; CF = chicken fat; PF = pork fat; the numbers indicate the layer the soaps were taken from the centrifuged mixture: 2= 2nd layer; 3= 3rd layer).

Among the soaps, calcium sulfate-based pork fat soap from the third layer exhibited the highest apparent viscosity (4.37 Pa.s) at 100s⁻¹ shear rate (Figure 4.13), which reflects its high resistance to flow. This type of soap had a higher percentage of oleic acid, C18:1 (43%) and palmitic acid, C16:0 (23%) (Table 4.1). The fatty acid combination is considered to greatly influence the resistance to flow of the soap since based on the study of He et al. (2013), calcium soaps with high oleic to palmitic acid ratio are harder. Moreover, oleic acid is known to produce sticky soaps (Girgis et al., 1998; He et al., 2013), while palmitic acid is recognized to produce hard soaps (Beetseh and Godwin, 2015). Additionally, calcium sulfate-based coconut oil soap from the third layer registered the second highest apparent viscosity reading (4.17 Pa.s). This is

reasonable since it contained a huge portion of saturated fatty acids such as lauric acid, C12:0 (45%) and myristic acid, C14:0 (21%) that are identified to solidify at a lower temperature (Fennema et al., 2008; Rosell, 1999).

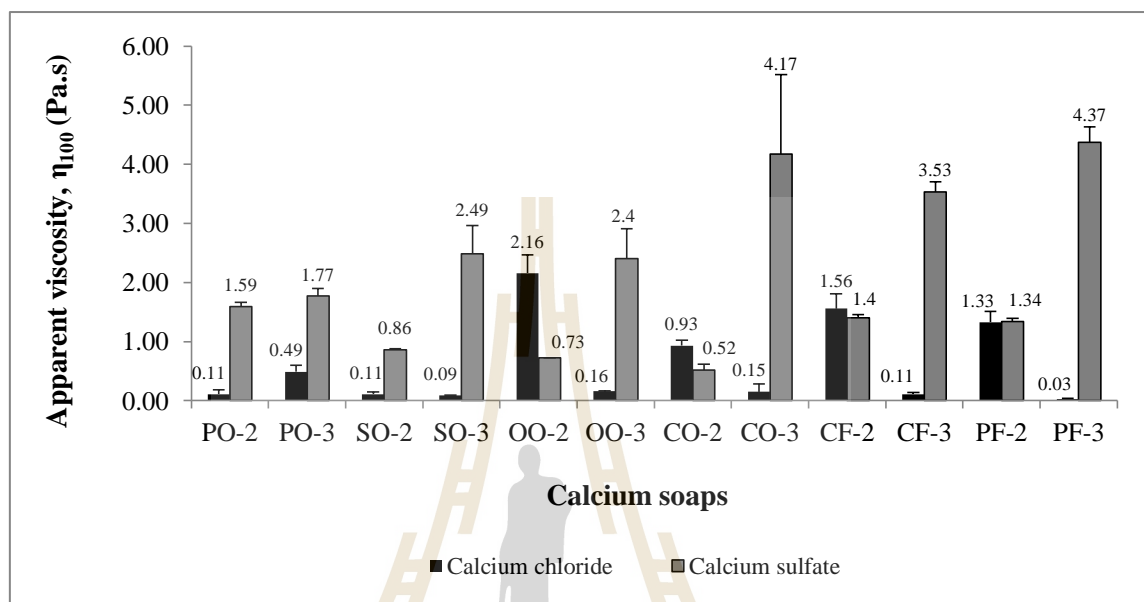


Figure 4.13 Apparent viscosity (η_{100} at 25°C) of the soaps from different fat/oil and calcium sources (PO = palm olein oil, SO = soybean oil, OO = olive oil, CO = coconut oil, CF = chicken fat, PF = pork fat; the numbers indicate the layer the soaps were taken from the centrifuged mixture: 2= 2nd layer; 3= 3rd layer).

It can be recalled that calcium sulfate-based coconut oil soap from the third layer had the highest yield (Figure 4.9), while calcium sulfate-based pork fat soap from the third layer had the highest melting endset (Figure 4.11). This suggests that the saponification of coconut oil and pork fat with calcium sulfate, which is a product of concrete corrosion, can potentially cause higher incidence of sewer blockages since they can either occur in large quantity or can withstand warmer temperature.

4.4.2 Viscoelasticity

The calcium soaps were further scrutinized for their viscoelastic behavior through oscillatory temperature sweep test. Typically, a sewer temperature ranges from 5-25°C (Iasmin et al., 2014), but some industries, household, and FSEs release warmer wastewater due to their processing and dishwashing activities (Ashan et al., 2005; Fabiyi and Larrea, 2015; Emmel et al., 2003; Heger, 2017). Therefore, the temperature range of the oscillatory test was broadened to 5-60°C to determine the possible effects of warmer wastewater or sewer environment on FOG deposits.

Figure 4.14 illustrates the viscoelastic profile of calcium chloride-based soaps under temperature sweep test. Palm olein oil soap from the second layer initially indicated a dynamic rearrangement of particles with its overlaps in G' and G'' . It finally manifested a stable gel point and maximum G' (8.4×10^3 Pa) at 17°C. However, its G' gradually decreased as temperature further increased. This reflected the weakening of the soap structure. Palm olein oil soap from the third layer remained solid-like within the temperature range. It showed maximum G' (1.3×10^4 Pa) at 12°C, but it eventually decreased as the temperature elevated. Soybean oil soap from the second layer exhibited solid-like behavior throughout the temperature range. Its G' consistently increased until it reached its maximum peak (3.6×10^3 Pa) at 48°C. Beyond this, its G' started to decrease. Soybean oil soap from the third layer indicated a solid-like behavior throughout the temperature range. It started with high G' (7.8×10^2 Pa) at 5°C, which gradually reached to its lowest value (5.5×10^2 Pa) at 40°C. However, it signified structure recovery above 40°C as its G' started to increase and attained its peak (8.3×10^2 Pa) at 60°C. Olive oil soap from the second layer showed a solid-like behavior throughout the temperature range. It exhibited an increasing trend in G' as the temperature progressed. Its maximum G' (2.4×10^3 Pa) was noted at 58°C. Olive oil soap from the third layer also displayed a

solid-like behavior within the temperature range. It started with high G' that reached its peak (1.7×10^3 Pa) at 17°C . However, its G' steadily decreased to its lowest value (1.3×10^3 Pa) at 49°C . Nevertheless, its G' began to increase as it approached 60°C . Coconut oil soap from the second layer had its gel point at 24°C , but its G' steadily decreased until 45°C . It showed structure recovery above 45°C and its maximum G' (8.6×10^3 Pa) was recorded at 57°C . Coconut oil soap from the third layer consistently manifested a solid-like behavior. Its maximum G' (2.6×10^5 Pa) was recorded at 8°C , while its minimum G' (1.0×10^3 Pa) was noted at 44°C . Above this temperature, its G' manifested structure recovery. Chicken fat soap from the second layer showed a stable gel point and maximum G' (2.0×10^4 Pa) at 23°C . However, its G' consistently decreased as the temperature increased. Chicken fat soap from the third layer showed a solid-like behavior within the temperature range. It had its maximum G' (9.7×10^3 Pa) at 17°C , which progressively decreased as the temperature increased. Pork fat soap from the second layer exhibited a stable gel point and maximum G' (3.6×10^4 Pa) at 19°C . However, the soap became weak and transitioned from solid to liquid-like ($G'' > G'$) above 33°C . Pork fat soap from the third layer maintained its solid-like property within the temperature range. It had a maximum G' (8.8×10^3 Pa) at 13°C , which gradually decreased as the temperature increased.

Figure 4.15 displays the viscoelastic profile of calcium sulfate-based soaps. Palm olein oil soap from the second layer manifested crystallization at 7°C based on its G' peak (4.5×10^3 Pa). As the temperature progressed, its G' decreased and reached its minimum value (9.0×10^2 Pa) at 20°C . Nevertheless, the soap showed gradual structure recovery above 20°C as its G' began to increase. Palm oil soap from the third layer also showed a similar trend, but it exhibited the highest G' (1.3×10^5 Pa) at a more elevated temperature of 17°C . It had minimum G' (7.9×10^4 Pa) at 28°C but started

to recover as the temperature progressed. Soybean oil soap from the second layer displayed solid-like behavior throughout the temperature range. It had its G' peak (3.0×10^3 Pa) at 49°C , but eventually manifested structure weakening as the temperature progressed. Soybean oil soap from the third layer followed the same trend, but had its peak G' (2.1×10^5 Pa) at 51°C . Olive oil soap from the second layer exhibited a stable solid-like form when exposed to increasing temperature. Its G' even increased at temperatures above 46°C and reached its maximum value (2.9×10^3 Pa) at 60°C . Olive oil soap from the third layer demonstrated the same inclination, although it was more stable based on its maximum G' (1.4×10^5 Pa) at 60°C . Coconut oil soap from the second layer gained its stable gel point and maximum G' (2.6×10^4 Pa) at 23°C . Its G' slowly decreased as the temperature accelerated. Coconut oil soap from the third layer maintained its solid-like nature the entire temperature range. Its maximum G' (4.62×10^5 Pa) was noted at 13°C . However, its G' steadily decreased above 29°C . Chicken fat soap from the second layer embodied attained its gel point and maximum G' (2.8×10^4 Pa) at 21°C . Its G' gradually decreased and reached its minimum value (1.26×10^3 Pa) at 38°C . As the temperature further progressed, the soap indicated structure recovery with its increasing G' . Chicken fat soap from the third layer maintained its solid-like behavior all throughout the test. It had its peak G' (2.9×10^5 Pa) at 13°C , but it decreased as temperature increased. Pork fat soap from the second layer signified a stable gel point and maximum G' (9.8×10^3 Pa) at 27°C . As the temperature accelerated, its G' decreased and reached its minimum value (1.36×10^2 Pa) at 54°C . Pork fat soap from the third layer remained solid-like the entire temperature range with its peak G' (3.9×10^5 Pa) at 15°C . As the temperature progressed, its G' slowly decreased.

The important observations noted from the temperature sweep test are summarized in Table 4.2. Based on the results, calcium sulfate-based soaps from the

third layer had constantly higher G' values than calcium-chloride based soaps. This is consistent with the work of Iasmin et al. (2014) as calcium sulfate-based canola oil soap had higher G' values than calcium chloride-based canola oil soap under oscillatory stress sweep test. On the other hand, regardless of the calcium source, coconut oil, chicken fat, and pork fat soaps from the second layer did not instantly manifest a solid-like behavior but attained their gel point at a certain temperature. This was also noticed in calcium chloride-based palm olein oil soap from the second layer. As discussed earlier, soaps from the second layer were paste-like, thus, they may be more vulnerable to changes in temperature. Moreover, palm olein oil, coconut oil, chicken fat, and pork fat soaps had many types of fatty acids (Table 4.1), which may have affected their viscoelastic properties given the temperature range.

Among the soaps tested, soybean and olive oil soaps showed a more stable gel within the temperature range based on their increased G' as temperature increased. Their behavior is may be caused by their fatty acid profile, which was largely composed of linoleic acid, C18:2 and oleic acid, C18:1, respectively. According to Adhvaryu et al. (2005), an increase in fatty acid chain length promotes the formation of interlocking and long chain fibers that are more flexible to external stress. However, since soybean and olive oil soaps are highly unsaturated, their soap structure is still unstable under extreme condition as evidenced by their low melting endset (Figure 4.11).

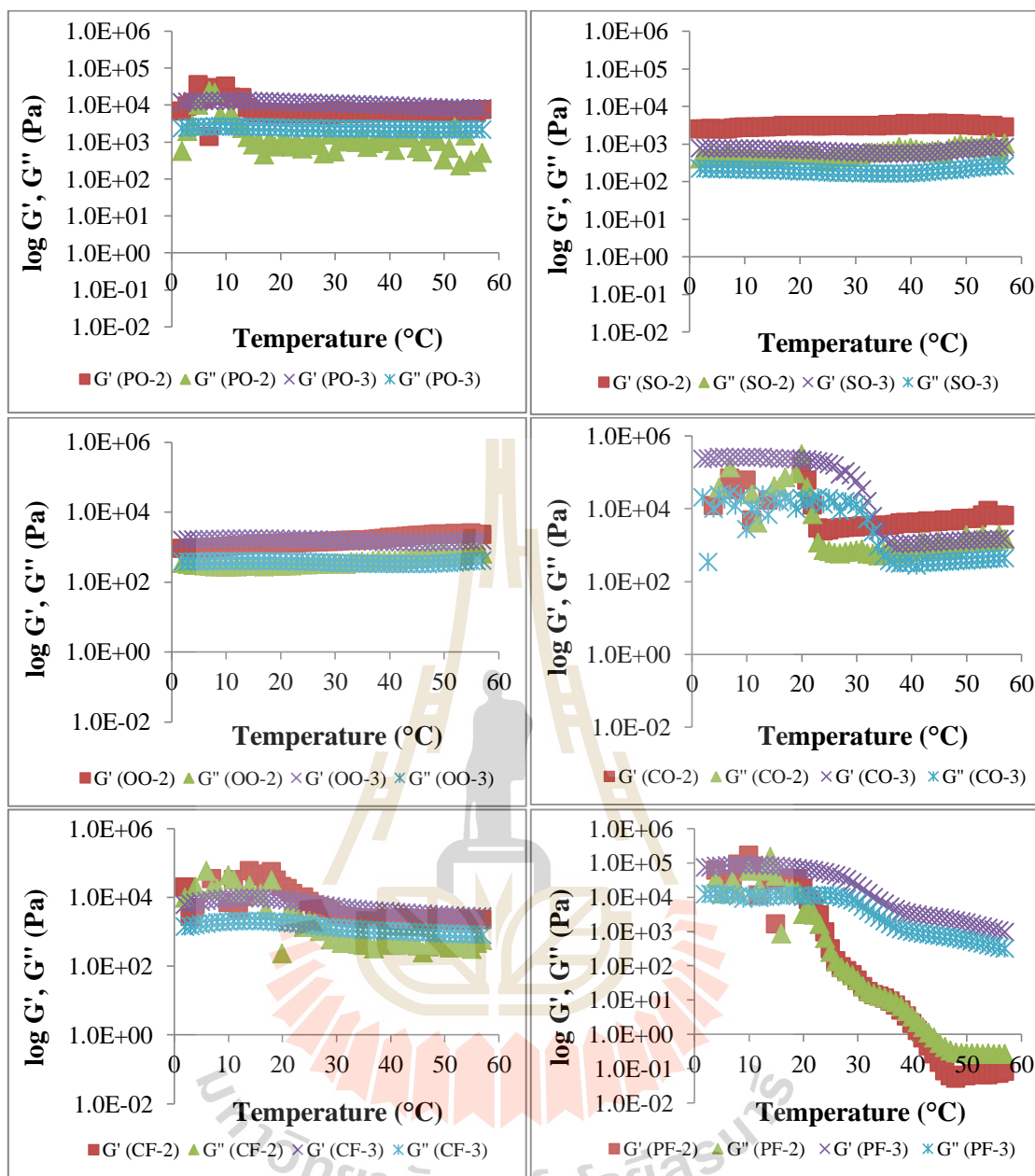


Figure 4.14 Temperature stress dependence of the soaps prepared from calcium chloride and various fats/oils (PO = palm olein oil; SO = soybean oil; OO = olive oil; CO = coconut oil; CF = chicken fat; PF = pork fat; the numbers indicate the layer the soaps were taken from the centrifuged mixture: 2= 2nd layer; 3= 3rd layer).

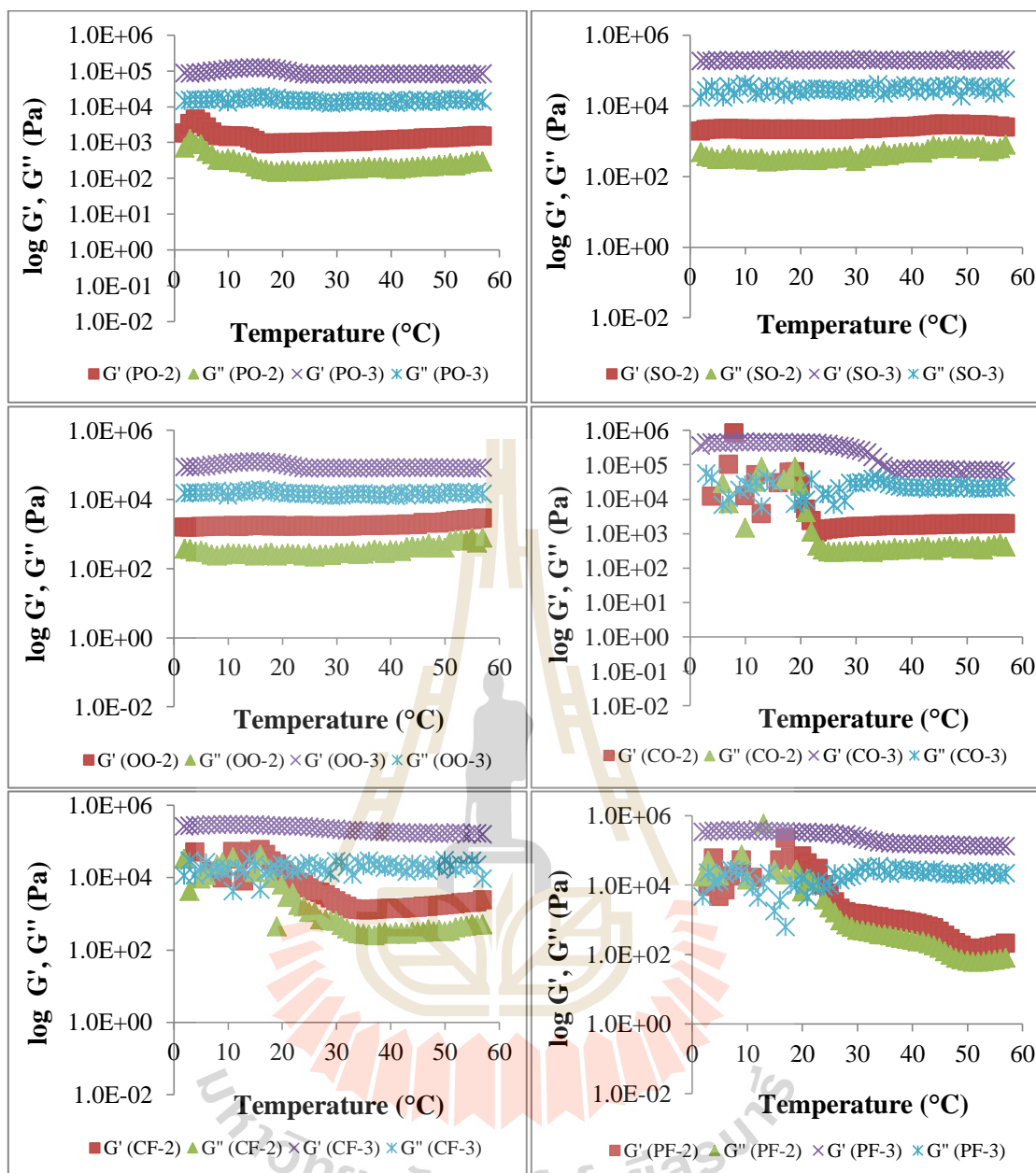


Figure 4.15 Temperature stress dependence of the soaps prepared from calcium sulfate and various fats/oils (PO = palm olein oil; SO = soybean oil; OO = olive oil; CO = coconut oil; CF = chicken fat; PF = pork fat; the numbers indicate the layer the soaps were taken from the centrifuged mixture: 2= 2nd layer; 3= 3rd layer).

Table 4.2 Summary of the viscoelastic properties of calcium soaps under oscillatory temperature sweep test.

| Soaps | Observations | |
|-------|---|---|
| | CaCl ₂ | CaSO ₄ |
| PO-2 | Gel point and maximum G' (8.4 x 10 ³ Pa) at 17°C | Consistent solid-like behavior; maximum G' (4.5 x 10 ³ Pa) at 7°C |
| PO-3 | Consistent solid-like behavior; maximum G' (1.3 x 10 ⁴ Pa) at 12°C | Consistent solid-like behavior; maximum G' at 1.3 x 10 ⁵ (17°C) |
| SO-2 | Consistent solid-like behavior; maximum G' (3.6 x 10 ³ Pa) at 48°C | Consistent solid-like behavior; maximum G' (3.0 x 10 ³ Pa) at 49°C |
| SO-3 | Consistent solid-like behavior; maximum G' (8.3 x 10 ² Pa) at 60°C | Consistent solid-like behavior; maximum G' (2.1 x 10 ⁵ Pa) at 51°C |
| OO-2 | Consistent solid-like behavior; maximum G' (2.4 x 10 ³ Pa) at 58°C | Consistent solid-like behavior; maximum G' (2.9 x 10 ³ Pa) at 60°C |
| OO-3 | Consistent solid-like behavior; maximum G' (1.7 x 10 ³ Pa) at 17°C | Consistent solid-like behavior; maximum G' (1.4 x 10 ⁵ Pa) at 60°C |
| CO-2 | Gel point and maximum G' (5.9 x 10 ⁴ Pa) at 24°C | Gel point and maximum G' (2.6 x 10 ⁴ Pa) at 23°C |
| CO-3 | Consistent solid-like behavior; maximum G' (2.6 x 10 ⁵ Pa) at 8°C | Consistent solid-like behavior; maximum G' (4.6 x 10 ⁵ Pa) at 13°C |
| CF-2 | Gel point and maximum G' (2.0 x 10 ⁴ Pa) at 23°C | Gel point and maximum G' (2.8 x 10 ⁴ Pa) at 21°C |
| CF-3 | Consistent solid-like behavior; maximum G' (9.7 x 10 ³ Pa) at 17°C | Consistent solid-like behavior; maximum G' (2.9 x 10 ⁵ Pa) at 13°C |
| PF-2 | Gel point and maximum G' (3.6 x 10 ⁴ Pa) at 19°C; Liquid-like (G''>G') above 33°C | Gel point and maximum G' (9.8 x 10 ³ Pa) at 27°C |
| PF-3 | Consistent solid-like behavior; maximum G' (8.8 x 10 ³ Pa) at 13°C | Consistent solid-like behavior; maximum G' (3.9 x 10 ⁵ Pa) at 15°C |

*PO = palm olein oil; SO = soybean oil; OO = olive oil; CO = coconut oil; CF = chicken fat; PF = pork fat; the numbers indicate the layer the soaps were taken from the centrifuged mixture: 2= 2nd layer; 3= 3rd layer.

At 25°C, the $\text{Tan } \delta$ or G''/G' ratio of the soaps were calculated. $\text{Tan } \delta$ lesser than 1 indicates predominantly elastic (solid-like) behavior, while $\text{Tan } \delta$ greater than 1 signifies predominantly viscous (liquid-like) behavior (Choi and Chang, 2012). Based on their $\text{Tan } \delta$ values (Figure 4.16), the soaps from the third layer mainly exhibited more solid-like characteristics. This is most especially observed in calcium sulfate-based soaps from the third layer. Incidentally, these soaps were also found to generally manifest higher apparent viscosity (η_{100}) at 25°C.

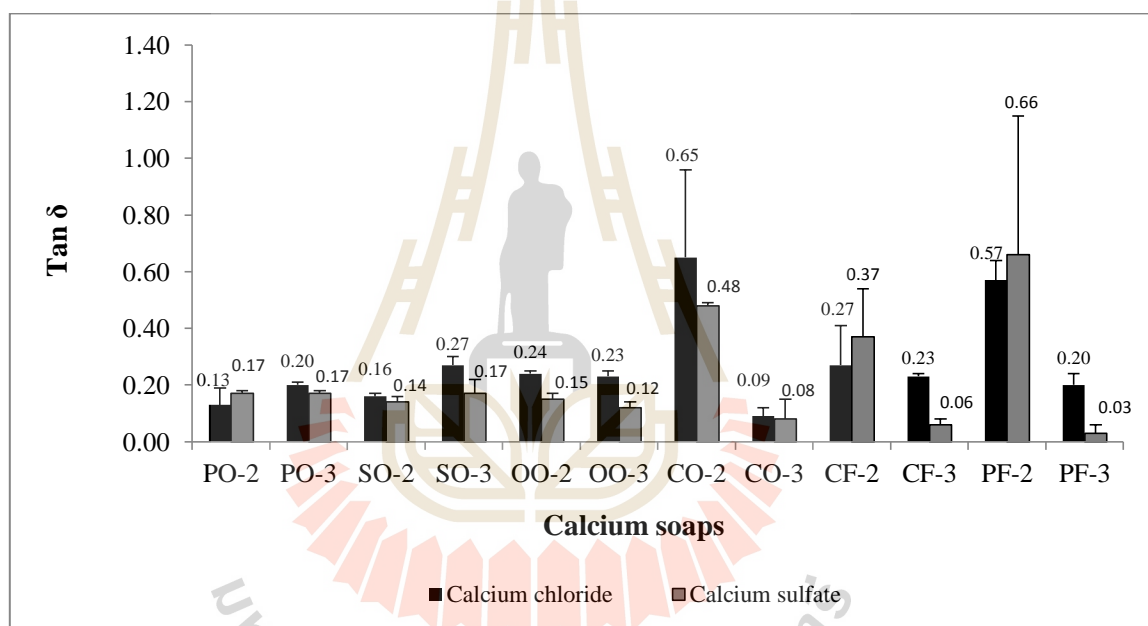


Figure 4.16 $\text{Tan } \delta$ of the soaps at 25°C prepared from different fat/oil and calcium sources (PO = palm olein oil, SO = soybean oil, OO = olive oil, CO = coconut oil, CF = chicken fat, PF = pork fat; the numbers indicate the layer the soaps were taken from the centrifuged mixture: 2= 2nd layer; 3= 3rd layer).

4.5 Microstructure of calcium soaps

4.5.1 ESEM images

To further comprehend the stability of the calcium soaps, their microstructure was probed through environmental scanning electron microscope (ESEM). As shown in Figures 4.17 and 4.18, the soaps made from the same fat/oil source displayed a distinct microstructure depending on the calcium source and the layer they were recovered.

Figure 4.17 presents the ESEM images of calcium chloride-based soaps. The palm olein oil soap from the second layer had an uneven solid surface with large hollow spaces, while the palm olein oil soap from the third layer had elongated networks with irregular pores. Both soybean oil soaps from the second and third layer exhibited flocculation and aggregation. However, a larger number of big and small aggregates were observed in the second layer, while the majority of the flocs in the third layer were bigger and seemingly bound in a more aqueous environment. The olive oil soap from the second layer had an uneven but solid surface, while the olive oil soap from the third layer had evident network branching. The coconut oil soap from the second layer had a sponge-like structure with small pores, whereas the coconut oil soap from the third layer had thicker networks with irregularly shaped gaps. The chicken fat soap from the second layer exhibited a solid network with large holes, whereas the chicken fat soap from the third layer had tightly packed and ellipsoidal shaped inner portion. The pork fat soap from the second layer had thin and entwined networks, while the pork fat soap from the third layer had a closely arranged capsule-like structure.

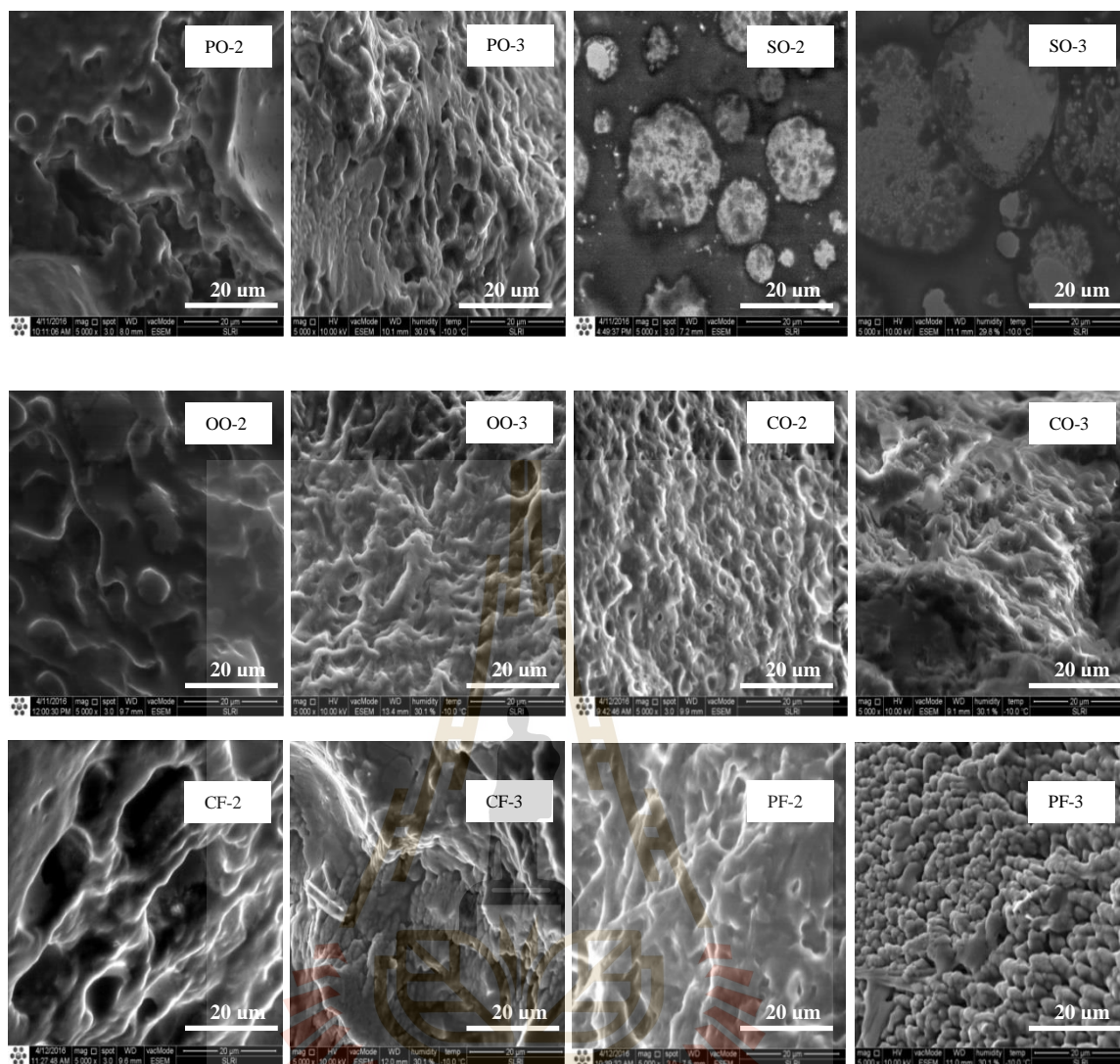


Figure 4.17 ESEM image (5000x, 20 μ m) of the soaps prepared from calcium chloride and various fat/oil sources (PO = palm olein oil; SO = soybean oil; OO = olive oil; CO = coconut oil; CF = chicken fat; PF = pork fat; the numbers indicate the layer the soaps were taken from the centrifuged mixture: 2= 2nd layer; 3= 3rd layer).

Figure 4.18 displays the ESEM images of calcium sulfate-based soaps. Palm olein oil soap from the second layer displayed rough protrusions and loosely chained networks, while palm olein oil soap from the third layer showed capsule-like

assemblages. Soybean oil soap from the second layer exhibited seemingly stretched network with hollow spaces, while soybean oil soap from the third layer demonstrated thinner capsule-like aggregates. Olive oil soap from the second layer had a similar microstructure with palm olein oil soap from the same layer, but it showed distinct bulges and chains; while olive oil soap from the third layer looked cottony. Coconut oil soap from the second layer exhibited network with sharp edges, while coconut oil from the third layer demonstrated sharper edges with dispersed capsule-like structures. Chicken fat soap from the second layer showed circular network pattern with huge holes, while chicken fat soap from the third layer displayed a mass of predominantly capsule-like clusters. Pork fat soap in the second layer showed elongated lumps, while pork fat soap from the third layer displayed a stacked rectangular-structure with some gaps.

Compared to calcium chloride-based soaps, the microstructure of most calcium sulfate-based soaps from the third layer exhibited capsule-like features, which may be associated with crystals. It is deduced that the greater apparent viscosity and more solid-like behavior recorded from calcium sulfate-based soaps were also due to aggregation and crystallization as demonstrated by their microstructure.

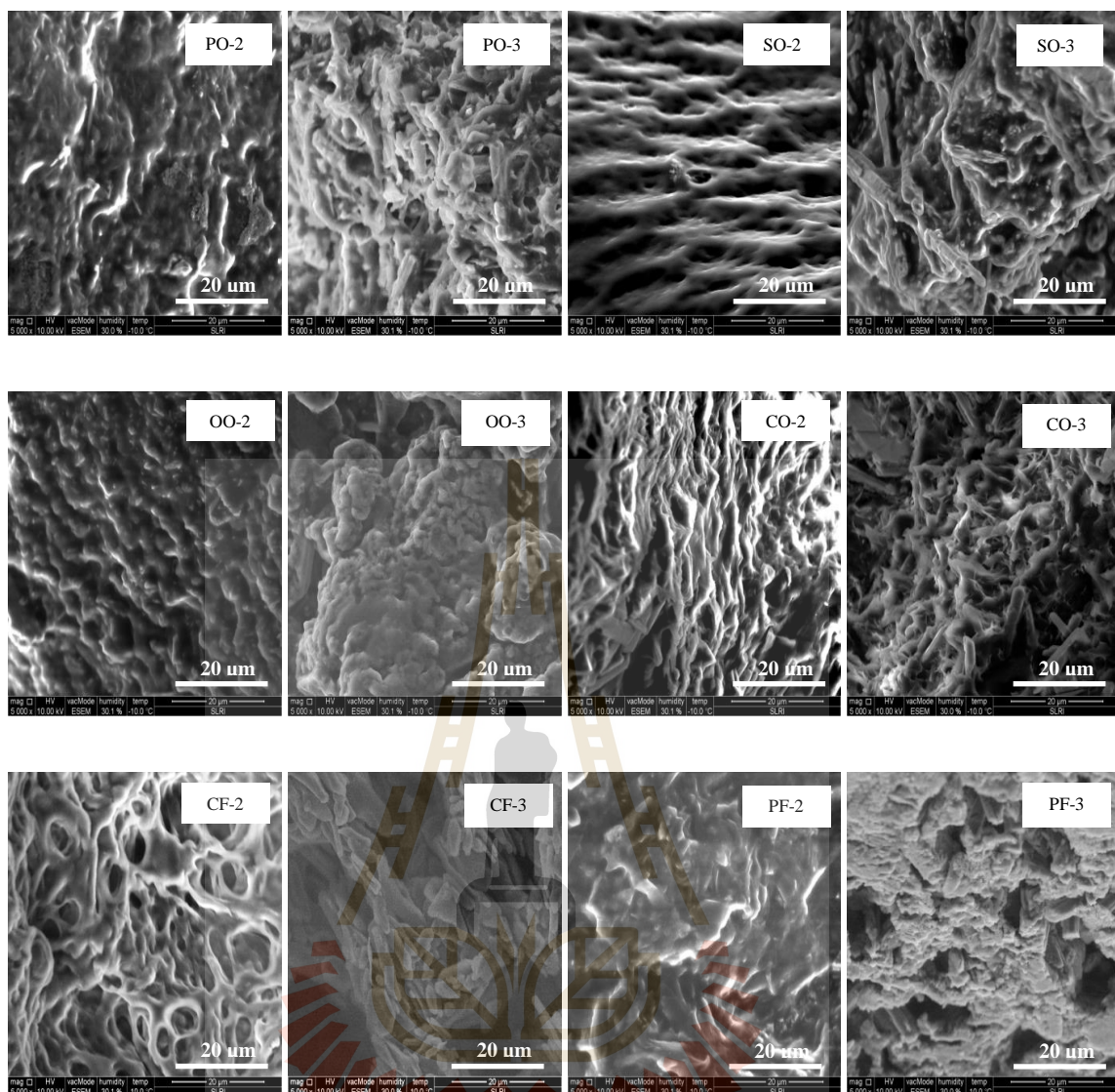


Figure 4.18 ESEM image (5000x, 20 μ m) of the soaps prepared from calcium sulfate and various fat/oil sources (PO = palm olein oil; SO = soybean oil; OO = olive oil; CO = coconut oil; CF = chicken fat; PF = pork fat; the numbers indicate the layer the soaps were taken from the centrifuged mixture: 2= 2nd layer; 3= 3rd layer).

4.5.2 CLSM images

To supplement the ESEM findings, the calcium soaps were also observed under confocal laser scanning microscope (CLSM). As shown in Figures 4.19 and 4.20, the kind of calcium source influenced the microstructure of the soaps, especially in terms of porosity. This attribute was quantified as percent void and presented in Figure 4.21. Generally, calcium sulfate-based soaps demonstrated lesser voids than calcium chloride-based soaps. It is theorized that their low porosity was caused by their low solubility, which limited the incorporation of water into the FOG deposit matrix (Gross et al., 2017). This is supported by their FTIR spectra, which mainly exhibited lower O-H absorbance (3400 cm^{-1}) than calcium chloride-based soaps (Figures 4.5 and 4.6).

The voids were further evaluated in terms of circularity in order to visualize the homogeneity of the soap microstructure. A void with a perfectly circular shape is indicated by a circularity value of 1.0, while a more elongated or irregular void is designated by a circularity value near zero (Rasband, 2000). As shown in Figure 4.22, the calcium chloride-based soaps from the third layer mainly had higher void circularity than their counterpart from the second layer. This may be due to their more uniform hollow spaces based on ESEM (Figure 4.17). Conversely, the calcium sulfate-based soaps from the third layer had lower void circularity than their counterpart from the second layer. This may be attributed to their more irregular holes and gaps based on ESEM (Figure 4.18).

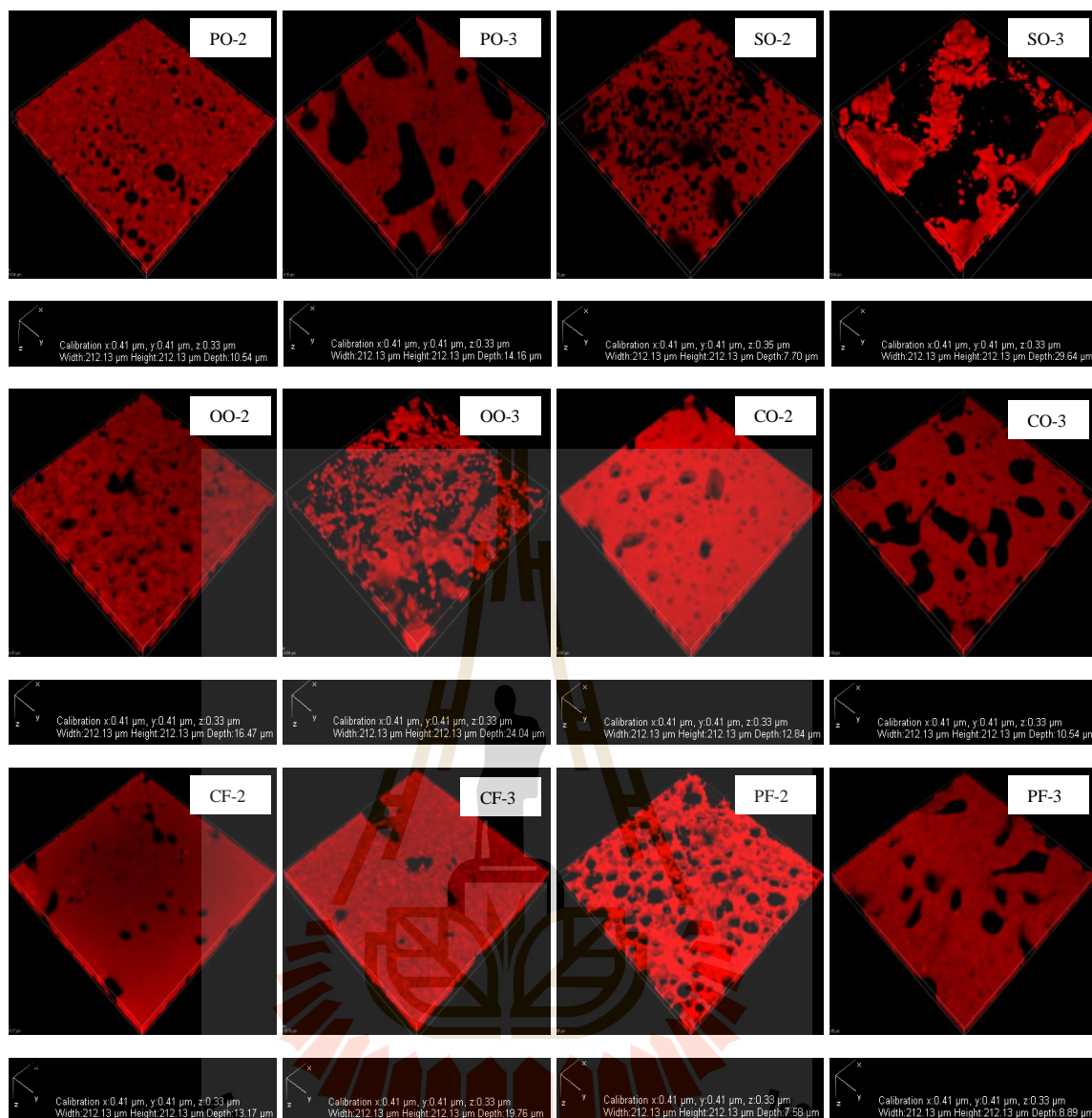


Figure 4.19 CLSM 3-D image of the soaps prepared from calcium chloride and various fat/oil sources soaps (PO = palm olein oil; SO = soybean oil; OO = olive oil; CO = coconut oil; CF = chicken fat; PF = pork fat; the numbers indicate the layer the soaps were taken from the centrifuged mixture: 2= 2nd layer; 3= 3rd layer).

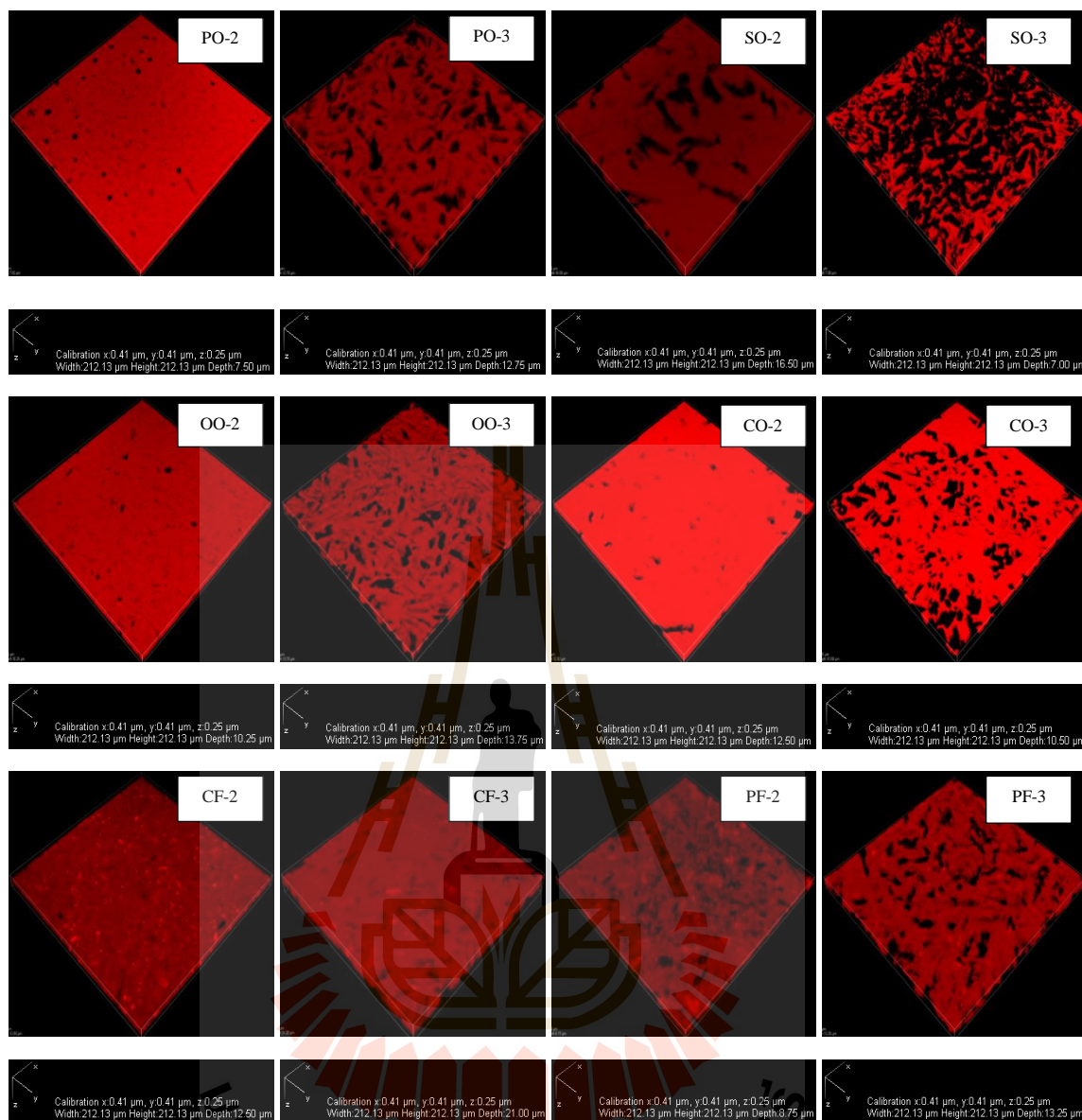


Figure 4.20 CLSM 3-D image of the soaps prepared from calcium sulfate and various fat/oil sources soaps (PO = palm olein oil; SO = soybean oil; OO = olive oil; CO = coconut oil; CF = chicken fat; PF = pork fat; the numbers indicate the layer the soaps were taken from the centrifuged mixture: 2= 2nd layer; 3= 3rd layer).

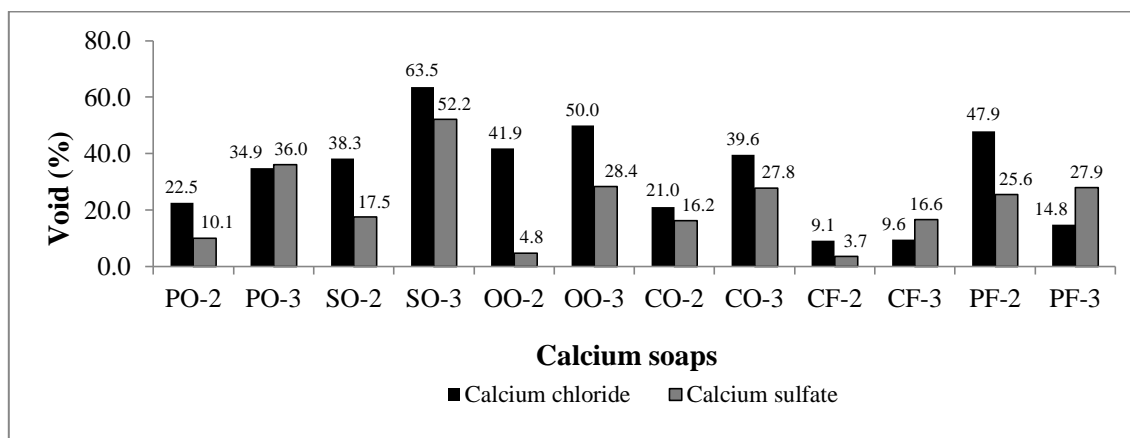


Figure 4.21 Percent void of the soaps prepared from different fat/oil and calcium sources (PO = palm olein oil, SO = soybean oil, OO = olive oil, CO = coconut oil, CF = chicken fat, PF = pork fat; the numbers indicate the layer the soaps were taken from the centrifuged mixture: 2= 2nd layer; 3= 3rd layer).

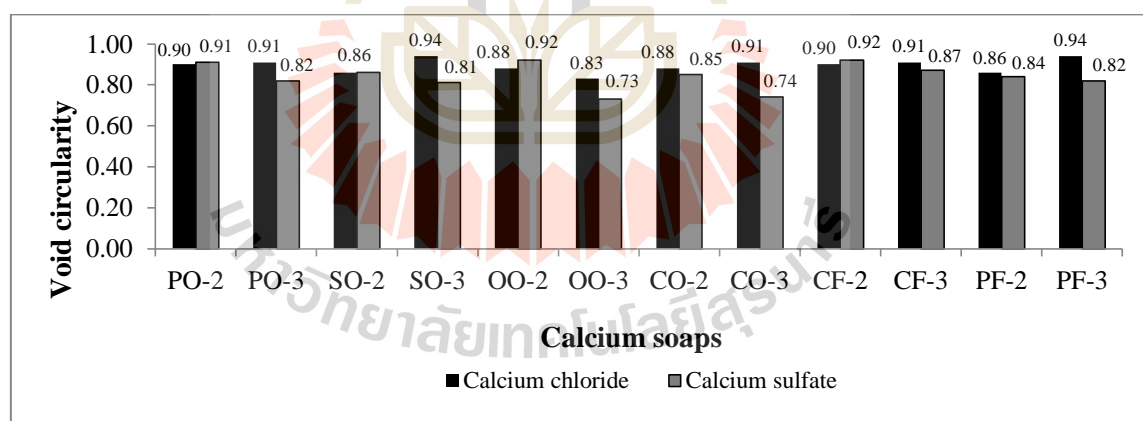


Figure 4.22 Void circularity of the soaps prepared from different fat/oil and calcium sources (PO = palm olein oil, SO = soybean oil, OO = olive oil, CO = coconut oil, CF = chicken fat, PF = pork fat; the numbers indicate the layer the soaps were taken from the centrifuged mixture: 2= 2nd layer; 3= 3rd layer).

4.6 X-ray diffraction of calcium soaps

It is anticipated that the melting, rheological behavior, and microstructure of FOG deposits are greatly influenced by their structural identity. Thus, the calcium soaps were subjected to X-ray analyses to get their X-ray diffraction pattern, which is considered as one of the essential data in understanding the structural states of metal soaps (Sagitani and Komoriya, 2015; Shoeb et al., 1999; Zhu et al., 2005).

4.6.1 SAXS diffraction pattern

In this study, SAXS measurement was employed in order to determine the structure of the calcium soaps. From the diffraction pattern, the bilayer long spacing was derived, which describes the perpendicular separation between carboxylate heads in the soap bilayer (Hill and Moaddel, 2016; Nadarajan and Ismail, 2011; Sawada and Konaka, 2004). The bilayer long spacing was calculated by getting the average of the d-spacings on each peak (Nadarajan and Ismail, 2011). Identification of the lamellar structure was based on the d-spacing ratio equivalent to $1:1/2:1/3:1/4$ (Li et al., 2017; Nadarajan and Ismail, 2011).

Figure 4.23 displays the SAXS diffraction patterns of the calcium soaps. The soaps were made from fats and oils, which contained a mixture of fatty acids; hence they had their own characteristic profile. Interestingly, the soaps produced from the same calcium and fat/oil source did not reflect a uniform pattern. This is probably due to the location they were recovered from the centrifuged mixture. Based on the FTIR analysis, soaps from the second layer had more unreacted fat, while soaps from the third layer had more bound water. Therefore, the presence of impurities in crude soaps had caused the differences in diffraction patterns (Vold and Hattiangdi, 1949).

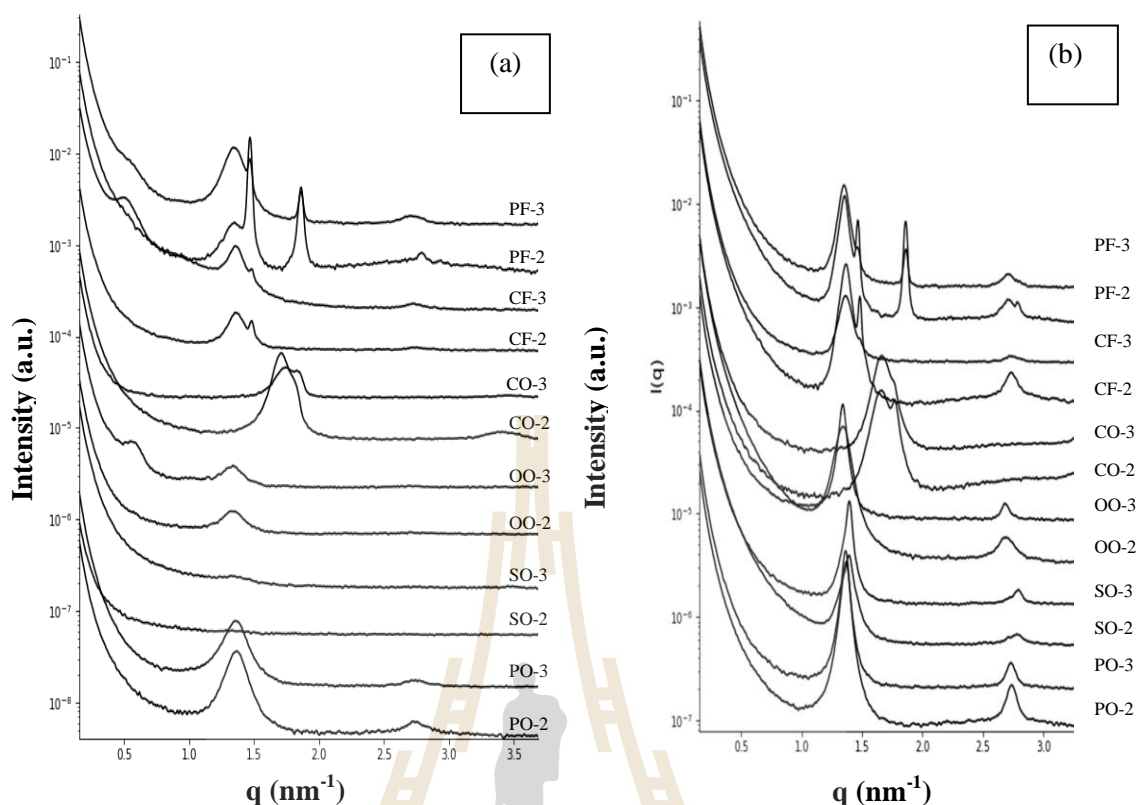


Figure 4.23 SAXS diffraction patterns of the calcium soaps prepared from various fats/oils: (a) calcium chloride; (b) calcium sulfate (PO = palm olein oil; SO = soybean oil; OO = olive oil; CO = coconut oil; CF = chicken fat; PF = pork fat; the numbers indicate the layer the soaps were taken from the centrifuged mixture: 2= 2nd layer; 3= 3rd layer).

To further characterize the calcium soaps, their long spacings were calculated from their respective SAXS diffraction patterns. Table 4.3 presents the SAXS data of soaps prepared from calcium chloride and various fat/oil sources. Based on the SAXS data of calcium chloride-based soaps, it was identified that long spacing was mainly influenced by the chain length of major fatty acid components of fat/oil source (Table 4.1). Case in point, olive oil that was comprised of a large amount of oleic acid, C18:1

(75%) produced soaps with highest long spacing (4.67-4.69 nm). This was followed by palm olein and soybean oil soap (4.61 nm). Palm olein oil was composed of palmitic acid, C16:0 (38%) and oleic acid, C18:1 (43%); while soybean oil was mainly made up of oleic acid, C18:1 (22%) and linoleic acid, C18:2 (55%). Coconut oil soaps acquired the least long spacing (3.41-3.68 nm) since coconut oil contained large quantities of lauric acid, C12:0 (44%) and myristic acid, C14:0 (22%). Distinctively, chicken and pork fat soaps exhibited a lamellar structure of more planes with various long spacings (4.24-4.61 nm and 3.36-4.63 nm, respectively). This is possibly due to a number of fatty acids found in animal fats. In particular, chicken fat contained considerable fractions of palmitic acid, C16:0 (27%), oleic acid, C18:1 (39%), and linoleic acid, C18:2 (21%). Pork fat had the same fatty acid components but in varied amount. Its main composition included palmitic acid, C16:0 (24%), oleic acid, C18:1 (41%), and linoleic acid, C18:2 (17%).

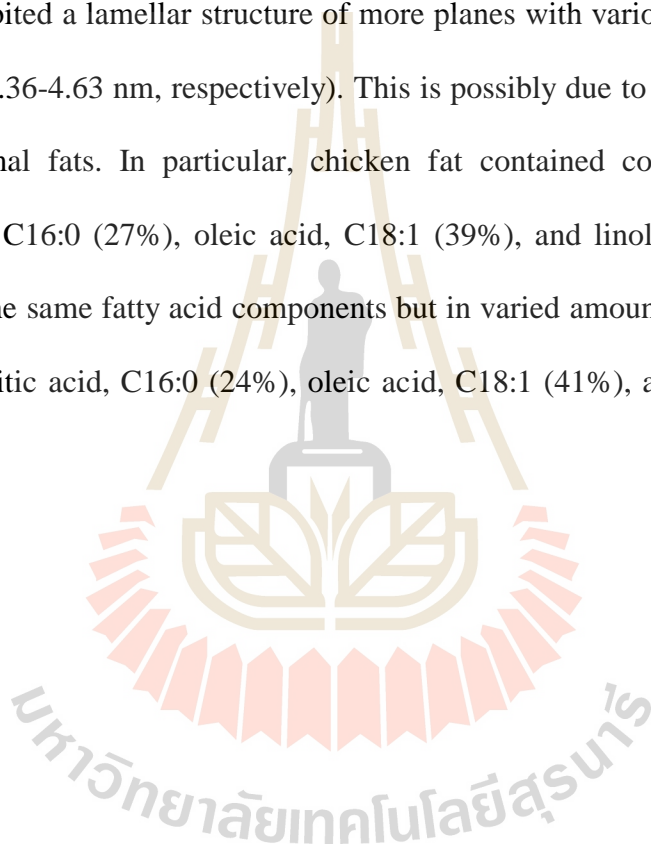


Table 4.3 SAXS data of soaps prepared from calcium chloride and various fat/oil sources.

| Soaps* | Plane | Peak Position, q (nm^{-1}) (Peak position ratio) | Long spacing (nm) |
|--------|-------|---|-------------------|
| PO-2 | 1 | 1.36 (1), 2.73 (2) | 4.61 |
| PO-3 | 1 | 1.35 (1), 2.75 (2) | 4.61 |
| SO-2 | | No peak | - |
| SO-3 | 1 | 1.36 (1) | 4.61 |
| OO-2 | 1 | 1.33 (1), 2.72 (2) | 4.67 |
| OO-3 | 1 | 0.57 (1) | 11.02 |
| | 2 | 1.34 (1) | 4.69 |
| CO-2 | 1 | 1.71 (1), 3.41 (2) | 3.68 |
| CO-3 | 1 | 1.74 (1) | 3.61 |
| | 2 | 1.84 (1) | 3.41 |
| CF-2 | 1 | 1.36 (1), 2.74 (2) | 4.60 |
| | 2 | 1.48 (1) | 4.24 |
| CF-3 | 1 | 0.51 (1) | 12.31 |
| | 2 | 1.36 (1), 2.73 (2) | 4.61 |
| | 3 | 1.48 (1) | 4.24 |
| PF-2 | 1 | 1.35 (1), 2.80 (2) | 4.57 |
| | 2 | 1.47 (1), 2.94 (2) | 4.27 |
| | 3 | 1.87 (1) | 3.36 |
| PF-3 | 1 | 1.35 (1), 2.72 (2) | 4.63 |
| | 2 | 1.47 (1) | 4.27 |
| | 3 | 2.72 (1) | 3.38 |

* (PO = palm olein oil; SO = soybean oil; OO = olive oil; CO = coconut oil; CF = chicken fat; PF = pork fat; the numbers indicate the layer the soaps were taken from the centrifuged mixture: 2= 2nd layer; 3= 3rd layer).

Table 4.4 SAXS data of soaps prepared from calcium sulfate and various fat/oil sources.

| Soaps* | Plane | Peak Position, q (nm^{-1}) (Peak position ratio) | Long spacing, (nm) |
|--------|-------|---|--------------------|
| PO-2 | 1 | 1.38 (1), 2.74 (2) | 4.57 |
| PO-3 | 1 | 1.37 (1), 2.74 (2) | 4.58 |
| SO-2 | 1 | 1.39 (1), 2.79 (2) | 4.51 |
| SO-3 | 1 | 1.40 (1), 2.79 (2) | 4.49 |
| OO-2 | 1 | 1.35 (1), 2.69 (2) | 4.66 |
| OO-3 | 1 | 1.34 (1), 2.68 (2) | 4.69 |
| CO-2 | 1 | 1.66 (1), 3.31 (2) | 3.79 |
| | 2 | 1.77 (1) | 3.55 |
| CO-3 | 1 | 1.67 (1), 3.31 (2) | 3.78 |
| | 2 | 1.77 (1) | 3.55 |
| CF-2 | 1 | 1.37 (1), 2.74 (2) | 4.58 |
| | 2 | 1.48 (1) | 4.24 |
| CF-3 | 1 | 1.37 (1), 2.73 (2) | 4.59 |
| | 2 | 1.49 (1) | 4.21 |
| PF-2 | 1 | 1.36 (1), 2.71 (2) | 4.63 |
| | 2 | 1.47 (1), 2.79 (2) | 4.39 |
| | 3 | 1.86 (1) | 3.38 |
| PF-3 | 1 | 1.36 (1), 2.71 (2) | 4.63 |
| | 2 | 1.47 (1) | 4.27 |
| | 3 | 1.86 (1) | 3.38 |

* (PO = palm olein oil; SO = soybean oil; OO = olive oil; CO = coconut oil; CF = chicken fat; PF = pork fat; the numbers indicate the layer the soaps were taken from the centrifuged mixture: 2= 2nd layer; 3= 3rd layer).

Table 4.4 details the SAXS data of soaps prepared from calcium sulfate and various fat/oil sources. The results clarified that the relatively lower long spacing of soybean oil soaps was influenced by linoleic acid, C18:2 that was found as the major fatty acid component of soybean oil (Table 4.1). Linoleic acid has two double bonds in *cis* configuration that cause bending in the carbon backbone molecule, thereby preventing the formation of closely packed soap structure (Nadarajan and Ismail, 2011). Additionally, the results verified that soaps with many types of fatty acids may lead to a lamellar structure with planes of different long spacings. Specifically, chicken and animal fat soaps exhibited greater long spacing range values (4.21-4.59 nm and 3.38-4.63 nm, respectively).

Based on the SAXS data, the lamellar plane models of the calcium soaps were developed. For calcium chloride-based soaps, four types of patterns were identified. First, a uniform lamellar structure with two peaks, which represent first and second orders. The profile corresponds to a structural model that illustrates planes with identical d-spacings (Figure 4.24a). This property is recorded in palm olein oil soaps, olive oil soap from the second layer, and coconut oil soap from the second layer. Second, a mixed lamellar structure that contains two or more planes with varied d-spacings (Figure 4.24b). This feature is noted in olive oil soap from the third layer, coconut oil soap from the third layer, chicken fat soaps, and pork fat soaps. Third, a distributed lamellar structure with a very broad peak in the first order, which resulted in the absence of a peak in the second order. The broad peak is caused by individual plane with dissimilar d-spacings (Figure 4.24c). This attribute is recognized in soybean oil soap from the third layer. Fourth, a phase with no peak due to the absence of periodic structure. This is observed in soybean oil soap from the second layer. The lack of a peak or the existence of a very broad peak in soybean oil soaps may be associated to their microstructure, which showed

flocculation and large void area. For calcium sulfate-based soaps, two kinds of lamellar patterns were recognized. First, a uniform lamellar structure (Figure 4.24a) as seen in palm olein oil, soybean oil, and olive oil soaps. Second, a mixed lamellar structure (Figure 4.24b) as recorded in coconut oil, chicken fat, and pork fat soaps. Olive oil soaps consistently obtained the highest long spacing (4.66-4.69 nm), followed by palm olein oil soaps (4.57-4.58 nm), soybean oil soaps (4.49-4.51 nm), and coconut oil soaps (3.55-3.79 nm).

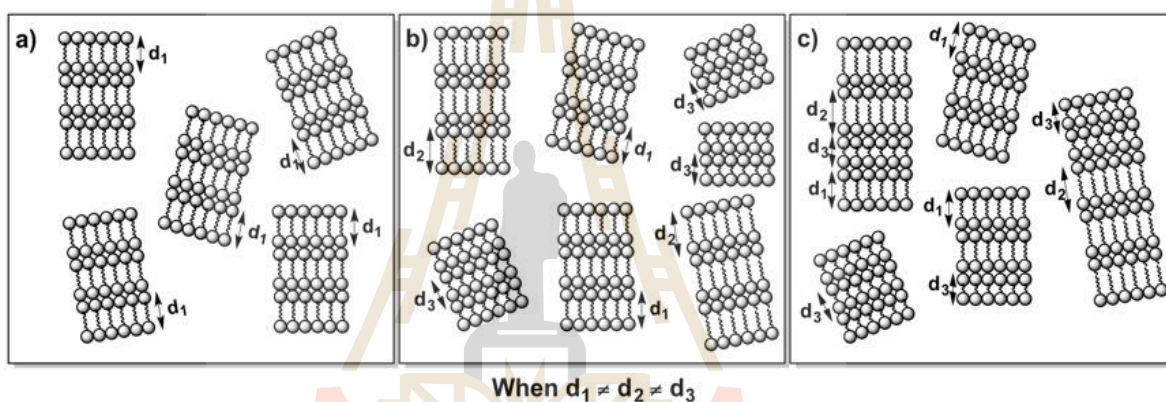


Figure 4.24 Proposed lamellar plane models of the calcium soaps from various fat/oil sources: (a) uniform lamellar plane; (b) mixed lamellar planes; (c) distributed lamellar plane.

Regardless of the calcium source, the d-spacings recorded from the soaps are mainly dictated by their fatty acid profile. Their values are also closely within the range noted from commercial and metal soaps made from a particular fat/oil (Gönen, 2010; Zhu, 2005; Hill and Moaddel, 2004; Sawada, 2004; Vold, 1949; Hattiangdi, 1949; Harkins, 1945). This proves that SAXS analysis is a highly credible technique in identifying the main fat/oil source or fatty acid component of a certain FOG deposit.

4.6.2 WAXS diffraction pattern

WAXS analysis was also employed in order to understand the complex ordered structuring between the hydrocarbon chains of the soaps (Zhu et al., 2005). The diffraction patterns obtained from WAXS determination were analyzed to get the crystallinity of the soaps. Crystallinity is equivalent to the ratio of peak areas between the crystalline peaks and the total peak area that includes the amorphous peak (Rugmai and Soontaranon, 2017).

Figure 4.25 illustrates the WAXS diffraction patterns of the soaps from different calcium and fat/oil sources. As shown, all soaps displayed partially crystalline and partially amorphous structure, but calcium sulfate-based soaps exhibited sharper multiple diffraction peaks that indicates more crystallinity.

From the diffraction patterns, the degree of crystallinity of the soaps was quantified and presented in Figure 4.26. Generally, calcium sulfate-based soaps were more crystalline than calcium chloride-based soaps. It is inferred that their distinct physical characteristics had caused the remarkable difference in crystallinity. Calcium chloride and calcium sulfate-based soaps from the second layer appeared smooth and paste-like, but calcium sulfate-based soaps were thicker. Calcium chloride and calcium sulfate-based soaps from the third layer had a coarse texture, but calcium sulfate-based soaps had a lumpy appearance. The higher crystallinity values recorded from calcium sulfate-based soaps are also attributed to their compact microstructure and/or the presence of crystal-like assemblages under ESEM, as well as their lower void/porosity under CLSM.

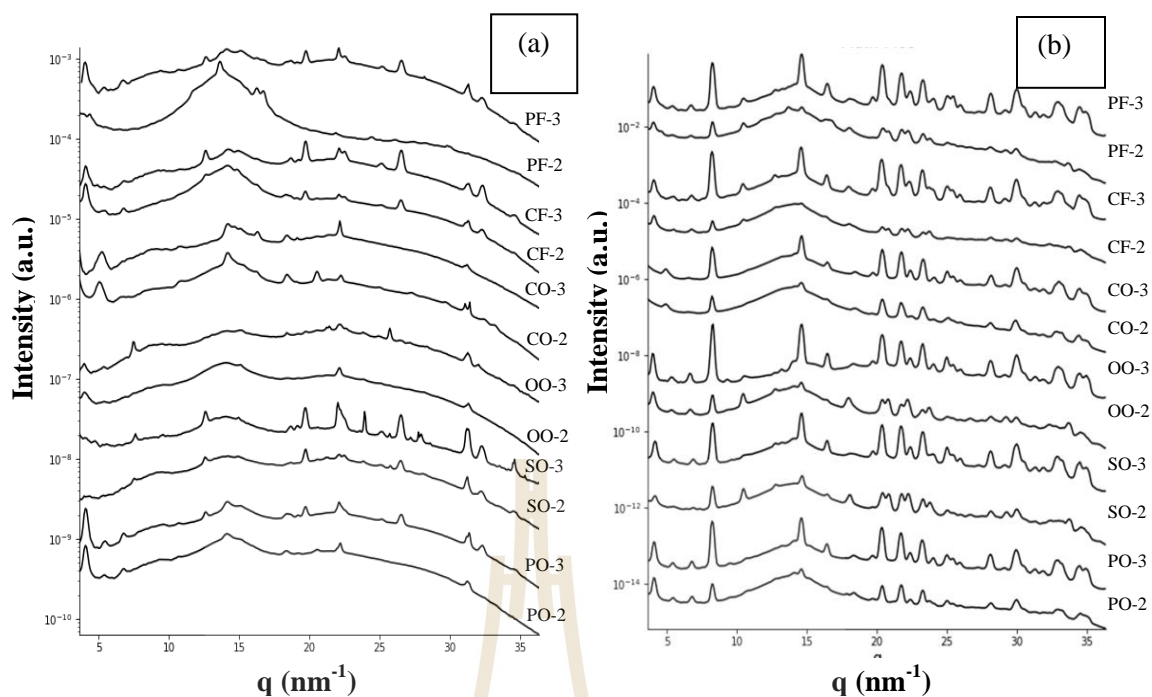


Figure 4.25 WAXS diffraction patterns of calcium soaps prepared from various fats/oils: (a) calcium chloride; (b) calcium sulfate (PO = palm olein oil; SO = soybean oil; OO = olive oil; CO = coconut oil; CF = chicken fat; PF = pork fat; the numbers indicate the layer the soaps were taken from the centrifuged mixture: 2= 2nd layer; 3= 3rd layer).

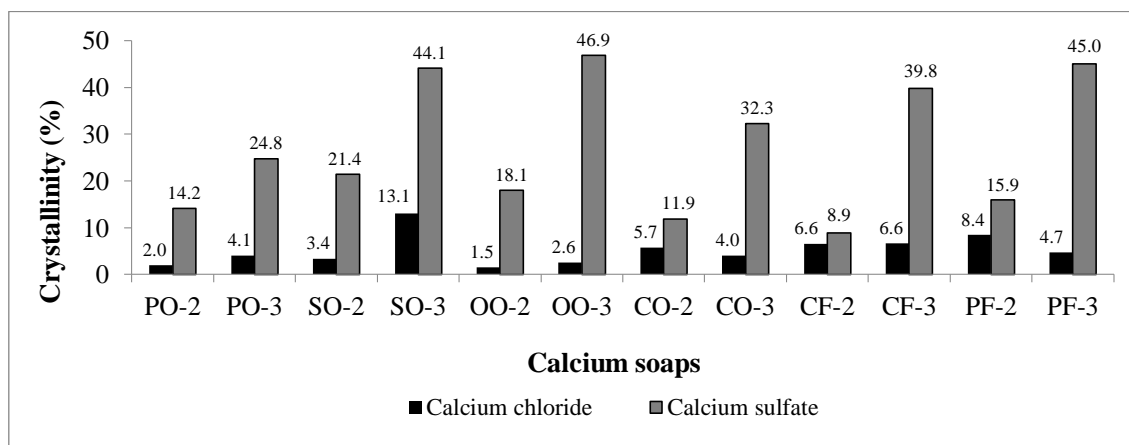


Figure 4.26 Percent crystallinity of soaps prepared from different fat/oil and calcium sources (PO = palm olein oil, SO = soybean oil, OO = olive oil, CO = coconut oil, CF = chicken fat, PF = pork fat; the numbers indicate the layer the soaps were taken from the centrifuged mixture: 2= 2nd layer; 3= 3rd layer).

Overall, the soaps from the third layer commonly demonstrated a higher degree of crystallinity than the soaps from the second layer. This is due to the fact that the soaps from the third layer had a higher degree of saponification and calcium content, which contributed to a more rigid structure. Concerning all calcium chloride-based soaps, soybean oil soap from the third layer reflected the highest crystallinity reading. This is believed to be linked to its bigger flocs under ESEM. It is also confirmed that the absence peak in soybean oil soap from the second layer in SAXS analysis was related to its low degree of crystallinity. Considering all calcium sulfate-based soaps, olive oil soap from the third layer obtained the highest crystallinity value. This is probably caused by its cottony structure under ESEM. Upon further scrutiny, it can be observed that the degree of crystallinity of calcium sulfate-based soaps from the third layer was generally

more than twice the crystallinity of calcium sulfate-based soaps from the second layer. This is expected since the soaps from the second layer were paste-like, while the soaps from the third layer were coarse and lumpy.

The SAXS and WAXS results were found to be complementary. The SAXS diffraction profile of soaps with sharper peaks corresponded to a WAXS profile with higher degree of crystallinity. Thus, SAXS and WAXS techniques are powerful tools in elucidating the structural properties of the soaps. In consideration of other properties evaluated, crystallinity, melting endset, apparent viscosity (η_{100}), and solid-like behavior ($\text{Tan } \delta$) of calcium sulfate-based soaps were generally directly related. However, in calcium chloride-based soaps crystallinity was inversely related to apparent viscosity, and viscoelasticity. This is theorized to be due to their more heterogeneous physical feature.

4.7 Correlation of calcium soap composition and physico-chemical properties

Understanding the critical factors and conditions that may cause high FOG deposit formation and stability is very valuable in properly addressing FOG deposit accumulation in the sewer system. The influence of FOG deposit composition on its physico-chemical properties may disclose its crucial role on stability, while the interrelationship of the physico-chemical properties may reveal how to effectively manage the deposits. As shown in Table 4.5, calcium content played a vital role in the formation of more FOG deposits, regardless of the calcium source. Moreover, calcium chloride-based soaps with high calcium content were more heat-stable and solid-like ($\text{Tan } \delta$). On the other hand, the heat stability of calcium sulfate-based soaps was

attributed to the presence of more saturated fatty acids. Nevertheless, calcium sulfate-based soaps with high calcium content indicated a solid-like behavior and resistance to flow (η_{100}). In contrast, calcium chloride-based soaps with high calcium content did not have a positive relationship with resistance to flow. It is postulated that this is due to their thinner and moister appearance and texture. Table 4.6 presents the significant association among the physico-chemical properties of the calcium soaps. The high soap yield signified heat stability in calcium chloride-based soaps, while it implied more resistance to flow and solid-like behavior in calcium sulfate-based soaps. In both calcium sources, saponification resulted in a large amount of solids formed. Moreover, it enhanced the heat stability and solid-like behavior of calcium chloride-based soaps. The resistance to flow specifically intensified the heat stability and solid-like behavior of calcium sulfate-based soaps.

Table 4.5 Significant correlations between the physico-chemical properties and composition of calcium soaps.

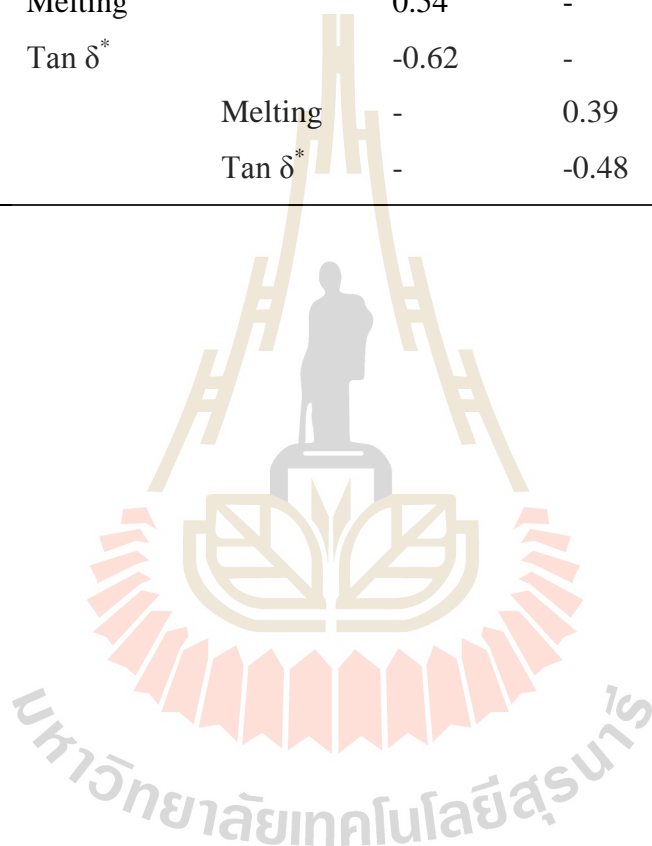
| Property | Soap composition | | Correlation coefficient | | p-value | |
|----------------|-------------------|-------------------|-------------------------|-------------------|-------------------|-------------------|
| | CaCl ₂ | CaSO ₄ | CaCl ₂ | CaSO ₄ | CaCl ₂ | CaSO ₄ |
| Soap yield | Ca content | Ca content | 0.42 | 0.81 | 0.010 | 0.000 |
| Saponification | Ca content | C16:0 | 0.74 | 0.54 | 0.001 | 0.001 |
| Melting | Ca content | C18:0 | 0.55 | 0.63 | 0.001 | 0.000 |
| | | C18:2 | - | -0.54 | - | 0.001 |
| | | Total SFA | - | 0.55 | - | 0.000 |
| | | Total UFA | - | -0.55 | - | 0.001 |
| η_{100} * | Ca content | Ca content | -0.60 | 0.56 | 0.000 | 0.000 |
| Tan δ * | Ca content | Ca content | -0.44 | -0.51 | 0.008 | 0.001 |

* at 25°C

Table 4.6 Significant correlations among the physico-chemical properties of calcium soaps.

| Property | | | Correlation coefficient | | p-value | |
|----------------|-------------------|-------------------|-------------------------|-------------------|-------------------|-------------------|
| | CaCl ₂ | CaSO ₄ | CaCl ₂ | CaSO ₄ | CaCl ₂ | CaSO ₄ |
| Soap yield | η_{100}^* | η_{100}^* | -0.40 | 0.79 | 0.015 | 0.000 |
| | Melting | Tan δ^* | 0.63 | -0.46 | 0.000 | 0.005 |
| Saponification | Soap yield | Soap yield | 0.69 | 0.40 | 0.000 | 0.015 |
| | Melting | | 0.54 | - | 0.001 | - |
| | Tan δ^* | | -0.62 | - | 0.000 | - |
| η_{100}^* | | Melting | - | 0.39 | - | 0.019 |
| | | Tan δ^* | - | -0.48 | - | 0.003 |

* at 25°C



CHAPTER V

CONCLUSIONS

Calcium content is a critical indicator of the enhanced formation and stability of FOG deposits. It corresponded to deposits with higher melting endset and solid-like behavior. Furthermore, the solubility of the calcium source greatly influences the properties of the FOG deposits. The more soluble calcium chloride generated highly saponified solids but in smaller quantity, whereas the less soluble calcium sulfate produced less saponified solids but in larger amount. Calcium sulfate-based soaps are predicted to cause faster sewer blockages due to their bulky nature, while calcium chloride-based soaps are expected to accumulate on sewer walls due to their higher melting endset.

The fatty acids in the sewer fundamentally dictate the stability of FOG deposits. Case in point, calcium soaps with a certain combination of palmitic acid ($\approx 21-39\%$) and oleic acid ($\approx 40-42\%$) were highly saponified. Calcium soaps with a certain proportion of palmitic acid ($\approx 21-23\%$), oleic acid ($\approx 42-43\%$), and linoleic acid ($\approx 17-18\%$) were more heat-stable. Also, calcium soaps with a certain percentage of oleic acid ($\approx 43\%$) and palmitic acid ($\approx 23\%$) were more flow-resistant. Additionally, when exposed to a corroded sewer environment, the more saturated lipids such as coconut oil and pork fat can result to FOG deposits that are more problematic. Coconut oil has the tendency to cause faster sewer blockages since it formed large amount of soaps. On the other hand, pork fat is foreseen to cause FOG

deposit accumulation because it produced soaps with higher melting endset, apparent viscosity, and solid-like characteristics.

The properties of the calcium soaps were better understood through microstructure and X-ray diffraction analyses. Calcium soaps with higher heat and flow stability had tightly-packed, crystal-like, and less porous microstructure. They also had mixed lamellar structure and higher degree of crystallinity as shown by their X-ray diffraction pattern.

Based on the results, it is proposed that institutions dealing with saturated fats/oils explore the utilization of less saturated fat/oil alternatives to prevent FOG deposit accumulation in the drainage system. As a long-term solution, they may also consider the construction of a sewer system with materials that are not prone to concrete corrosion. In case there is an occurrence of FOG deposition, immediate cleanup is necessary, which can be facilitated with pumps with higher shear rate and/or water with warmer temperature.

To further expand our knowledge on FOG deposit formation and stability, it is recommended that preceding studies explore a saponification formulation that will not exceed the solubility limit of the calcium source. Moreover, it is also advised to utilize processed fats/oils.

REFERENCES

- Adhvaryu, A., Sung, C. and Erhan, S. (2005). Fatty acids and antioxidant effects on grease microstructures. **Industrial Crops and Products**. 21(3): 285-291.
- Alade, A.O., Jameel, A.T., Muyubi, S.A., Karim, M.I.A. and Alam, M.Z. (2011). Removal of oil and grease as emerging pollutants of concern (EPC) in wastewater stream. **IIUM Engineering Journal**. 12(4): 161-169.
- Alm, M. (2013). Animal Fats: Edible oil processing. **AOCS Lipid Library**. (online) available: <http://lipidlibrary.aocs.org/OilsFats/content.cfm?ItemNumber=40320>. (Accessed 12 June 2018).
- AlMubaddal, F., AlRumaihi, K. and Ajbar, A. (2009). Performance optimization of coagulation/flocculation in the treatment of wastewater from a polyvinyl chloride plant. **Journal of Hazardous Materials**. 161(1): 431-438.
- Arnaud, E., Relkin, P., Pina, M. and Collignan, A. (2004). Characterisation of chicken fat dry fractionation at the pilot scale. **European Journal of Lipid Science and Technology**. 106(9): 591-598.
- Arthur, S. and Blanc, J. (2013). **Management and recovery of FOG (fats, oils and greases)**. (online) available: http://www.crew.ac.uk/sites/default/files/sites/default/files/publication/CREW_FOG.pdf. (Accessed 11 April 2016).
- Ahsan, S., Rahman, M.A., Kaneco, S., Katsumata, H., Suzuki, T. and Ohta, K. (2005). Effect of temperature on wastewater treatment with natural and waste materials. **Clean Technologies and Environmental Policy**. 7(3): 198-202.

- Bhatnagar, A.S., Prasanth Kumar, P.K., Hemavathy, J. and Gopala Krishna, A.G. (2009). Fatty acid composition, oxidative stability, and radical scavenging activity of vegetable oil blends with coconut oil. **Journal of the American Oil Chemists' Society**. 86(10): 991-999.
- Beetseh, C. and Godwin, J. (2015). A study of distinctive characteristics of soaps made of saw dust ash (lye) with palm and olive oils and their oil blends in Benue State Nigeria. **Journal of Environment and Earth Science**. 5(12): 98-105.
- BSR (2010). **Sustainable water group water quality guidelines**. (online) available: https://www.bsr.org/reports/awqwg/BSR_AWQWG_Guidelines-TestingStandards.pdf. (Accessed 23 May 2018).
- Choi, D.W. and Chang, Y.H. (2012). Steady and dynamic shear rheological properties of buckwheat starch-galactomannan mixtures. **Preventive Nutrition and Food Science**. 17(3): 192-196.
- Daborganes, C. (2009). **Formation of new compounds during frying-general observations**. (online) available: <http://aocs.files.cmsplus.com/annualmeeting/images/lipidimporthtml/lipidlibrary/frying/c-newcpds/index.htm>. (Accessed 23 May 2018).
- da Silva Lannes, S. and Ignacio, R. (2013). **Structuring fat foods**. (online) available: <https://www.intechopen.com/books/food-industry/structuring-fat-foods>. (Accessed 5 June 2018).
- Davis, J.L., Nica, D., Shields, K. and Roberts, D.J. (1998). Analysis of concrete from corroded sewer pipe. **International Biodeterioration & Biodegradation**. 42(1): 75-84.

- DAWR (1994). **Guidelines for Sewerage Systems Acceptance of Trade Waste (Industrial Waste)**. (online) available: <http://www.agriculture.gov.au/SiteCollectionDocuments/water/sewerage-systems-trade-waste-paper12.pdf>. (Accessed 23 May 2018).
- dos Santos, M.T., Viana, I., Ract, J. and Le Roux, G. (2016). Thermal properties of palm stearin, canola oil and fully hydrogenated soybean oil blends: coupling experiments and modeling. **Journal of Food Engineering**. 185: 17-25.
- Ducoste, J.J. (2013). EPA Research Forum: **Factors that influence the formation of FOG deposits in sewer collection systems**. (online) available: <https://archive.epa.gov/ncer/events/calendar/archive/web/pdf/ducoste.pdf>. (Accessed 20 June 2018).
- Emmel, J., Parott, K. and Beamish, J. (2003). Dishwashing and water conservation: an opportunity for environmental education. **Journal of Extension** 41(1).
- Engineering Toolbox (2008). **Melting points of oils**. (online) available: https://www.engineeringtoolbox.com/oil-melting-point-d_1088.html. (Accessed 18 June 2018).
- EPA (2004). **Report to Congress on impacts and control of CSO's and SSO's**. (online) available: https://www.epa.gov/sites/production/files/2015-10/documents/csos_sortc_2004_full.pdf. (Accessed 26 April 2018).
- EPD (1990). **Technical memorandum standards for effluents discharged into drainage and sewerage systems, inland and coastal waters**. (online) available: https://www.epd.gov.hk/epd/sites/default/files/epd/english/envir_standards/files/GN2014P240-1991c-e.pdf. (Accessed 23 May 2018).

- Fabiyi, M. and Larrea, A. (2015). Effect of High Temperature Operations on Wastewater Treatment: Reviewing the Resilience of High Temperature Industrial Wastewater Treatment Systems Using Microbiological Population Studies and Kinetic Dynamics. **Proceedings of the Water Environment Federation**. 2015(13): 1658-1669.
- FAO (2017). **Food outlook: Biannual report on global food markets**. (online) available: <http://www.fao.org/3/a-I8080e.pdf>. (Accessed 23 May 2018).
- Fennema, O.R., Damodaran, S. and Parkin, K.L. (2008). **Fennema's Food Chemistry (fourth ed.)**. CRC, Florida.
- Gönen, M., Öztürk, S., Balköse, D., Okur, S. and Ülkü, S. (2010). Preparation and characterization of calcium stearate powders and films prepared by precipitation and Langmuir-Blodgett techniques. **Industrial & Engineering Chemistry Research**. 49(4): 1732-1736.
- Ghotra, B.S., Dyal, S.D. and Narine, S.S. (2002). Lipid shortenings: a review. **Food Research International**. 35(10): 1015-1048.
- García, J.M., Herrera, S. and Morilla, A. (1996). Effects of postharvest dips in calcium chloride on strawberry. **Journal of Agricultural and Food Chemistry**. 44(1): 30-33.
- George, R.P. (2012). Current understanding and future approaches for controlling microbially influenced concrete corrosion: a review. **Concrete Research Letters**. 3(3): 491-506.
- Girgis, A.Y., El-Aziz, N.A. and El-Salam, S.A. (1998). Physical and chemical characteristics of toilet soap made from apricot kernel oil and palm stearin. **Grasas y Aceites**. 49(5-6): 434-439.

- Goodrum, J.W., Geller, D.P. and Adams, T.T. (2002). Rheological characterization of yellow grease and poultry fat. **Journal of the American Oil Chemists' Society.** 79(10): 961-964.
- Gross, M.A., Jensen, J.L., Gracz, H.S., Dancer, J. and Keener, K.M. (2017). Evaluation of physical and chemical properties and their interactions in fat, oil, and grease (FOG) deposits. **Water Research.** 123: 173-182.
- Gu, Z., Huang, W., Wang, S. and Zhou, A. (2015). Study on the formation of Fat, Oil, and Grease (FOG) deposits in sewer pipes. **J. Water Wastewater Eng. Assoc.** 1(1): 132-137.
- Guillen, M.D. and Cabo, N. (1997). Infrared spectroscopy in the study of edible oils and fats. **Journal of the Science of Food and Agriculture.** 75(1): 1-11.
- Gunstone, F.D. (2004). **The chemistry of oils and fats: Sources, composition, properties and uses.** Great Britain: Blackwell Publishing Ltd.
- Gupta (2005). **Frying Oils** **Bailey's Industrial Oil and Fat Products** (6th ed., Volume 6). New Jersey: John Wiley & Sons, Inc.
- Harkins, W.D., Mattoon, R.W. and Corrin, M.L. (1946). Structure of soap micelles indicated by X-rays and the theory of molecular orientation. I. Aqueous solutions¹. **Journal of the American Chemical Society.** 68(2): 220-228.
- Hattiangdi, G.S. (1949). Characterization of some commercial soaps by X-ray diffraction. **Journal of Research of the National Bureau of Standards.** 42(4): 331-341.
- Haynes, W.M. (2010). **CRC Handbook of Chemistry and Physics**, 91st Edition. Florida: Taylor & Francis Group.

- He, X., de los Reyes III, F.L. and Ducoste, J.J. (2017). A critical review of fat, oil, and grease (FOG) in sewer collection systems: challenges and control. **Critical Reviews in Environmental Science and Technology**. 47(13): 1191-1217.
- He, X., Francis, L., Leming, M.L., Dean, L.O., Lappi, S.E. and Ducoste, J.J. (2013). Mechanisms of fat, oil and grease (FOG) deposit formation in sewer lines. **Water Research**. 47(13): 4451-4459.
- He, X., Iasmin, M., Dean, L.O., Lappi, S.E., Ducoste, J.J. and de los Reyes III, F.L. (2011) Evidence for fat, oil, and grease (FOG) deposit formation mechanisms in sewer lines. **Environmental Science & Technology**. 45(10): 4385-4391.
- Heger, S. (2017). **How temperature impacts onsite wastewater treatment**. (online) available:https://www.onsiteinstaller.com/online_exclusives/2017/05/how_temperature_impacts_onsite_wastewater_treatment. (Accessed 9 August 2018).
- Hill, M. and Moaddel, T. (2016). **Soap Manufacturing Technology** (Second Edition). Elsevier.
- Husain, I.A., Alkhatib, M.a.F., Jammi, M.S., Mirghani, M.E., Zainudin, Z.B. and Hoda, A. (2014). Problems, control, and treatment of fat, oil, and grease (FOG): a review. **Journal of Oleo Science**. 63(8): 747-752.
- Iasmin, M., Dean, L.O. and Ducoste, J.J. (2016). Quantifying fat, oil, and grease deposit formation kinetics. **Water Research**. 88: 786-795.
- Iasmin, M., Dean, L.O., Lappi, S.E. and Ducoste, J.J. (2014). Factors that influence properties of FOG deposits and their formation in sewer collection systems. **Water Research**. 49: 92-102.
- Ikhu - Omoregbe, D. and Bushi, G.M. (2008). Rheological characteristics of South African commercial sauces. **International Journal of Food Science &**

Technology. 43(12): 2230-2236.

Jayadas, N. and Nair, K.P. (2006). Coconut oil as base oil for industrial lubricants-evaluation and modification of thermal, oxidative and low temperature properties. **Tribology International.** 39(9): 873-878.

Keener, K.M., Ducoste, J.J. and Holt, L.M. (2008). Properties influencing fat, oil, and grease deposit formation. **Water Environment Research.** 80(12): 2241-2246.

Koushki, M., Nahidi, M. and Cheraghali, F. (2015). Physico-chemical properties, fatty acid profile and nutrition in palm oil. **Journal of Paramedical Sciences.** 6(3).

Lee, K.-T. and Foglia, T.A. (2000). Synthesis, purification, and characterization of structured lipids produced from chicken fat. **Journal of the American Oil Chemists' Society.** 77(10): 1027-1034.

Lerma-García, M., Ramis-Ramos, G., Herrero-Martínez, J. and Simó-Alfonso, E. (2010). Authentication of extra virgin olive oils by Fourier-transform infrared spectroscopy. **Food Chemistry.** 118(1): 78-83.

Li, F., Chen, M. and Zhang, W. (2017). Effect of binary/ternary fatty acids ratio and glycerin on the phase behaviors of soap solutions. **Journal of Surfactants and Detergents.** 20(2): 425-434.

Lucke, N. (2013). **Industrial wastewater requirements and supervision.** (online) available: http://www.prestobalticsea.eu/download.php/dms/presto/Water%20Fair%20in%20Berlin/Presentations%20eng/Lucke_Norbert.pdf. (Accessed 23 May 2018).

Madani, B., Mirshekari, A. and Yahia, E. (2016). Effect of calcium chloride treatments on calcium content, anthracnose severity and antioxidant activity in papaya

- fruit during ambient storage. **Journal of the Science of Food and Agriculture**. 96(9): 2963-2968.
- Mancini, A., Imperlini, E., Nigro, E., Montagnese, C., Daniele, A., Orrù, S. and Buono, P. (2015). Biological and nutritional properties of palm oil and palmitic acid: effects on health. **Molecules**. 20(9): 17339-17361.
- Marikkar, J., Ghazali, H., Man, Y.C. and Lai, O. (2002). The use of cooling and heating thermograms for monitoring of tallow, lard and chicken fat adulterations in canola oil. **Food Research International**. 35(10): 1007-1014.
- Metin, S. and Hartel, R.W. (2005). **Crystallization of fats and oils. Bailey's industrial oil and fat products** (6th ed., Vol. 6). New Jersey: John Wiley & Sons, Inc.
- Mills, P. (2010). **Framing the Problem. In FOG build up and removal**. (online) available: http://www.policyconsulting.co.uk/downloads/FOGs_Cranfield_March_2010.pdf. (Accessed 26 April 2018).
- Montefrio, M.J., Xinwen, T. and Obbard, J.P. (2010). Recovery and pre-treatment of fats, oil and grease from grease interceptors for biodiesel production. **Applied Energy**. 87(10): 3155-3161.
- Montoya, C., Cochard, B., Flori, A., Cros, D., Lopes, R., Cuellar, T., Espeout, S., Syaputra, I., Villeneuve, P. and Pina, M. (2014). Genetic architecture of palm oil fatty acid composition in cultivated oil palm (*Elaeis guineensis* Jacq.) compared to its wild relative *E. oleifera* (HBK) Cortés. **PLoS One**. 9(5): e95412.
- Naghshineh, M., Ariffin, A.A., Ghazali, H.M., Mirhosseini, H. and Mohammad, A.S. (2010). Effect of saturated/unsaturated fatty acid ratio on physicochemical

- properties of palm olein–olive oil blend. **Journal of the American Oil Chemists' Society.** 87(3): 255-262.
- Nadarajan, R. and Ismail, R. (2011). Performance and microstructural study on soap using different fatty acids and cations. **Journal of Surfactants and Detergents.** 14(4): 463-471.
- NEA (2018). **Allowable limits for trade effluent discharge to watercourse/controlled watercourse.** (online) available: <http://www.nea.gov.sg/anti-pollution-radiation-protection/water-pollution-control/allowable-limits>. (Accessed 23 May 2018).
- Nielsen, S.S. (2003). **Food Analysis** (third ed.). New York: Kluwer Academic/Plenum Publishers.
- Nora, A., Szczepanek, A. and Koenen, G. (2005). **Metallic Soaps.** Ullmann's Encyclopedia of Industrial Chemistry. Wiley-VCH, Weinheim.
- O'Brein, R. (2009). **Fats and Oils: formulating and Processing for Applications.** Richard D. O'Brien, editor, CRC Press, Boca Raton, FL.
- Osborne, S. (2017). **The Independent online newspaper: 'Monster fatberg' weighing more than 10 double deckers found clogging east London sewer.** (online) available: <https://www.independent.co.uk/news/uk/home-news/fatberg-east-london-sewer-10-double-decker-buses-kingston-monster-fat-whitechapel-thames-water-a7943036.html>. (Accessed 18 June 2018).
- Panpipat, W. and Yongsawatdigul, J. (2008). Stability of potassium iodide and omega-3 fatty acids in fortified freshwater fish emulsion sausage. **LWT-Food Science and Technology.** 41(3): 483-492.

- Poulenat, G., Sentenac, S. and Mouloungui, Z. (2003). Fourier-transform infrared spectra of fatty acid salts-Kinetics of high-oleic sunflower oil saponification. **Journal of Surfactants and Detergents**. 6(4): 305-310.
- Rasband, W. (2000). **Circularity**. (online) available: <https://imagej.nih.gov/ij/plugins/circularity.html>. (Accessed 15 July 2017).
- Ren, T., Gao, X., Zheng, T. and Wang, P. (2016). **Study on treatment of acidic and highly concentrated fluoride waste water using calcium oxide-calcium chloride**. (online) available: <http://iopscience.iop.org/article/10.1088/1755-1315/39/1/012003/pdf>. (Accessed 12 June 2018).
- Roberts, D., Nica, D., Zuo, G. and Davis, J. (2002). Quantifying microbially induced deterioration of concrete: initial studies. **International Biodeterioration & Biodegradation**. 49(4): 227-234.
- Rohman, A. and Che Man, Y.B. (2011). The optimization of FTIR spectroscopy combined with partial least square for analysis of animal fats in quaternary mixtures. **Journal of Spectroscopy**. 25(3-4): 169-176.
- Romanova, A., Mahmoodian, M. and Alani, M.A. (2014). Influence and interaction of temperature, H₂S and pH on concrete sewer pipe corrosion. **International Journal of Civil, Architectural, Structural, Urban Science and Engineering**. 8(6): 592-595.
- Rosell, B. (1999). **Vegetable oils and fats** (vol. 1), Leatherhead Publishing, London.
- Rugmai, S. and Soontaranon, S. (2017). **SAXSIT Version 4.34**. Synchrotron Light Research Institute (SLRI), Thailand.
- Sagitani, H. and Komoriya, M. (2015). Stability conditions and mechanism of cream soaps: Effect of polyols. **Journal of Oleo Science**. 64(8): 809-816.

- Sawada, K. and Konaka, M. (2004). Characterization of fine metallic soap particles by X-ray diffraction, differential scanning calorimetry, and specific surface area analysis. **Journal of Oleo Science**. 53(12): 627-640.
- Sawyer, C.N. (2003). **Chemistry for environmental engineering and science**. McGraw-Hill.
- Scottish Water (2012). **Your guide to disposing cooking fats**. (online) available: http://www.scottishwater.co.uk/assets/domestic/files/you%20and%20your%20home/save%20your%20drains/swfog2012_single%20pages_lowres.pdf. (Accessed 23 May 2018).
- Scrimgeour (2005). **Chemistry of fatty acids. Bailey's industrial oil and fat products** (6th ed., Vol. 6). New Jersey: John Wiley & Sons, Inc.
- Shahidi, F. and Zhong, Y. (2005). **Lipid oxidation: measurement methods. Bailey's industrial oil and fat products** (6th ed., Vol. 6). New Jersey: John Wiley & Sons, Inc.
- Shoeb, Z.E., Hammad, B.M. and Yousef, A. (1999). Oleochemicals I: Studies on the preparation and the structure of lithium soaps. **Grasas y Aceites**. 50(6): 426-434.
- Soult, A. (2016). Lipids and Triglycerides. (online) available: [https://chem.libretexts.org/LibreTexts/University_of_Kentucky/UK%3A_CHE_103_-_Chemistry_for_Allied_Health_\(Soult\)/Chapters/Chapter_14%3A_Biological_Molecules/14.2%3A_Lipids_and_Triglycerides](https://chem.libretexts.org/LibreTexts/University_of_Kentucky/UK%3A_CHE_103_-_Chemistry_for_Allied_Health_(Soult)/Chapters/Chapter_14%3A_Biological_Molecules/14.2%3A_Lipids_and_Triglycerides). (Accessed 18 June 2018).
- Steffe, J.F. (1996). **Rheological methods in food process engineering** (second ed.), Michigan: Freeman Press.

- Stoll, U. and Gupta, H. (1997). Management strategies for oil and grease residues. **Waste Management & Research**. 15(1): 23-32.
- Tang, D. and Marangoni, A.G. (2006). Quantitative study on the microstructure of colloidal fat crystal networks and fractal dimensions. **Advances in Colloid and Interface Science**. 128: 257-265.
- Thames Water (2017). **Could your bus be soon powered by a fatberg?** (online) available: <https://corporate.thameswater.co.uk/Media/News-releases/Could-your-bus-soon-be-powered-by-a-fatberg>. (Accessed 18 June 2018).
- Tieko Nassu, R. and Guaraldo Gonçalves, L. (1995). Solid fat content determination: Comparison between pNMR and DSC techniques. **Grasas y Aceites**. 46(6): 337-343.
- Trampitsch, C. (2009). **Multiwave 3000 Classified list of applications**. Anton Paar, Austria.
- Vold, R. and Hattiangdi, G. (1949). Characterization of heavy metal soaps by X-ray diffraction. **Industrial & Engineering Chemistry**. 41(10): 2311-2320.
- Wallace, T., Gibbons, D., O'Dwyer, M. and Curran, T.P. (2016). International evolution of fat, oil and grease (FOG) waste management—A review. **Journal of Environmental Management**. 187: 424-435.
- WCHD (2018). **FOG- fats, oils and grease**. (online) available: <https://www.washtenaw.org/1567/Fats-Oils-Grease-FOG>. (Accessed 4 June 2018).
- WEPA (2018). **Industrial effluent standard in Thailand**. (online) available: http://www.wepa-db.net/policies/law/thailand/std_industrial.htm. (Accessed 23 May 2018).
- Williams, J., Clarkson, C., Mant, C., Drinkwater, A. and May, E. (2012). Fat, oil and grease

- deposits in sewers: Characterisation of deposits and formation mechanisms. **Water Research**. 46(19): 6319-6328.
- Adhvaryu, A., Sung, C. and Erhan, S. (2005). Fatty acids and antioxidant effects on grease microstructures. **Industrial Crops and Products**. 21(3): 285-291.
- Alade, A.O., Jameel, A.T., Muyubi, S.A., Karim, M.I.A. and Alam, M.Z. (2011). Removal of oil and grease as emerging pollutants of concern (EPC) in wastewater stream. **IIUM Engineering Journal**. 12(4): 161-169.
- Alm, M. (2013). Animal Fats: Edible oil processing. **AOCS Lipid Library**. (online) available: <http://lipidlibrary.aocs.org/OilsFats/content.cfm?ItemNumber=40320>. (Accessed 12 June 2018).
- AlMubaddal, F., AlRumaihi, K. and Ajbar, A. (2009). Performance optimization of coagulation/flocculation in the treatment of wastewater from a polyvinyl chloride plant. **Journal of Hazardous Materials**. 161(1): 431-438.
- Arnaud, E., Relkin, P., Pina, M. and Collignan, A. (2004). Characterisation of chicken fat dry fractionation at the pilot scale. **European Journal of Lipid Science and Technology**. 106(9): 591-598.
- Arthur, S. and Blanc, J. (2013). **Management and recovery of FOG (fats, oils and greases)**. (online) available:http://www.crew.ac.uk/sites/default/files/sites/default/files/publication/CREW_FOG.pdf. (Accessed 11 April 2016).
- Ahsan, S., Rahman, M.A., Kaneco, S., Katsumata, H., Suzuki, T. and Ohta, K. (2005). Effect of temperature on wastewater treatment with natural and waste materials. **Clean Technologies and Environmental Policy**. 7(3): 198-202.
- Bhatnagar, A.S., Prasanth Kumar, P.K., Hemavathy, J. and Gopala Krishna, A.G. (2009). Fatty acid composition, oxidative stability, and radical scavenging activity of

vegetable oil blends with coconut oil. **Journal of the American Oil Chemists' Society**. 86(10): 991-999.

Beetseh, C. and Godwin, J. (2015). A study of distinctive characteristics of soaps made of saw dust ash (lye) with palm and olive oils and their oil blends in Benue State Nigeria. **Journal of Environment and Earth Science**. 5(12): 98-105.

BSR (2010). **Sustainable water group water quality guidelines**. (online) available: https://www.bsr.org/reports/awqwg/BSR_AWQWG_Guidelines-TestingStandards.pdf. (Accessed 23 May 2018).

Choi, D.W. and Chang, Y.H. (2012). Steady and dynamic shear rheological properties of buckwheat starch-galactomannan mixtures. **Preventive Nutrition and Food Science**. 17(3): 192-196.

Daborganes, C. (2009). **Formation of new compounds during frying-general observations**. (online) available: <http://aocs.files.cmsplus.com/annualmeeting/images/lipidimporthtml/lipidlibrary/frying/c-newcpds/index.htm>. (Accessed 23 May 2018).

da Silva Lannes, S. and Ignacio, R. (2013). **Structuring fat foods**. (online) available: <https://www.intechopen.com/books/food-industry/structuring-fat-foods>. (Accessed 5 June 2018).

Davis, J.L., Nica, D., Shields, K. and Roberts, D.J. (1998). Analysis of concrete from corroded sewer pipe. **International Biodeterioration & Biodegradation**. 42(1): 75-84.

DAWR (1994). **Guidelines for Sewerage Systems Acceptance of Trade Waste (Industrial Waste)**. (online) available: <http://www.agriculture.gov.au/>

SiteCollectionDocuments/water/sewerage-systems-trade-waste-paper12.pdf.

(Accessed 23 May 2018).

dos Santos, M.T., Viana, I., Ract, J. and Le Roux, G. (2016). Thermal properties of palm stearin, canola oil and fully hydrogenated soybean oil blends: coupling experiments and modeling. **Journal of Food Engineering**. 185: 17-25.

Ducoste, J.J. (2013). EPA Research Forum: **Factors that influence the formation of FOG deposits in sewer collection systems**. (online) available: <https://archive.epa.gov/ncer/events/calendar/archive/web/pdf/ducoste.pdf>. (Accessed 20 June 2018).

Emmel, J., Parott, K. and Beamish, J. (2003). Dishwashing and water conservation: an opportunity for environmental education. **Journal of Extension** 41(1).

Engineering Toolbox (2008). **Melting points of oils**. (online) available: https://www.engineeringtoolbox.com/oil-melting-point-d_1088.html. (Accessed 18 June 2018).

EPA (2004). **Report to Congress on impacts and control of CSO's and SSO's**. (online) available: https://www.epa.gov/sites/production/files/2015-10/documents/csos_sortc_2004_full.pdf. (Accessed 26 April 2018).

EPD (1990). **Technical memorandum standards for effluents discharged into drainage and sewerage systems, inland and coastal waters**. (online) available: https://www.epd.gov.hk/epd/sites/default/files/epd/english/envir_standards/files/GN2014P240-1991c-e.pdf. (Accessed 23 May 2018).

Fabiyi, M. and Larrea, A. (2015). Effect of High Temperature Operations on Wastewater Treatment: Reviewing the Resilience of High Temperature Industrial Wastewater Treatment Systems Using Microbiological Population

- Studies and Kinetic Dynamics. **Proceedings of the Water Environment Federation**. 2015(13): 1658-1669.
- FAO (2017). **Food outlook: Biannual report on global food markets**. (online) available: <http://www.fao.org/3/a-I8080e.pdf>. (Accessed 23 May 2018).
- Fennema, O.R., Damodaran, S. and Parkin, K.L. (2008). **Fennema's Food Chemistry (fourth ed.)**. CRC, Florida.
- Gönen, M., Öztürk, S., Balköse, D., Okur, S. and Ülkü, S. (2010). Preparation and characterization of calcium stearate powders and films prepared by precipitation and Langmuir–Blodgett techniques. **Industrial & Engineering Chemistry Research**. 49(4): 1732-1736.
- Ghotra, B.S., Dyal, S.D. and Narine, S.S. (2002). Lipid shortenings: a review. **Food Research International**. 35(10); 1015-1048.
- García, J.M., Herrera, S. and Morilla, A. (1996). Effects of postharvest dips in calcium chloride on strawberry. **Journal of Agricultural and Food Chemistry**. 44(1): 30-33.
- George, R.P. (2012). Current understanding and future approaches for controlling microbially influenced concrete corrosion: a review. **Concrete Research Letters**. 3(3): 491-506.
- Girgis, A.Y., El-Aziz, N.A. and El-Salam, S.A. (1998). Physical and chemical characteristics of toilet soap made from apricot kernel oil and palm stearin. **Grasas y Aceites**. 49(5-6): 434-439.
- Goodrum, J.W., Geller, D.P. and Adams, T.T. (2002). Rheological characterization of yellow grease and poultry fat. **Journal of the American Oil Chemists' Society**. 79(10): 961-964.

- Gross, M.A., Jensen, J.L., Gracz, H.S., Dancer, J. and Keener, K.M. (2017). Evaluation of physical and chemical properties and their interactions in fat, oil, and grease (FOG) deposits. **Water Research**. 123: 173-182.
- Gu, Z., Huang, W., Wang, S. and Zhou, A. (2015). Study on the formation of Fat, Oil, and Grease (FOG) deposits in sewer pipes. **J. Water Wastewater Eng. Assoc.** 1(1): 132-137.
- Guillen, M.D. and Cabo, N. (1997). Infrared spectroscopy in the study of edible oils and fats. **Journal of the Science of Food and Agriculture**. 75(1): 1-11.
- Gunstone, F.D. (2004). **The chemistry of oils and fats: Sources, composition, properties and uses**. Great Britain: Blackwell Publishing Ltd.
- Gupta (2005). **Frying Oils** **Bailey's Industrial Oil and Fat Products** (6th ed., Volume 6). New Jersey: John Wiley & Sons, Inc.
- Harkins, W.D., Mattoon, R.W. and Corrin, M.L. (1946). Structure of soap micelles indicated by X-rays and the theory of molecular orientation. I. Aqueous solutions I. **Journal of the American Chemical Society**. 68(2): 220-228.
- Hattiangdi, G.S. (1949). Characterization of some commercial soaps by X-ray diffraction. **Journal of Research of the National Bureau of Standards**. 42(4): 331-341.
- Haynes, W.M. (2010). **CRC Handbook of Chemistry and Physics**, 91st Edition. Florida: Taylor & Francis Group.
- He, X., de los Reyes III, F.L. and Ducoste, J.J. (2017). A critical review of fat, oil, and grease (FOG) in sewer collection systems: challenges and control. **Critical Reviews in Environmental Science and Technology**. 47(13): 1191-1217.
- He, X., Francis, L., Leming, M.L., Dean, L.O., Lappi, S.E. and Ducoste, J.J. (2013).

- Mechanisms of fat, oil and grease (FOG) deposit formation in sewer lines. **Water Research**. 47(13): 4451-4459.
- He, X., Iasmin, M., Dean, L.O., Lappi, S.E., Ducoste, J.J. and de los Reyes III, F.L. (2011) Evidence for fat, oil, and grease (FOG) deposit formation mechanisms in sewer lines. **Environmental Science & Technology**. 45(10): 4385-4391.
- Heger, S. (2017). **How temperature impacts onsite wastewater treatment**. (online) available:https://www.onsiteinstaller.com/online_exclusives/2017/05/how_temperature_impacts_onsite_wastewater_treatment. (Accessed 9 August 2018).
- Hill, M. and Moaddel, T. (2016). **Soap Manufacturing Technology** (Second Edition). Elsevier.
- Husain, I.A., Alkhatib, M.a.F., Jammi, M.S., Mirghani, M.E., Zainudin, Z.B. and Hoda, A. (2014). Problems, control, and treatment of fat, oil, and grease (FOG): a review. **Journal of Oleo Science**. 63(8): 747-752.
- Iasmin, M., Dean, L.O. and Ducoste, J.J. (2016). Quantifying fat, oil, and grease deposit formation kinetics. **Water Research**. 88: 786-795.
- Iasmin, M., Dean, L.O., Lappi, S.E. and Ducoste, J.J. (2014). Factors that influence properties of FOG deposits and their formation in sewer collection systems. **Water Research**. 49: 92-102.
- Ikhu - Omoregbe, D. and Bushi, G.M. (2008). Rheological characteristics of South African commercial sauces. **International Journal of Food Science & Technology**. 43(12): 2230-2236.
- Jayadas, N. and Nair, K.P. (2006). Coconut oil as base oil for industrial lubricants-evaluation and modification of thermal, oxidative and low temperature properties. **Tribology International** 39(9), 873-878.

- Keener, K.M., Ducoste, J.J. and Holt, L.M. (2008). Properties influencing fat, oil, and grease deposit formation. **Water Environment Research**. 80(12): 2241-2246.
- Koushki, M., Nahidi, M. and Cheraghali, F. (2015). Physico-chemical properties, fatty acid profile and nutrition in palm oil. **Journal of Paramedical Sciences**. 6(3).
- Lee, K.-T. and Foglia, T.A. (2000). Synthesis, purification, and characterization of structured lipids produced from chicken fat. **Journal of the American Oil Chemists' Society**. 77(10): 1027-1034.
- Lerma-García, M., Ramis-Ramos, G., Herrero-Martínez, J. and Simó-Alfonso, E. (2010). Authentication of extra virgin olive oils by Fourier-transform infrared spectroscopy. **Food Chemistry**. 118(1): 78-83.
- Li, F., Chen, M. and Zhang, W. (2017). Effect of binary/ternary fatty acids ratio and glycerin on the phase behaviors of soap solutions. **Journal of Surfactants and Detergents**. 20(2): 425-434.
- Lucke, N. (2013). **Industrial wastewater requirements and supervision**. (online) available: http://www.prestobalticsea.eu/download.php/dms/presto/Water%20Fair%20in%20Berlin/Presentations%20eng/Lucke_Norbert.pdf. (Accessed 23 May 2018).
- Madani, B., Mirshekari, A. and Yahia, E. (2016). Effect of calcium chloride treatments on calcium content, anthracnose severity and antioxidant activity in papaya fruit during ambient storage. **Journal of the Science of Food and Agriculture**. 96(9): 2963-2968.
- Mancini, A., Imperlini, E., Nigro, E., Montagnese, C., Daniele, A., Orrù, S. and Buono, P. (2015). Biological and nutritional properties of palm oil and palmitic acid: effects on health. **Molecules**. 20(9): 17339-17361.

- Marikkar, J., Ghazali, H., Man, Y.C. and Lai, O. (2002). The use of cooling and heating thermograms for monitoring of tallow, lard and chicken fat adulterations in canola oil. **Food Research International**. 35(10): 1007-1014.
- Metin, S. and Hartel, R.W. (2005). **Crystallization of fats and oils**. **Bailey's industrial oil and fat products** (6th ed., Vol. 6). New Jersey: John Wiley & Sons, Inc.
- Mills, P. (2010). **Framing the Problem**. In **FOG build up and removal**. (online) available:http://www.policyconsulting.co.uk/downloads/FOGs_Cranfield_March_2010.pdf. (Accessed 26 April 2018).
- Montefrio, M.J., Xinwen, T. and Obbard, J.P. (2010). Recovery and pre-treatment of fats, oil and grease from grease interceptors for biodiesel production. **Applied Energy**. 87(10): 3155-3161.
- Montoya, C., Cochard, B., Flori, A., Cros, D., Lopes, R., Cuellar, T., Espeout, S., Syaputra, I., Villeneuve, P. and Pina, M. (2014). Genetic architecture of palm oil fatty acid composition in cultivated oil palm (*Elaeis guineensis* Jacq.) compared to its wild relative *E. oleifera* (HBK) Cortés. **PLoS One**. 9(5): e95412.
- Naghshineh, M., Ariffin, A.A., Ghazali, H.M., Mirhosseini, H. and Mohammad, A.S. (2010). Effect of saturated/unsaturated fatty acid ratio on physicochemical properties of palm olein–olive oil blend. **Journal of the American Oil Chemists' Society**. 87(3): 255-262.
- Nadarajan, R. and Ismail, R. (2011). Performance and microstructural study on soap using different fatty acids and cations. **Journal of Surfactants and Detergents**. 14(4): 463-471.

- NEA (2018). **Allowable limits for trade effluent discharge to watercourse/controlled watercourse.** (online) available: <http://www.nea.gov.sg/anti-pollution-radiation-protection/water-pollution-control/allowable-limits>. (Accessed 23 May 2018).
- Nielsen, S.S. (2003). **Food Analysis** (third ed.). New York: Kluwer Academic/Plenum Publishers.
- Nora, A., Szczepanek, A. and Koenen, G. (2005). **Metallic Soaps.** Ullmann's Encyclopedia of Industrial Chemistry. Wiley-VCH, Weinheim.
- O'Brein, R. (2009). **Fats and Oils: formulating and Processing for Applications.** Richard D. O'Brien, editor, CRC Press, Boca Raton, FL.
- Osborne, S. (2017). **The Independent online newspaper: 'Monster fatberg' weighing more than 10 double deckers found clogging east London sewer.** (online) available: <https://www.independent.co.uk/news/uk/home-news/fatberg-east-london-sewer-10-double-decker-buses-kingston-monster-fat-whitechapel-times-water-a7943036.html>. (Accessed 18 June 2018).
- Panpipat, W. and Yongsawatdigul, J. (2008). Stability of potassium iodide and omega-3 fatty acids in fortified freshwater fish emulsion sausage. **LWT-Food Science and Technology.** 41(3): 483-492.
- Poulenat, G., Sentenac, S. and Mouloungui, Z. (2003). Fourier-transform infrared spectra of fatty acid salts-Kinetics of high-oleic sunflower oil saponification. **Journal of Surfactants and Detergents.** 6(4): 305-310.
- Rasband, W. (2000). **Circularity.** (online) available: <https://imagej.nih.gov/ij/plugins/circularity.html>. (Accessed 15 July 2017).
- Ren, T., Gao, X., Zheng, T. and Wang, P. (2016). **Study on treatment of acidic and highly**

concentrated fluoride waste water using calcium oxide-calcium chloride.

(online) available: [http://iopscience.iop.org/article/10.1088/1755-1315/](http://iopscience.iop.org/article/10.1088/1755-1315/39/1/012003/pdf)

[39/1/012003/pdf](http://iopscience.iop.org/article/10.1088/1755-1315/39/1/012003/pdf). (Accessed 12 June 2018).

Roberts, D., Nica, D., Zuo, G. and Davis, J. (2002). Quantifying microbially induced deterioration of concrete: initial studies. **International Biodeterioration &**

Biodegradation. 49(4): 227-234.

Rohman, A. and Che Man, Y.B. (2011). The optimization of FTIR spectroscopy combined with partial least square for analysis of animal fats in quaternary mixtures. **Journal of Spectroscopy.** 25(3-4): 169-176.

Romanova, A., Mahmoodian, M. and Alani, M.A. (2014). Influence and interaction of temperature, H₂S and pH on concrete sewer pipe corrosion. **International Journal of Civil, Architectural, Structural, Urban Science and Engineering.** 8(6): 592-595.

Rosell, B. (1999). **Vegetable oils and fats** (vol. 1), Leatherhead Publishing, London.

Rugmai, S. and Soontaranon, S. (2017). **SAXSIT Version 4.34.** Synchrotron Light Research Institute (SLRI), Thailand.

Sagitani, H. and Komoriya, M. (2015). Stability conditions and mechanism of cream soaps: Effect of polyols. **Journal of Oleo Science.** 64(8): 809-816.

Sawada, K. and Konaka, M. (2004). Characterization of fine metallic soap particles by X-ray diffraction, differential scanning calorimetry, and specific surface area analysis. **Journal of Oleo Science.** 53(12): 627-640.

Sawyer, C.N. (2003). **Chemistry for environmental engineering and science.** McGraw-Hill.

- Scottish Water (2012). **Your guide to disposing cooking fats.** (online) available: http://www.scottishwater.co.uk/assets/domestic/files/you%20and%20your%20home/save%20your%20drains/swfog2012_single%20pages_lowres.pdf. (Accessed 23 May 2018).
- Scrimgeour (2005). **Chemistry of fatty acids. Bailey's industrial oil and fat products** (6th ed., Vol. 6). New Jersey: John Wiley & Sons, Inc.
- Shahidi, F. and Zhong, Y. (2005). **Lipid oxidation: measurement methods. Bailey's industrial oil and fat products** (6th ed., Vol. 6). New Jersey: John Wiley & Sons, Inc.
- Shoeb, Z.E., Hammad, B.M. and Yousef, A. (1999). Oleochemicals I: Studies on the preparation and the structure of lithium soaps. **Grasas y Aceites.** 50(6): 426-434.
- Soult, A. (2016). Lipids and Triglycerides. (online) available: [https://chem.libretexts.org/LibreTexts/University_of_Kentucky/UK%3A_CHE_103_-_Chemistry_for_Allied_Health_\(Soult\)/Chapters/Chapter_14%3A_Biological_Molecules/14.2%3A_Lipids_and_Triglycerides](https://chem.libretexts.org/LibreTexts/University_of_Kentucky/UK%3A_CHE_103_-_Chemistry_for_Allied_Health_(Soult)/Chapters/Chapter_14%3A_Biological_Molecules/14.2%3A_Lipids_and_Triglycerides). (Accessed 18 June 2018).
- Steffe, J.F. (1996). **Rheological methods in food process engineering** (second ed.), Michigan: Freeman Press.
- Stoll, U. and Gupta, H. (1997). Management strategies for oil and grease residues. **Waste Management & Research.** 15(1): 23-32.
- Tang, D. and Marangoni, A.G. (2006). Quantitative study on the microstructure of colloidal fat crystal networks and fractal dimensions. **Advances in Colloid and Interface Science.** 128: 257-265.

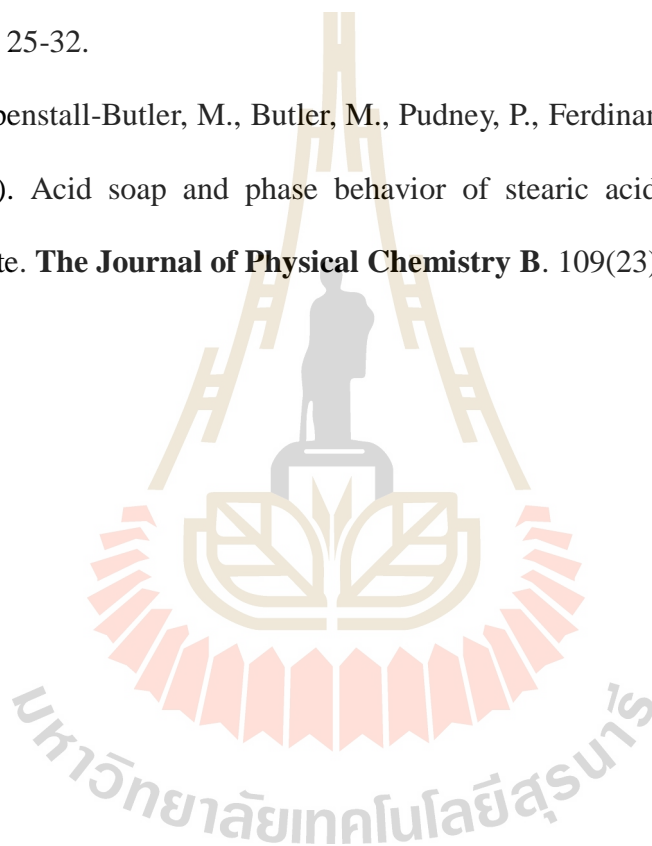
- Thames Water (2017). **Could your bus be soon powered by a fatberg?** (online) available: <https://corporate.thameswater.co.uk/Media/News-releases/Could-your-bus-soon-be-powered-by-a-fatberg>. (Accessed 18 June 2018).
- Tieko Nassu, R. and Guaraldo Gonçalves, L. (1995). Solid fat content determination: Comparison between pNMR and DSC techniques. **Grasas y Aceites**. 46(6): 337-343.
- Trampitsch, C. (2009). **Multiwave 3000 Classified list of applications**. Anton Paar, Austria.
- Vold, R. and Hattiangdi, G. (1949). Characterization of heavy metal soaps by X-ray diffraction. **Industrial & Engineering Chemistry**. 41(10): 2311-2320.
- Wallace, T., Gibbons, D., O'Dwyer, M. and Curran, T.P. (2016). International evolution of fat, oil and grease (FOG) waste management—A review. **Journal of Environmental Management**. 187: 424-435.
- WCHD (2018). **FOG-fats, oils and grease**. (online) available: <https://www.washtenaw.org/1567/Fats-Oils-Grease-FOG>. (Accessed 4 June 2018).
- WEPA (2018). **Industrial effluent standard in Thailand**. (online) available: http://www.wepa-db.net/policies/law/thailand/std_industrial.htm. (Accessed 23 May 2018).
- Williams, J., Clarkson, C., Mant, C., Drinkwater, A. and May, E. (2012). Fat, oil and grease deposits in sewers: Characterisation of deposits and formation mechanisms. **Water Research**. 46(19): 6319-6328.
- Wu, B.-c., Degner, B. and McClements, D.J. (2013). Creation of reduced fat foods: Influence of calcium-induced droplet aggregation on microstructure and rheology

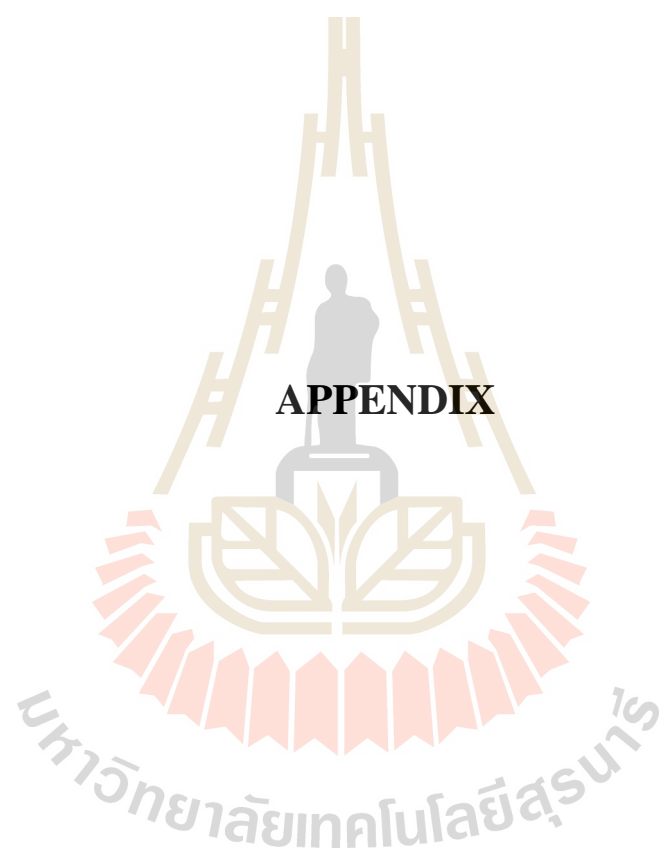
of mixed food dispersions. **Food Chemistry**. 141(4): 3393-3401.

Valenzuela, R., and Valenzuela, A. (2013). Overview about lipid structure. (online) available: <http://www.intechopen.com/books/lipid-metabolism/overview-about-lipid-structure>. (Accessed 31 March 2018).

Yang, H., Irudayaraj, J. and Paradkar, M.M. (2005). Discriminant analysis of edible oils and fats by FTIR, FT-NIR and FT-Raman spectroscopy. **Food Chemistry**. 93(1): 25-32.

Zhu, S., Heppenstall-Butler, M., Butler, M., Pudney, P., Ferdinando, D. and Mutch, K. (2005). Acid soap and phase behavior of stearic acid and triethanolamine stearate. **The Journal of Physical Chemistry B**. 109(23): 11753-11761.





APPENDIX

มหาวิทยาลัยเทคโนโลยีสุรนารี

Table A1 ANOVA-Tukey results of the Absorbance of characteristic metallic soap bands observed from CaCl₂-based soaps.

| Soaps* | Absorbance | | | | |
|--------|----------------------------|----------------------------|----------------------------|---------------------------|---------------------------|
| | 670 cm ⁻¹ | 1300-1420 cm ⁻¹ | 1550-1610 cm ⁻¹ | 1745 cm ⁻¹ | 3400 cm ⁻¹ |
| PO-2 | 0.09±0.01 ^{abcde} | 2.27±0.07 ^{abcd} | 0.83±0.25 ^{cde} | 0.19±0.02 ^{def} | 0.06±0.03 ^{bcd} |
| PO-3 | 0.19±0.02 ^{fg} | 2.57±0.11 ^{de} | 2.19±0.39 ^h | 0.12±0.11 ^a | 0.11±0.01 ^{de} |
| SO-2 | 0.15±0.02 ^{defg} | 2.33±0.04 ^{abcd} | 0.73±0.04 ^{abc} | 0.20±0.00 ^{efg} | 0.03±0.00 ^{abc} |
| SO-3 | 0.21±0.01 ^{gh} | 2.51±0.02 ^{bcd} | 0.91±0.07 ^{de} | 0.18±0.01 ^{def} | 0.06±0.00 ^{bcd} |
| OO-2 | 0.05±0.00 ^{ab} | 2.25±0.06 ^{abc} | 0.64±0.09 ^{bcd} | 0.21±0.00 ^{efgh} | 0.01±0.01 ^{ab} |
| OO-3 | 0.31±0.02 ⁱ | 2.57±0.04 ^{de} | 1.04±0.01 ^{ef} | 0.17±0.01 ^{cde} | 0.03±0.01 ^{abc} |
| CO-2 | 0.05±0.03 ^{ab} | 2.55±0.02 ^{cde} | 0.41±0.14 ^{abcd} | 0.26±0.01 ^{hij} | 0.04±0.02 ^{abc} |
| CO-3 | 0.28±0.09 ^{hi} | 2.83±0.16 ^{ef} | 1.53±0.46 ^{fg} | 0.14±0.05 ^{abc} | 0.16±0.08 ^{ef} |
| CF-2 | 0.033±0.01 ^a | 2.27±0.03 ^{abcd} | 0.41±0.05 ^{abcd} | 0.23±0.00 ^{ghij} | 0.00±0.00 ^a |
| CF-3 | 0.20±0.02 ^{fg} | 3.05±0.14 ^f | 2.37±0.12 ^h | 0.13±0.01 ^{bc} | 0.09±0.01 ^{cd} |
| PF-2 | 0.02±0.02 ^a | 2.22±0.00 ^{ab} | 0.10±0.01 ^{ab} | 0.23±0.00 ^{ghij} | 0.00±0.00 ^a |
| PF-3 | 0.15±0.10 ^{defg} | 3.01±0.39 ^f | 1.46±0.41 ^f | 0.15±0.02 ^{bcd} | 0.05±0.03 ^{abcd} |

*PO = palm olein oil; SO = soybean oil; OO = olive oil; CO = coconut oil; CF = chicken fat; PF = pork fat; the numbers indicate the layer the soaps were taken from the centrifuged mixture. Readings are compared with CaSO₄ results. Values followed by the same letter within the column are not significantly different (p<0.05).

Table A2 ANOVA-Tukey results of the Absorbance of characteristic metallic soap bands observed from CaSO₄-based soaps.

| Soaps* | Absorbance | | | | |
|--------|----------------------------|----------------------------|----------------------------|----------------------------|--------------------------|
| | 670 cm ⁻¹ | 1300-1420 cm ⁻¹ | 1550-1610 cm ⁻¹ | 1745 cm ⁻¹ | 3400 cm ⁻¹ |
| PO-2 | 0.06±0.00 ^{ab} | 2.39±0.11 ^{abcd} | 0.64±0.14 ^{bcde} | 0.22±0.00 ^{efgh} | 0.02±0.00 ^{ab} |
| PO-3 | 0.31±0.02 ⁱ | 2.35±0.07 ^{abcd} | 2.04±0.14 ^{gh} | 0.06±0.01 ^a | 0.21±0.02 ^f |
| SO-2 | 0.08±0.01 ^{abc} | 2.24±0.04 ^{abc} | 0.36±0.06 ^{abc} | 0.23±0.00 ^{fghij} | 0.01±0.01 ^{ab} |
| SO-3 | 0.15±0.02 ^{cdefg} | 2.22±0.05 ^{ab} | 0.67±0.12 ^{cde} | 0.19±0.01 ^{defg} | 0.03±0.01 ^{abc} |
| OO-2 | 0.07±0.01 ^{ab} | 2.23±0.02 ^{ab} | 0.56±0.00 ^{abcde} | 0.22±0.00 ^{efgh} | 0.02±0.00 ^{ab} |
| OO-3 | 0.08±0.01 ^{abcd} | 2.14±0.01 ^a | 0.01±0.00 ^a | 0.22±0.00 ^{efghi} | 0.01±0.00 ^{ab} |
| CO-2 | 0.02±0.00 ^a | 2.47±0.01 ^{bcd} | 0.49±0.01 ^{abcd} | 0.27±0.00 ⁱ | 0.01±0.00 ^{ab} |
| CO-3 | 0.03±0.00 ^a | 2.48±0.02 ^{bcd} | 0.62±0.10 ^{bcde} | 0.26±0.00 ^{ij} | 0.00±0.00 ^{ab} |
| CF-2 | 0.04±0.00 ^a | 2.21±0.00 ^{ab} | 0.41±0.03 ^{abcd} | 0.23±0.00 ^{ghij} | 0.01±0.00 ^{ab} |
| CF-3 | 0.16±0.02 ^{efg} | 2.32±0.01 ^{abcd} | 0.92±0.10 ^{de} | 0.18±0.01 ^{cde} | 0.06±0.01 ^{bcd} |
| PF-2 | 0.06±0.00 ^{ab} | 2.28±0.01 ^{abcd} | 0.50±0.01 ^{abcde} | 0.22±0.00 ^{efgh} | 0.02±0.00 ^{ab} |
| PF-3 | 0.12±0.01 ^{bcdef} | 2.24±0.04 ^{abc} | 0.71±0.04 ^{cde} | 0.20±0.01 ^{efg} | 0.03±0.01 ^{abc} |

*PO = palm olein oil; SO = soybean oil; OO = olive oil; CO = coconut oil; CF = chicken fat; PF = pork fat; the numbers indicate the layer the soaps were taken from the centrifuged mixture. Readings are compared with CaCl₂ results. Values followed by the same letter within the column are not significantly different (p<0.05).

Table A3 ANOVA-Tukey results of the saponification and yield of THE soaps from different lipid and calcium sources.

| Soaps* | Saponification (%) | | Yield (%) | |
|--------|--------------------------|---------------------------|------------------------|-------------------------|
| | CaCl ₂ | CaSO ₄ | CaCl ₂ | CaSO ₄ |
| PO-2 | 94.4±1.1 ^{def} | 93.4 ±0.6 ^{bcde} | 4.1±0.1 ^{ab} | 4.3±0.5 ^{ab} |
| PO-3 | 97.6±0.4 ^{ij} | 98.7 ±0.2 ^j | 22.7±.2 ^{gh} | 26.1±1.7 ^{hi} |
| SO-2 | 94.2±0.2 ^{def} | 92.2 ±0.3 ^{ab} | 3.2±0.8 ^{ab} | 1.2±0.1 ^a |
| SO-3 | 95.2±0.2 ^{fg} | 94.0 ±0.6 ^{cdef} | 7.2±1.4 ^{bc} | 28.4±0.5 ^{ij} |
| OO-2 | 93.4±0.6 ^{bcde} | 92.9 ±0.0 ^{bcd} | 5.1±0.6 ^{ab} | 4.8±0.3 ^{ab} |
| OO-3 | 95.7±0.2 ^{fgh} | 91.1 ±0.2 ^a | 20.6±0.7 ^{fg} | 25.4±3.7 ^{hi} |
| CO-2 | 92.1±0.8 ^{ab} | 91.8 ±0.0 ^{ab} | 3.4±0.5 ^{ab} | 1.1±0.0 ^a |
| CO-3 | 97.0±1.5 ^{hij} | 92.3 ±0.4 ^{abc} | 12.7±0.9 ^{de} | 32.1±4.6 ^j |
| CF-2 | 92.1±0.2 ^{ab} | 92.0 ±0.2 ^{ab} | 3.4±0.1 ^{ab} | 3.5±0.2 ^{ab} |
| CF-3 | 97.7±0.2 ^{ij} | 95.1 ±0.4 ^{efg} | 14.4±1.0 ^{de} | 25.1±1.3 ^{ghi} |
| PF-2 | 91.0±0.1 ^a | 92.9 ±0.1 ^{bcd} | 10.8±0.8 ^{cd} | 7.1±0.8 ^{bc} |
| PF-3 | 97.0±1.1 ^{ghi} | 94.0 ±0.4 ^{cdef} | 16.5±0.2 ^{ef} | 22.9±1.5 ^{gh} |

*PO = palm olein oil; SO = soybean oil; OO = olive oil; CO = coconut oil; CF = chicken fat; PF = pork fat; the numbers indicate the layer the soaps were taken from the centrifuged mixture.

Values followed by the same letter within the category are not significantly different (p<0.05).

Table A4 ANOVA-Tukey results of the calcium content of THE soaps from different lipid and calcium sources.

| Soaps* | Calcium content (mg Ca/mg crude soap) | |
|--------|---------------------------------------|--------------------------|
| | CaCl ₂ | CaSO ₄ |
| PO-2 | 0.15±0.00 ^f | 0.04±0.00 ^{ab} |
| PO-3 | 0.20±0.01 ^{ij} | 0.15±0.02 ^f |
| SO-2 | 0.16±0.00 ^{fg} | 0.09±0.01 ^{de} |
| SO-3 | 0.23±0.01 ^j | 0.18±0.02 ^{ghi} |
| OO-2 | 0.15±0.01 ^{fg} | 0.06±0.00 ^{bcd} |
| OO-3 | 0.23±0.02 ^j | 0.20±0.02 ^{hij} |
| CO-2 | 0.16±0.01 ^{fg} | 0.04±0.01 ^{ab} |
| CO-3 | 0.20±0.01 ^{ij} | 0.10±0.02 ^e |
| CF-2 | 0.08±0.00 ^{cde} | 0.05±0.00 ^{bc} |
| CF-3 | 0.20±0.00 ^{ij} | 0.15±0.01 ^f |
| PF-2 | 0.01±0.00 ^a | 0.05±0.01 ^{bc} |
| PF-3 | 0.17±0.01 ^{fgh} | 0.16±0.01 ^{fg} |

*PO = palm olein oil; SO = soybean oil; OO = olive oil; CO = coconut oil; CF = chicken fat; PF = pork fat; the numbers indicate the layer the soaps were taken from the centrifuged mixture.

Values followed by the same letter are not significantly different (p<0.05).

Table A5 ANOVA-Tukey results of the melting onset of the soaps from different lipid and calcium sources.

| Samples* | Melting onset (°C) | |
|----------|-------------------------|-----------------------|
| | CaCl ₂ | CaSO ₄ |
| | Raw | |
| PO | 12.4±0.1 ^{abc} | |
| SO | -2.8±0.2 ^a | |
| OO | 10.8±0.7 ^b | |
| CO | 32.1±0.5 ^e | |
| CF | 35.9±0.6 ^{efg} | |
| PF | 32.4±0.3 ^e | |
| | CaCl ₂ | CaSO ₄ |
| PO-2 | 19.2±0.2 ^d | 20.6±0.8 ^d |
| PO-3 | 56.3±4.4 ^j | 20.9±0.5 ^d |
| SO-2 | 48.4±0.5 ⁱ | 2.5±0.4 ^a |
| SO-3 | 57.9±1.9 ^j | 17.2±1.5 ^c |
| OO-2 | 44.5±0.2 ^{hi} | 12.3±0.6 ^b |
| OO-3 | 59.5±3.5 ^j | 16.4±0.3 ^c |
| CO-2 | 42.6±3.3 ^h | 35.7±0.6 ^e |
| CO-3 | 44.8±2.9 ^{hi} | 35.4±1.0 ^e |
| CF-2 | 34.9±0.9 ^{ef} | 34.9±0.1 ^e |
| CF-3 | 56.9±3.8 ^j | 34.2±0.9 ^e |
| PF-2 | 39.7±0.9 ^{fgh} | 42.4±0.4 ^f |
| PF-3 | 40.6±0.5 ^j | 40.6±0.5 ^f |

*PO = palm olein oil; SO = soybean oil; OO = olive oil; CO = coconut oil; CF = chicken fat; PF = pork fat; the numbers indicate the layer the soaps were taken from the centrifuged mixture.

Values followed by the same letter are not significantly different (p<0.05).

Table A6 ANOVA-Tukey results of the apparent viscosity and viscoelasticity of the soaps from different lipid and calcium sources.

| FOG deposit [*] | Apparent viscosity, η_{100} (Pa.s) | | Tan δ | |
|--------------------------|---|----------------------------|---------------------------|---------------------------|
| | CaCl ₂ | CaSO ₄ | CaCl ₂ | CaSO ₄ |
| PO-2 | 0.11±0.07 ^a | 1.59±0.07 ^{defg} | 0.13±0.06 ^{ab} | 0.17±0.01 ^{abc} |
| PO-3 | 0.49±0.11 ^{ab} | 1.77±0.13 ^{defg} | 0.20±0.01 ^{abc} | 0.17±0.01 ^{abc} |
| SO-2 | 0.11±0.04 ^a | 0.86±0.02 ^{abcd} | 0.16±0.01 ^{abc} | 0.14±0.02 ^{ab} |
| SO-3 | 0.09±0.00 ^a | 2.49±0.47 ^{gh} | 0.27±0.03 ^{abcd} | 0.17±0.05 ^{abc} |
| OO-2 | 2.16±0.31 ^{efg} | 0.73±0.00 ^{abcd} | 0.24±0.01 ^{abc} | 0.15±0.02 ^{ab} |
| OO-3 | 0.16±0.01 ^a | 2.40±0.51 ^{fg} | 0.23±0.02 ^{abc} | 0.12±0.02 ^{ab} |
| CO-2 | 0.93±0.09 ^{abcd} | 0.52±0.10 ^{abc} | 0.65±0.31 ^d | 0.48±0.01 ^{bcd} |
| CO-3 | 0.15±0.13 ^a | 4.17±1.35 ⁱ | 0.09±0.03 ^{ab} | 0.08±0.07 ^{ab} |
| CF-2 | 1.56±0.25 ^{cdefg} | 1.40±0.06 ^{bcdef} | 0.27±0.14 ^{abcd} | 0.37±0.17 ^{abcd} |
| CF-3 | 0.11±0.03 ^a | 3.53±0.17 ^{hi} | 0.23±0.01 ^{abc} | 0.06±0.02 ^a |
| PF-2 | 0.18±0.10 ^{bcde} | 1.34±0.05 ^{bcde} | 0.57±0.07 ^{cd} | 0.66±0.49 ^d |
| PF-3 | 0.03±0.01 ^a | 4.37±0.26 ⁱ | 0.20±0.04 ^{abc} | 0.03±0.03 ^a |

^{*}PO = palm olein oil; SO = soybean oil; OO = olive oil; CO = coconut oil; CF = chicken fat; PF = pork fat; the numbers indicate the layer the soaps were taken from the centrifuged mixture. All measurements were done at 25°C. Values followed by the same letter within the category are not significantly different (p<0.05).

BIOGRAPHY

Dann Marie Nuñez Del Mundo was born on October 9, 1979 in Digos City, Davao del Sur, Philippines. In 2001, she received her Bachelor of Science in Food Technology at the University of the Philippines Visayas, Miag-ao, Iloilo. Shortly after her graduation, she joined the Century Pacific Group of Companies as an R&D Researcher for tuna and meat processing. In 2006, she pursued her MS Environmental Science at the University of the Philippines Los Baños and was granted the UP Presidential Scholarship and Conservation International Thesis Award.

Since 2008, she is a faculty member of the Department of Food Science and Chemistry in the University of the Philippines Mindanao where she teaches courses in food processing, sensory evaluation, food analysis, food quality, and food processing waste management. In 2012, she was tapped by the Department of Science and Technology Region XI as one of the junior consultants for Small and Medium Enterprises. In 2013, she was awarded the SUT-PhD Scholarship for ASEAN and pursued a PhD degree in Food Technology. In 2017, she published her work in Water Research journal entitled, “Influence of fat and oil type on the yield, physico-chemical properties, and microstructure of fat, oil, and (FOG) grease deposits.”